UNIVERSITÀ DEGLI STUDI DI TRIESTE

XXXI CICLO DEL DOTTORATO DI RICERCA IN

SCIENZE DELLA RIPRODUZIONE E DELLO SVILUPPO

PHOTOBIOMODULATION THERAPY: *IN VIVO* AND *IN VITRO* MODELS FOR APPLICATIONS IN PEDIATRIC ONCOLOGY

Settore scientifico-disciplinare: MED/38 PEDIATRIA GENERALE E SPECIALISTICA

Ph.D. STUDENT

DR. LUISA ZUPIN

Ph.D. PROGRAM COORDINATOR

PROF. PAOLO GASPARINI

THESIS SUPERVISOR

PROF. SERGIO CROVELLA

ANNO ACCADEMICO 2017/2018

UNIVERSITÀ DEGLI STUDI DI TRIESTE

XXXI CICLO DEL DOTTORATO DI RICERCA IN

SCIENZE DELLA RIPRODUZIONE E DELLO SVILUPPO

PHOTOBIOMODULATION THERAPY: *IN VIVO* AND *IN VITRO* MODELS FOR APPLICATIONS IN PEDIATRIC ONCOLOGY

Settore scientifico-disciplinare: MED/38 PEDIATRIA GENERALE E SPECIALISTICA

Ph.D. STUDENT

DR. LUISA ZUPIN

Ph.D. PROGRAM COORDINATOR

PROF. PAOLO GASPARINI

THESIS SUPERVISOR

PROF. SERGIO CROVELLA

ANNO ACCADEMICO 2017/2018

CONTENTS

Abstract

Photobiomodulation (PBM) Therapy is a form of treatment that exploits laser light to elicit bio-stimulation, promoting cellular metabolism, reducing inflammation, driving analgesia and with an antimicrobial action at blue wavelength. PBM is currently used for the management of oral mucositis (OM) a severe side effect of chemo-radiotherapy characterized by painful atrophic / ulcerative lesions of oral mucosa that can affect pediatric and adult oncologic patients. Although the successful clinical employment of PBM, some issues remain regarding its mechanisms of action, moreover, a universal agreement regarding the most efficacious protocols is still lacking.

In this PhD project different aspects of PBM were investigated with the aim of describing the properties of laser light, and consecutively amplifying the scientific knowledge in the laser field.

Firstly, PBM effect on oxidative stress was inquired.
In OM patients, the clinical parameters improved with PBM at 970 nm with the amelioration of clinical scores and with the healing of oral ulcerations, moreover, PBM reduced salivary total oxidant status.
In an *in vitro* model of skin keratinocytes treated with 5-fluorouracil (5-FU), mimicking OM condition, PBM at 970, 905, 800 and 660 nm was able to increment the viability of 5-FU treated cells and to reduce reactive oxygen species (ROS) and gene expression of two antioxidant enzymes.

Secondly, PBM was tested for its immunoregulatory actions.
PBM was not able to impact on salivary β-defensins proteins production in OM patients.
However, in an oral mucosa epithelial cell line, PBM at 970, 800 and 660 nm reduced mRNA expression of *DEFB1, DEFB4, DEFB103* genes. Furthermore, when the cells were pre-treated with lipopolysaccharide, PBM at 660 nm reduced the expression of *DEFB103*. Moreover, PBM at 970 nm increased *IL1B* expression and decreased *NLRP3* one, meanwhile at 660 nm increased *NLRP1* expression.

Thirdly, the analgesic activities of PBM were investigated.
PBM at 970 nm was able to decrease the painful sensation referred by OM patients.
In primary murine sensory neurons from dorsal root ganglia, PBM at 970 and 800 nm reduced ATP and nitric oxide production and increased ROS level; PBM at 800 nm increased also superoxide anion and mitochondrial membrane potential, while at 970 nm decreased the calcium flow after capsaicin administration.

When capsaicin, as a painful stimulus, were subplantarly injected in mice, PBM at 970 nm reduced the pain related behavior.

Fourthly, the blue PBM was studied for its antibacterial properties.
PBM inhibited *Pseudomonas aeruginosa* growth on agar plate and in broth, inducing wall damaging. Blue light caused a lethal increment of ROS, that was rescued through a pre-treatment with a ROS scavenger. *P. aeruginosa* mutants for enzymes of the porphyrin biosynthetic pathway, producing less porphyrins, resulted less susceptible to irradiation.
Finally, PBM was able to inhibit bacterial replication in a murine *in vivo* model of skin abrasion infection. Blue PBM did not result cytotoxic for eukaryotic cells, rather it reduced the inflammatory infiltrate in the murine skin.

Lastly, blue PBM was examined for its antiviral activities.
Blue PBM was tested on an *in vitro* model of human skin keratinocytes infected with Herpes simplex virus type 1 (HSV-1).
The virus was irradiated alone and then the cells were infected: PBM exerted an antiviral effect, decreasing the viral load and increasing the viability of the cells infected with irradiated virus.
The plaque forming unit assay corroborated these results, proven the less infectivity capacity of irradiated HSV-1.

So, our results highlighted a pleiotropic action of PBM as anti-oxidant, immunoregulatory, analgesic, antibacterial and antiviral agent. These data corroborated the useful medical interventions based on laser light, possibly helping to increment a clinical thoughtful and justified usage of PBM in OM patients for routinely applications, especially in pediatric oncologic subjects.

List of abbreviations

5-FU = 5-fluorouracil
AMPs = antimicrobial peptides
ATP = adenosine triphosphate
CFU = colony forming unit
Cox = cytochrome C oxidase
COX2 = cyclooxygenase-2
CRT = chemo-radiotherapy
CTC = common toxicity criteria
CTRL = control
CW = continuous wave
DAMPs = damage-associated molecular patterns
DRG = dorsal root ganglia
ECM = extracellular matrix
hBD = human β-defensin
HSV-1 = Herpes simplex virus type 1
IL = Interleukin
IR = infrared
LB = Luria-Bertani
LPS = lipopolysaccharide
MMP = mitochondrial membrane potential
NF-κB = nuclear factor κB
NGF = nerve growth factor
NGS = normal goat serum
NIR = near infrared
NO = nitric oxide
NT = not treated
OD = optical density
OM = Oral Mucositis
PAMPs = pathogen associated molecular patterns
PBM = Photobiomodulation
PBS -T = phosphate buffer saline + TritonX100
PBS = phosphate buffer saline
PFA = paraformaldehyde
PFU = plaque forming unit
ROS = reactive oxygen species
SEM = Scanning Electron Microscope
TBARS = thiobarbituric acid reactive substances
TNF = Tumor Necrosis Factor
TOS = total oxidant status
TRPV1 = transient receptor potential cation channel subfamily V member 1
VAS = visual analogue scale

Introduction

L.A.S.E.R.

L.A.S.E.R. is the acronym for Light Amplification by Stimulated Emission of Radiation.
The creation of laser light in an active medium occurs when an excitation source (i.e. flash lamp, electric current) leads to transition of electrons towards a higher energy level, then the electrons returns to lower state emitting energy as photons. This process was then amplified by the emitted photons that stimulate the emission of further photons in the closer atoms and by mirrors inside the laser device. When the photon energy created by excited atoms is sufficient, the light is released as emission of a beam [reviewed by [Langtry, 1994]].

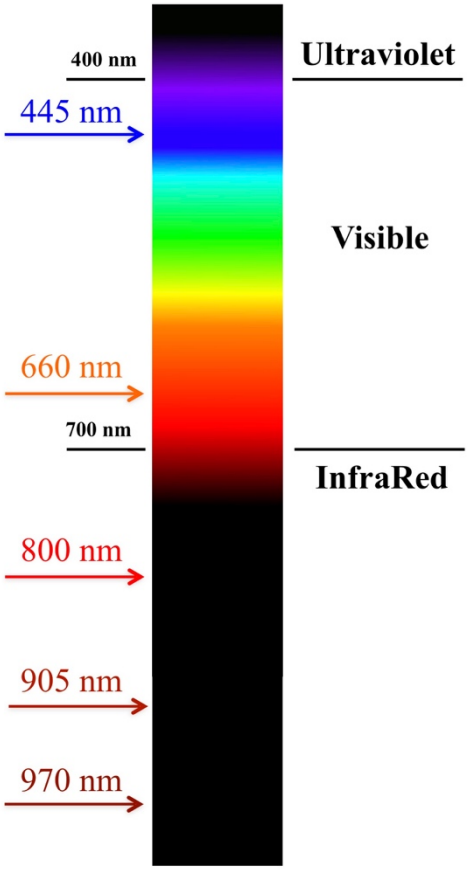

Laser light is characterized by coherence, unidirectionality and monochromaticity. Coherence means that light waves are in phase respecting space and time; unidirectionality indicates that light waves are collimated and parallel with no divergence; monochromaticity designates the characteristic that only a single defined wavelength is emitted [reviewed by [Bogdan Allemann, and Kaufman, 2011]].
Laser instruments present an active lasing medium (liquid, solid or gas) that determines the wavelength emitted [reviewed by [Bogdan Allemann, and Kaufman, 2011]]. In the laser medical field, the range from visible to near infrared (NIR) wavelengths (600 - 1070 nm) is commonly employed, moreover, recently, laser light at lower wavelength (400 - 470 nm) has been successfully used for antimicrobial purpose [reviewed by [Wang et al., 2017b]] (figure 1).

Figure 1. The electromagnetic spectrum.
On the left side are highlighted the wavelengths employed in the current study.
On the right the common names of the electromagnetic waves are reported.

Other important parameters in laser field are: energy, the number of photon delivered (expressed in Joules); fluence or energy density, the energy per area (measured in Joules/cm^2); power, the amount of energy delivered (expressed in Watts); irradiance or power density, the quotient of incident laser power on a unit surface area, (measured in Watt/cm^2). Lasers can emit light in continuous wave (CW) or with a pulse repetition rate (frequency measured in Hertz) [reviewed by [Bogdan Allemann, and Kaufman, 2011]].

Photobiomodulation

Low Level Laser Therapy also recently defined as Photobiomodulation (PBM) therapy is a form of treatment that employs the laser light to perform biostimulation, eliciting a response to light not due to heating [reviewed by [Tsai, and Hamblin, 2017]]. PBM is based on the principle that laser light is absorbed by cellular photoreceptors (chromophores) promoting photophysical and photochemical events [Anders et al., 2015]. Its application is separated from that of surgical medical laser where the photothermolysis is pursued: this type of procedure exploits the absorption of light from targeted molecules in the tissue leading to their destruction without affecting the adjacent structures [Anderson, and Parrish, 1981]. In fact, "low level" of energy density and power are applied in PBM respect to laser utilized for cutting, ablation and tissue coagulation, and for these characteristics PBM is also known as "cold laser" [reviewed by [Chung et al., 2012]].

The first utilization of laser for biostimulation dates back to the 1967 when Endre Mester observed that the application of laser light on shaven mice promoted a faster grow of the hair [Mester et al., 1968]; then, he showed that laser was also able to foster wound healing in mice [Mester et al., 1971]. After these findings, he soon translated them to human, treating successfully skin ulcers [Mester et al., 1972; Mester et al., 1976].

From these discoveries the use of PBM for medical applications has been grown worldwide comprising more than 5000 published articles in 2018 (using the MeSH term "Low-Level Laser Therapy" on NCBI available at URL https://www.ncbi.nlm.nih.gov) and it spreads out from the wound healing in diabetic (ulcers) or oncologic (oral mucositis) patients, to the pain relief in carpal tunnel syndrome and arthritis [reviewed by [Chung et al., 2012]].
So, it can be evinced that PBM has its utmost effectiveness in the treatment of superficial tissue of human organism, such as skin or mucosa [reviewed by [Chung et al., 2012]], although recently the transcranial application of light has been arisen [reviewed by [Salehpour et al., 2018]].

The tissue penetration of light depends on the wavelength employed. Indeed, under 600 nm tissue chromophores as hemoglobin, melanin and water absorb photon energy, therefore, PBM should be used in the range 600 - 700 nm to treat superficial tissues meanwhile in the range 780 - 950 nm for deeper tissues [reviewed by [Chung et al., 2012]]. Finally, blue wavelength has a very low penetration and it reaches only 1 mm in depth, but at the moment its application is limited to the research field as microbicide and only few studies reported its effects on human infections [reviewed by [Wang et al., 2017b]] (figure 2).

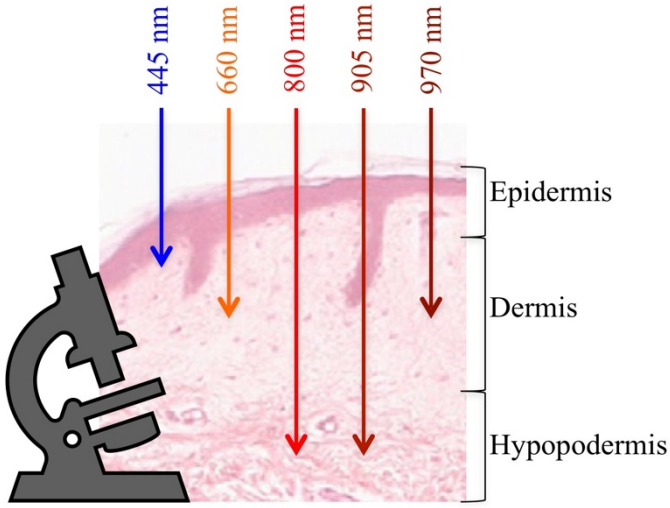

Figure 2. The penetration of the wavelengths into the skin.

The penetration of the 5 wavelengths employed in the current study are shown.

Apart from the wavelength employed, PBM effect is highly dependent on the dosimetry chosen. PBM presents a biphasic dose response that follows the Arndt-Schulz Law "a weak stimuli slightly accelerates activity, stronger stimuli raises it further, but a peak is reached and that a stronger stimulus will suppress activity" [Martius, 1923]: in laser field, it means that upper and lower threshold of energy and power exists, outside which the light is respectively too weak or too strong to have an efficacious outcome [reviewed by [Chung et al., 2012]] (figure 3 [Sommer et al., 2001]).

Huang et al. hypothesized that this effect could be due to generation of reactive oxygen species and nitric oxide, very low and with minimal effect in the left side of the curve, low but beneficial to activate intracellular pathways in the peak, too high and dangerous in the right side of the curve [reviewed by [Huang et al., 2009; Huang et al., 2011]].

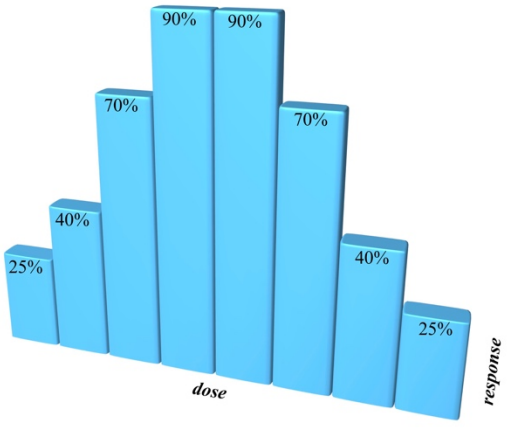

Figure 3. Idealized biphasic dose response curve similar to those conceived by Sommer et al. [Sommer et al., 2001].

Photobiomodulation Molecular Effects

It has been widely accepted that in the eukaryotic cells the main photoreceptor should be the mitochondria and specifically, the cytochrome C oxidase (Cox) seems to absorb most of the light in the red and NIR wavelengths received by the cells [Passarella, and Karu, 2014]. Cox is the terminal enzyme of the mitochondrial respiratory chain forming the complex IV; it presents two copper (Cu_A and Cu_B) and two iron ($Heme_a$ and $Heme_{a3}$) centers. The study of absorption and action spectra allows the researchers to identify in Cu_A and Cu_B (and their redox state) the main cellular chromophores [reviewed by [Karu, 1999]].

Since PBM treatment induces an increased oxygen consumption, it has been supposed that PBM is able to increment the availability of electrons for the reduction of molecular oxygen in the Cox's catalytic centers: so, PBM increases O_2 uptake, electron transfer and proton pumping of Cox [reviewed by [Karu, 2008]]. This action of PBM on cellular respiration leads to a transitory increment of mitochondrial membrane potential (MMP), an electrochemical gradient consisting of electrical transmembrane potential and a proton gradient (ΔpH), that propels adenosine triphosphate (ATP) production [reviewed by [Karu, 2008]].

On the other hand, during chemiosmosis for the production of ATP, oxidative phosphorylation could release a small quantity of electrons that are accepted by oxygen producing superoxide anion (O_2^-). This reactive oxygen species (ROS) at low concentration causes a intracellular redox change and it is an activator of different pathways [reviewed by [Prindeze et al., 2012]], however, when in the presence of a pre-existent oxidative stress PBM is able to decrease ROS levels [reviewed by [Rai, 2016]].

Besides these events, nitric oxide (NO) concentration increases after PBM, probably due to its release from metal centers of Cox, thus, driving back the mitochondrial inhibition caused by NO binding [reviewed by [Shiva, and Gladwin, 2009]]. Moreover, NO influences the redox state of the respiratory chain and O_2^- generation [reviewed by [Poyton, and Ball, 2011]].

These changes activate a retrograde mitochondrial signaling through which mitochondria communicate with nucleus and affect transcription factors and gene expressions [reviewed by [Karu, 2008]].

Moreover, mitochondria through internal structural changes could also communicate with nucleus: these organelles are dynamic in constant movement with fusion and fission events that change the mitochondrial size, number and mass. Calcium ion (Ca^{2+}) concentration could be affected by mitochondrial ultrastructure modification, moreover, it can also result from PBM induced cytosolic alkalinization that facilitates TRPV1 (transient receptor potential cation

channel subfamily V member 1) channels opening. On the other hand, when Ca^{2+} increases at high level for some stimuli, PBM decrements it [reviewed by [de Freitas, and Hamblin, 2016]].

Photobiomodulation Biological Effects

Thus, PBM can influence different types of processes inside eukaryotic cells impacting so on tissue functionality.

It was reported that PBM in fibroblast was able to induce cell cycle progression and proliferation, migration, metabolism with ATP production [reviewed by [Kuffler, 2016]]; additionally, PBM influenced collagen secretion [reviewed by [Kuffler, 2016]] and extracellular matrix remodeling probably through matrix metalloproteinases modulation [reviewed by [Ayuk et al., 2016]]. Similarly, PBM in keratinocytes promoted proliferation, migration and a rapid differentiation [Sperandio et al., 2015], helping and accelerating wound healing and tissue repair, reducing fibrous tissue formation [reviewed by [Kuffler, 2016]]. Moreover, PBM stimulated proliferation of endothelial cells and vascular smooth muscle relaxation, causing neoangiogenesis, release of oxygens and nutrients in the tissues and interstitial liquid reabsorption [Ottaviani et al., 2013]: the perfusion was increased, and locale ischemia reduced [reviewed by [Chung et al., 2012]]. These effects are beneficial for the treatment of different skin conditions in human, such as the diabetic foot ulcers, burns, hypertrophic scars, keloids, acne, and herpetic lesions [reviewed by [Avci et al., 2013]].

It was shown that PBM activated nuclear factor κB (NF-κB), via ROS generation in fibroblast *in vitro* [Chen et al., 2011], this transcription factor in turn regulates different intracellular pathways and it acts also as pro-inflammation inducer [Carmody, and Chen, 2007]. *In vivo* on skin of healthy volunteers PBM attracted neutrophils, macrophages and mast cells [Omi et al., 2005]. Despite this data, PBM was able to reduce pro-inflammatory markers, such as Tumor Necrosis Factor (TNF) - α, Interleukin (IL) - 1β, cyclooxygenase-2 (COX2), in activated inflammatory cells like synoviocytes (from rheumatoid arthritis patients), lipopolysaccharide (LPS) treated fibroblasts and macrophages; in macrophages PBM reduced also the markers of M1 phenotype (classically activated) [reviewed by [Hamblin, 2017]]. In neutrophils PBM incremented the respiratory burst and their fungicidal capacity [Cerdeira et al., 2016], but also reduced the neutrophils infiltrate in experimental oral mucositis in hamsters [Lopes et al., 2010]. So, PBM exerts double activity, increasing NF-κB in normal resting cells but also reducing inflammation

when it is present. Therefore, PBM is successful used in humans for Achilles tendinopathy, autoimmune thyroiditis, muscles trauma, psoriasis, and arthritis [reviewed by [Hamblin, 2017]].

PBM was able to partially block nerve conduction and action potential generation in peripheral neurons, possibly producing an analgesic effect. Indeed, PBM caused the formation of reversible varicosities, rich in mitochondria, along axons that reduced ATP availability and interfered with neuron electric transmission [reviewed by [Chow, and Armati, 2016]]. PBM was also able to inhibit sensory neuron activities when stimulated with pro-inflammatory substances, as formalin, or in case of neurogenic inflammation induced by neuropeptides, as substance P. PBM promoted also the release of neurotransmitters, such as serotonin and β-endorphin, both relevant for pain relief [reviewed by [Chow, and Armati, 2016]]. In animal models, PBM reduced the withdrawal latency using the tail-flick test [Ponnudurai et al., 1987], the sensitivity to cold or heat stimuli, and the mechanical hyperalgesia [Holanda et al., 2017].
For these characteristics, in humans, PBM is successfully currently used to treat chronic pain, musculoskeletal pain (e.g. low back pain), orthodontic pain, post-operative pain, and joints or tendinopathy related pain [reviewed by [Chow et al., 2011]].

The above-mentioned laser light actions are commonly and currently used in the clinical practice for the conditions above reported, however evidences from preclinical and clinical studies proposed other potential applications of laser light, for example it can be used through a transcranial application for treating neurological conditions. PBM was beneficially tested on traumatic brain injury and ischemic stroke, neurodegenerative diseases as Alzheimer and Parkinson, and psychological problems as depression and anxiety [reviewed by [Salehpour et al., 2018]]. PBM was also applied to retina to treat retinal degeneration, age-related macular degeneration, diabetic retinopathy, reducing cell loss and improving the view in animal models and in patients [reviewed by [Geneva, 2016]].
In peripheral nerve injury, PBM accelerated and improved the nerve repair and regeneration stimulating axon sprouting, leading to re-innervation of the tissues in animal models [de Oliveira et al., 2015], moreover, in humans PBM helped the recovery of sensibility in oral district [de Oliveira et al., 2015].
In animal experimental model, PBM was employed as vaccine adjuvants for enhancing the immunity response, acting mainly on motility and migration of dendritic cells [Chen et al., 2010]. PBM was also able to promote immune surveillance against cancerous cells and to reduce the tumor growth in mice [Ottaviani et al., 2016].

Additionally, PBM influenced osteoblasts and osteoclasts proliferation, promoting their maturation and alkaline phosphatase activities, so helping regeneration in extraction sites, bone fracture, experimentally induced bone defects and distraction osteogenesis in animals models [reviewed by [Ebrahimi et al., 2012]]; instead, in humans, PBM could act increasing bone density in maxillofacial bone defects [reviewed by [Santinoni et al., 2017]].

Concluding, PBM has multiple and differential effects depending on the state of the cells/tissues, indeed, it is important to consider that when PBM is applied on normal cells, the effect is poor, but its great effectiveness is achieved when there is a deviation from the homeostatic condition [Sommer et al., 2001].
In this description, the positive outcomes of PBM treatment are reported, nevertheless, some studies showed no effect. An old but interesting and actual approach to try to answer this discrepancy was indicated by Tunér and Hode [Tunér, and Hode, 1998]: the parameters of irradiation are of the utmost importance, indeed sometimes it is difficult to obtain the optimal dose, too low energy or power could have no effect; the inclusion criteria and the inter-individually variations should be taken into account, as the procedure of PBM outcome evaluation and the blinding of the experimenters.

The effect of PBM are schematically represented in figure 4.

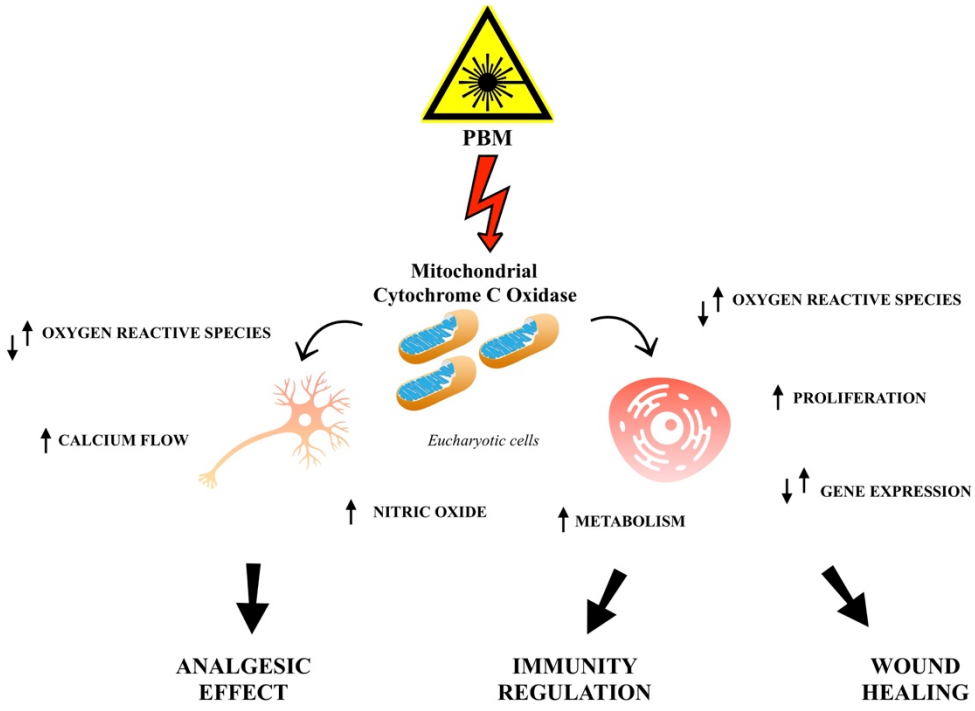

Figure 4. Schematic representation of the principal effects of photobiomodulation (PBM) at red and near-infrared λ on eukaryotic cells.

Blue Photobiomodulation Therapy

Regarding blue light antimicrobial properties, it was reported that endogenous bacterial porphyrins should be the receptors of blue light. Once the light is absorbed, the molecules change their state from basal to excited triple state, and they transfer their energy to molecular oxygen. Oxygen becomes excited and dissociated forming ROS (singlet oxygen ($^1O_2$), superoxide anion (O_2), hydrogen peroxide (H_2O_2), and hydroxyl radical ($\cdot OH$)), and damaging bacteria cells through lipid oxidation and protein cross linkage leading to death [Yang et al., 1995]. This hypothesis is supported by the fact that in anaerobic condition the antimicrobial effect does not occur as when ROS scavenger is added to the culture medium [Feuerstein et al., 2005].

Blue light is so active against different bacteria, such as *Propionibacterium acnes, Staphylococcus aureus, Staphylococcus epidermidis, Streptococcus pyogenes, Streptococcus mutans, Enterococcus faecalis, Clostridium perfringens, Acinetobacter baumannii, Pseudomonas aeruginosa, Helicobacter pylori, Escherichia coli, Proteus vulgaris, Klebsiella pneumoniae, Porphyromonas gingivalis, Prevotella spp, Fusobacterium nucleatum* [reviewed by [Dai et al., 2012]].

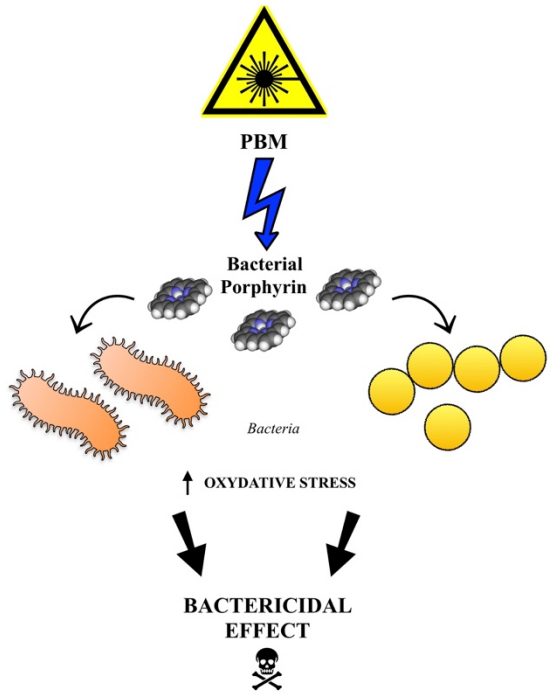

In vivo animal studies showed the antimicrobial action of blue light on wound and burns infections caused by *A. baumannii, P. aeruginosa, methicillin-resistant S. aureus* [reviewed by [Wang et al., 2017b]].

Few clinical studies were yet conducted, however blue irradiation showed efficacy in the treatment of acne vulgaris caused by *P. acnes*, *H. pylori* gastric infections, dental plaques induced by *P. gingivalis* and *Prevotella intermedia* [reviewed by [Dai et al., 2012; Wang et al., 2017b]].

The blue PBM effect is schematically represented in figure 5.

Figure 5. Antimicrobial mechanism of action of blue photobiomodulation (PBM).

Oral Mucositis

Oral Mucositis (OM) is a common severe side effect that can arise from chemo-radiotherapy (CRT) in oncologic patients, both adult and pediatric, and clinically ranges from atrophic erythematous lesions to ulcerative injuries of the oral mucosa [reviewed by [Sonis, 2004]].

Although OM can affect both children and adults, pediatric patients present a higher OM prevalence than adults, possibly due to more rapid cell proliferation in younger subjects [Kennedy, and Diamond, 1997]. Indeed, it is estimated that up to 80% of children treated with chemotherapy develop OM [Cheng et al., 2004], while, almost all children affected by hematologic malignancies and submitted to conditioning regimens for hematopoietic stem cell transplantation develop OM [Cheng, 2007], and in more severe form than other type of solid cancers [Otmani et al., 2011].

Among the mucotoxic drugs, 5-fluorouracil (5-FU) is correlated with more severe OM features respect to others such as doxorubicin, etoposide, or methotrexate [Rubenstein et al., 2004].

OM generally develops after 3-10 days from the beginning of the CRT and can persist until 3 weeks with a peak between 7-14 days [reviewed by [Miller et al., 2012]].

CRT affects cells with rapid division, so, the oral mucosa lining is severely damaged by the treatment, notably, CRT induced injury is a complex process that does not alter the superficial epithelium, but initiates its destructive action in the submucosal endothelium [reviewed by [Miller et al., 2012]].

OM development occurs in 5 stages: initiation, primary damage response, signal amplification, ulceration and healing [reviewed by [Sonis, 2004]]. In the “initiation” stage, CRT induce both DNA and non-DNA damage in the basal epithelium and submucosa causing ROS generation. In the “primary damage response” stage, DNA breaking activates intracellular pathways that in turn switch on transcription factor as p53 and nuclear factor κB (NF-κB). NF-κB is able to up-regulate about 200 different genes, among which, B cell lymphoma 2 associated X protein (BAX) that possesses pro-apoptotic effect, and TNF-α, IL-1β, IL-6 that present pro-inflammatory activities: their presence decrements oxygenation and produces early destruction of connective tissue and endothelium leading to death of epithelial basal cells. In fibroblast CRT promotes metalloproteinases secretion that amplifies the damage at the sub-epithelial matrix and basement membrane. In the “signal amplification” stage, the molecules and cytokines produced in the early phases provide a positive feedback that extends the primary damage; TNF-α for example can activate mitogen-activated protein kinase (MAPK) signaling, finally resulting in caspase 3 activation and cell death. Until this stage clinically the patients do not present any symptoms. In the “ulceration” stage, the loss of mucosal integrity occurs, and the lesions are prone to bacterial

colonization. The microorganisms can penetrate through the injury and promote further inflammation and infiltration of mononuclear immune cells. Moreover, since CRT impacts negatively on cells in rapid division, as immune cells, OM patients are often immunocompromised and more susceptible to infections. In the "healing" stage migration, proliferation and differentiation of epithelial cells heal the wound. Healing is generally spontaneous at the end of CRT, however it depends on the type of cancer treatments followed by the patients [reviewed by [Sonis, 2004]].

When OM lesions are clinically visible the patients experience painful sensations and various daily activities such as speaking, swallowing and chewing are affected. Patients often report difficulties in eating and drinking, needing in some cases of parental nutrition [reviewed by [Sonis, 2004]]. Therefore, OM impacts negatively on the quality of life of the affected patients and prejudices the adherence to the cancer regimens; moreover, the most severe situations require the reduction or the suppression of the CRT, leading to serious outcomes associated to increased risk of morbidity and mortality [reviewed by [Sonis, 2004]].

The extent of OM is commonly classified using the common toxicity criteria (CTC) by World Health Organization [World Health Organization, 1979] which are reported in table 1.

Grade 0	**Grade 1**	**Grade 2**	**Grade 3**	**Grade 4**
None	Erythema of the mucosa; asymptomatic or mild symptoms; normal diet	Patchy ulcerations; pseudomembranes; moderate pain; not interfering with oral intake; modified diet indicated	Confluent ulcerations or pseudomembrane; bleeding with minor trauma; severe pain; interfering with oral intake	Tissue necrosis; significant spontaneous bleeding; life-threatening consequences

Table 1. CTC scale by WHO (1979)

As above mentioned, OM can be associated with opportunistic infections, really, the CRT can alter the normal oral microflora, allowing some species to proliferate and cause oral infections, moreover, micro-organisms can penetrate through the oral ulcerations leading to systemic infections. Furthermore, the use of antimicrobial prophylactic drugs [reviewed by [Donnelly et al., 2003]] and the immunosuppression of the patients can exacerbate this condition and aggravate the risk of infections [reviewed by [Donnelly et al., 2003]]. The neutrophils depletion renders patients more susceptible to bacterial infection, instead the lymphocytes deficiency to fungal and viral infections [reviewed by [Lerman et al., 2008]].

In OM, oral infections from bacteria, fungi and virus were reported, the most common are: *viridans Streptococci, E. coli, K. pneumoniae, Enterobacter sp., P. aeruginosa, S. aureus, S. epidermidis, Candida sp., human herpes viruses (herpes simplex 1,2, varicella zoster virus, Epstein Barr virus, Cytomegalovirus), Papillomaviruses.* Sometimes these infections could also cause systemic fatal diseases if not properly prevented, indeed, antibacterial, antifungal and antiviral prophylaxis are the treatments of choice in the most severe cancer conditions [reviewed by [Donnelly et al., 2003; Lerman et al., 2008]].

To date, no treatment or therapy can prevent the arise of OM, but there exist only palliative drugs that can alleviate the symptoms [reviewed by [Sonis, 2004]].
The Multinational Association of Supportive Care in Cancer / International Society of Oral Oncology (MASCC/ISOO) guidelines recommend and suggest the use of oral care protocols, oral cryotherapy, recombinant keratinocytes growth factor-1, benzydamine mouthwash, zinc supplement, meanwhile for pain control, morphine, fentanyl, doxepin are indicated [Migliorati et al., 2013; Lalla et al., 2014]. Thus, OM, itself and for its medical consequences, impacts on the resources of health systems, and the research in this field with the introduction of other types of interventions is warranted by the clinical community.
In this framework, for its characteristics, PBM is universally considered a helpful type of approach for the management of OM. Indeed, PBM with its bio-stimulant effects is able to promote the wound healing of the ulceration, to reduce the inflammation, and to alleviate the pain sensation [reviewed by [de Freitas, and Hamblin, 2016]]. Tissue regeneration induced by PBM includes different cellular aspects, PBM increases ATP production and cell proliferation of both keratinocytes and fibroblasts *in vitro* [AlGhamdi et al., 2012], reduces the gene expression of NF-κB [Curra et al., 2015] and the neutrophils' infiltrate [Lopes et al., 2010] in OM hamster animal model, increments the angiogenesis, especially eliciting arterioles formation in mice [Ottaviani et al., 2013], slows nerve conduction velocity in peripheral nerves in humans [reviewed by [Chow et al., 2011]].
Based on the *in vitro* and *in vivo* studies conducted so far, and on the metanalysis recently published [Oberoi et al., 2014; He et al., 2018], the MASCC/ISOO in its last guidelines recommended PBM for the prevention of oral mucositis (OM) in adults [Migliorati et al., 2013; Lalla et al., 2014], and in children it was successful used both in the prevention [He et al., 2018] and in the lesions care [Chermetz et al., 2014; Gobbo et al., 2018; He et al., 2018].
He et al. [He et al., 2018] conducted an exhaustive metanalysis on the use of PBM with red and NIR wavelengths in young patients. They showed that, when prophylactic PBM is applied concomitant with the first day of CRT and kept on every day, the irradiation treatment reduces

the risk of developing OM of grade 3 or higher, decrements the severity of the condition when occurs, and fasters the healing (from 4 days to 2) [He et al., 2018]. Instead, when PBM is utilized as a therapeutic intervention when OM manifests itself for 4 consecutive days, PBM at the 7th day reduces the severity of OM, the duration (from 9 days to 6), and pain [He et al., 2018]. Intriguingly, the visual analogue scale (VAS) score for pain showed a major reduction of VAS with preventive PBM respect to therapeutic PBM [He et al., 2018].

Objectives

Nowadays, an efficacious remedy for oral mucositis (OM) is still missing and the current treatments are only palliative to cure the symptoms [reviewed by [Miller et al., 2012]].

Considering the bio-stimulant effects of laser light, photobiomodulation (PBM) should be a valid alternative supportive treatment to manage OM lesions in children and adults. We decide to focus our attention on pediatric patients where the pathology needs to be carefully managed by clinicians. Really, childhood is an age that requires particulate attention, since cancer therapies could affect negatively nutrition and growth, furthermore, the necessity of cancer treatment reduction for the worsening of the daily activities of patients should be considered [reviewed by [Bryant, 2003]].

PBM is painless, not invasive, without side effects and rapid, and could be particularly indicated for these patients.

Moreover, after the first expense for the device and personnel training it has no other operative cost, therefore, PBM utilization could reduce the economic charge of drugs, such as analgesic, antibiotics and parenteral nutrition.

Nevertheless, at the moment the PBM utilization remains controversial for two main issues.

On the one hand, there is not a universal agreement regarding the most efficacious protocol, really, the parameters of irradiation vary a lot between the different studies in terms of wavelength (or combination of different wavelengths), irradiance, power, energy, fluence employed. Moreover, the application can be repeated at different intervals and this enlarges the possible options of treatment that clinicians can apply to the patients. Therefore, the infinity possibility of dosimetry afforded by PBM renders difficult to obtain a consensus between different centers [reviewed by [Avci et al., 2013]].

On the other hand, although the photoreceptors and the pathways activated were largely analyzed, some uncertainties remain about the mechanisms of action of laser light, and about the link between intracellular changes and the final outcome in the human organism [reviewed by [Avci et al., 2013]].

The biphasic dose response is another emblematic issue that should be taken into account: too low dose of PBM could result in a less effectiveness and there could be not response to stimulation, meanwhile too high dose could cause the crossing through the threshold of stimulation leading to inhibition [reviewed by [Huang et al., 2009; Huang et al., 2011]].

Therefore, a deep overview of the PBM mechanisms of actions is still needed.

This research aims at:

- Exploring the PBM effect on oxidative stress on salivary total oxidant status in OM patients and in an *in vitro* cellular model of skin keratinocytes 5-fluorouracil treated mimicking OM. Evaluating also the general effect of PBM on OM condition.
- Investigating the repercussion of PBM on β-defensins protein production in saliva from OM patients and on gene expression of innate immunity molecules in a cellular model of oral mucosa.
- Analyzing the analgesic action of PBM on OM patients, in an *in vitro* cellular model of primary murine sensory neurons from dorsal root ganglia, studying mitochondria parameters, and *in vivo* in a behavioral murine model of nociception.
- Inquiring the anti-bacterial activity of blue PBM on *Pseudomonas aeruginosa in vitro,* trying to understand the mechanism of action of blue light and *in vivo* in a murine model of skin abrasion infection.
- Researching the anti-viral properties of blue PBM in an *in vitro* model of human keratinocytes infected with Herpes Simplex Virus type 1.

The final outcome of the current study is to extend the knowledge in the field of PBM in order to permit the optimization of the PBM protocols in the clinical practice. Often the PBM usage is quite empirical, “it works” but the question “how it works” still needs to be clarified in detail. Indeed, a better comprehension of PBM mechanism of action can be useful for a conscious and justified usage of PBM for routinely clinical employment and for amplifying the possible medical applications based on laser light.

Laser Irradiation

The PBM treatments were performed using two types of class IV diode lasers presenting gallium aluminum arsenide (GaAlAs) as active lasing medium (K-laser d.o.o., Sežana, Slovenia) (figure 6 A). One is the K-Laser Blue Med and the other the K-Laser Cube 4. The first emits wavelengths at 970, 660, 445 nm the other at 970, 905, 800, 660 nm. The laser source is composed by equal diodes, that emit a laser field with an equal distribution of irradiance. The devices present a handpiece that can be connected with a zoom tip that permits to irradiate area of 5 cm^2 or with an ENT tip to irradiate small areas of about 1 cm^2 (figure 6 B and C respectively). Moreover, a dedicated programmable prototype robot-scanner (figure 6 A) equipped with a specific optic fiber output (figure 6 D) to allow a uniform and reproducible irradiation to multiwell plates was employed, specifically provided by K-Laser company and carefully calibrated by its engineers (K-laser d.o.o., Sežana, Slovenia) (figure 6 A).

The power was quantified using the power-meter instrument (LaserPoint Plus+, Vimodrone, Milan, Italy) meanwhile the thermal monitoring was measured using the FLUKE Ti20 thermal imager infrared camera (Everett, Washington, U.S.A.).

Class IV laser instrument are those devices that exceed 0.5 W of power, thus, they can cause eye damage for a direct, indirect or diffuse beam viewing [K-laser instruments datasheet]; both operator and patients wore protective glasses during the laser application.

The irradiation was conducted in light condition as dark as possible to avoid interference from environmental light. During irradiation the lid of the plates were opened to avert plastic light diffraction and the tip was positioned perpendicularly over the wells with a beam able to cover completely the well. To prevent the laser light absorption, in the *in vitro* experiments the medium of cell culture was without phenol red, meanwhile in the *in vivo* experiments on C57BL/6 mice (presenting black hair) the back was shaved.

The protocols employed combined irradiance 0.1-1 W/cm^2, fluence 6-120 J/cm^2, in pulsed modalities or continuous wave. The specific protocols employed were defined in each section.

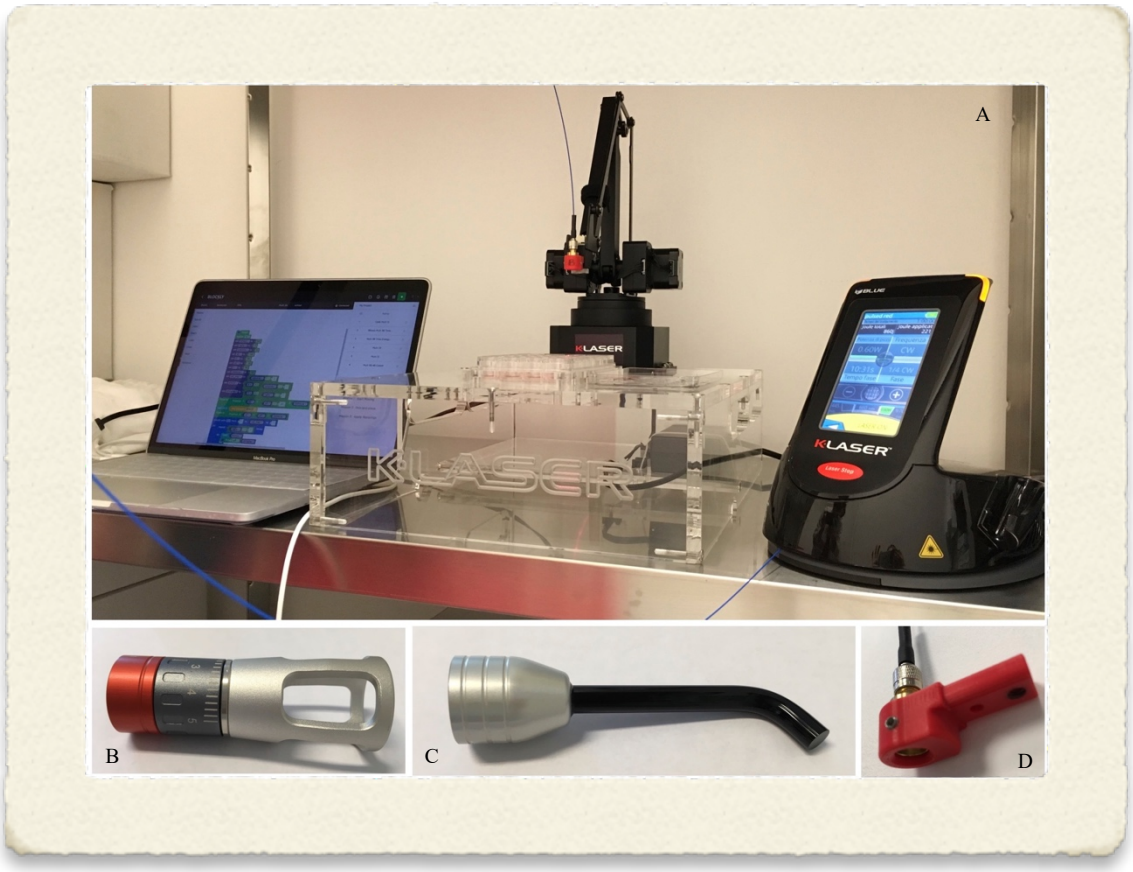

Figure 6. The equipment used in the experiments.

A The laser device (on the right) and the scanner (in the middle) employed in the experiments

The tip used in the irradiation: the zoom (B), the ENT (C) and the tip for the scanner (D).

Statistical Analysis and Figures

Apple inc. Keynote application version 8.3 (Cupertino, California, U.S.A.) was used to create the vector images.
Graphpad Prism version 7.0a (GraphPad Software, La Jolla, California, U.S.A.) was used for the statistical analysis and graphs creation.
The statistical tests employed were defined in each section.

Photobiomodulation Effect on Oxidative Stress in Oral Mucositis

In oral mucositis (OM) development, oxygen receive species (ROS) play a fundamental role. In the first phase of OM, chemo-radiotherapy (CRT) induces both DNA and non-DNA damage leading to the production of localized ROS [reviewed by [Sonis, 2004]], especially superoxide O_2^-, probably generated by mitochondria from neutrophils migrating to the site of injury [Lee et al., 2000]. When ROS levels exceed cellular antioxidant mechanisms, the oxidation of protein, cytokines, lipids and DNA initiate the damaging pathways that lead to mucosa destruction. These events drive to the second phase of OM, with the activation of transcription factors, as nuclear factor kappa-B (NF-κB) that in turn impacts on different genes and on the production of pro-inflammatory cytokines [reviewed by [Sonis, 2004]].
Different chemotherapic drugs, as for example 5-fluorouracil (5-FU), were reported as deleterious for oral mucosa causing OM [Sung et al., 2017]. 5-FU is a fluoropyrimidine and acts as a thymidylate synthase inhibitor resulting in a decrement of thymidine monophosphate, one of the three nucleotides that form thymine [reviewed by [Longley et al., 2003]]. 5-FU generates ROS in biological system, and this action can be related to the antitumoral activity of the drug [Matsunaga et al., 2010].
In a hamster model of OM, 5-FU increased the level of malondialdehyde, a marker of lipid peroxidation, in the pouch region affected by OM and incremented ROS measured using an *in vivo* L-band electron spin resonance ESR technique. The authors suggested that OM presents an acute inflammation that exacerbates the oxidative stress at level higher respect those that organism can counteract [Yoshino et al., 2013].

Photobiomodulation (PBM) is a therapy currently used for the treatment of OM patients. Indeed, Oberoi et al., in a meta-analysis, highlighted the beneficial effects of PBM (at red wavelength) on OM as prophylactic treatment: PBM reduced the grade of severity and the duration of OM grade 3 or 4 [Oberoi et al., 2014]. Similar results were reported in another meta-analysis conducted on children where both red and near infrared (NIR) wavelengths were considered [He et al., 2018]. However, the experience in PBM of the Division of Oral Medicine and Pathology of "Maggiore" Hospital in Trieste (Italy) showed that PBM was also efficacious as a cure when the lesions occur [Chermetz et al., 2014; Ottaviani et al., 2013; Gobbo et al., 2018]. The advantages observed are probably due to the anti-inflammatory and analgesic action of PBM together with the increased vascularization and the wound healing of the tissue [reviewed by [Bensadoun, and Nair, 2012]]. These effects are clearly visible when the OM patients manifest the ulcerations, as well as when the OM is at the first stage and the injury is present but not

clinically evident. Another possible complementary action could be due to detoxification or reduction of free radicals caused by CRT [reviewed by [Bensadoun, and Nair, 2012]].
In fact, PBM was able to reduce oxidative stress in primary neurons treated with hydrogen peroxide, cobalt chloride and rotenone [Huang et al., 2013], in neural cells exposed to oxidative stress PBM increased the viability [Giuliani et al., 2009], meanwhile in $CoCl_2$-induced hypoxic human umbilical vein endothelial cells PBM decreased ROS increasing cell viability [Lim et al., 2011]. Moreover, PBM was able to reduce oxidative stress *in vivo* in skin wound in normal [Silveira et al., 2011] and diabetic [Tatmatsu-Rocha et al., 2016] mice.

This work aims at investigating the effect of PBM on oxidative stress both *in vivo* and *in vitro.* The total oxidant status (TOS) assay was used to check the oxidative stress on cancer patients affected by OM before and after PBM, moreover, the PBM effect on clinical and subjective parameters was assessed. Finally, an *in vitro* OM model was developed treating human keratinocytes with 5-FU: the ROS level and the expression of two antioxidant genes (*SOD2* and *HMOX1*) after PBM were evaluated.

Materials and Methods

Study Population

A total of 10 patients affected by OM were enrolled at the Division of Oral Medicine and Pathology of "Maggiore" Hospital in Trieste (Italy).
Inclusion criteria: age between 40-95 years old, diagnosis of hematological tumor or solid cancer, presence of OM from grade 2 to grade 4 [World Health Organization, 1979] related to ongoing chemotherapy and/or radiotherapy, patients' availability for 5 consecutive days (4 laser sessions and 1 follow up recall).
Exclusion criteria will be: OM already treated by PBM therapy, smokers, uncontrolled or severe periodontal disease, patients' application of topical oral medications, systemic corticosteroids and anti-inflammatory assumption.
During the first visit at day 0, the clinicians registered information about patients' clinical history and scored OM severity according to the common toxicity criteria (CTC) scale, considering ulceration and erythema distribution and size [World Health Organization, 1979]. Voice alteration, swallowing and chewing difficulties were also recorded. The patients were then treated with PBM, at days 0, 1, 2, 3, according to clinical protocols (λ 970 nm, 200 mW/cm^2, 6 J/cm^2, in continuous wave, CW) [Ottaviani et al., 2013; Ottaviani et al., 2016] by a specialized team of

pathologists. A rotatory motion was used all over the oral cavity to cover both ulcerated and healthy areas, keeping a 3-cm distance between the laser probe and the tissue.

Irradiation time was calculated considering a mean oral mucosa surface area of 215 cm^2 [Collins, and Dawes, 1987]. Moreover, photographs of affected areas will be taken at each session.

Unstimulated saliva samples were collected for 5 minutes before and immediately after each PBM treatment and at day 4. Patients were asked to fast for at least 2 hours before sampling, avoiding tooth brushing, excess alcohol intake and physical activity since the previous evening. Patients rinsed the mouth with water for 1 minute and then spit saliva for 5 minutes in a sterile collection tube.

The samples were centrifuged for 10 minutes at 10000 xg and the supernatants were than collected and stored at -80°C before analysis.

All subjects signed an informed consent to participate in the study and all the research experiments were performed in agreement with ethical standards of the 1975 Declaration of Helsinki (7^{th} revision, 2013).

The schematic representation of the clinical study design is reported in figure 7.

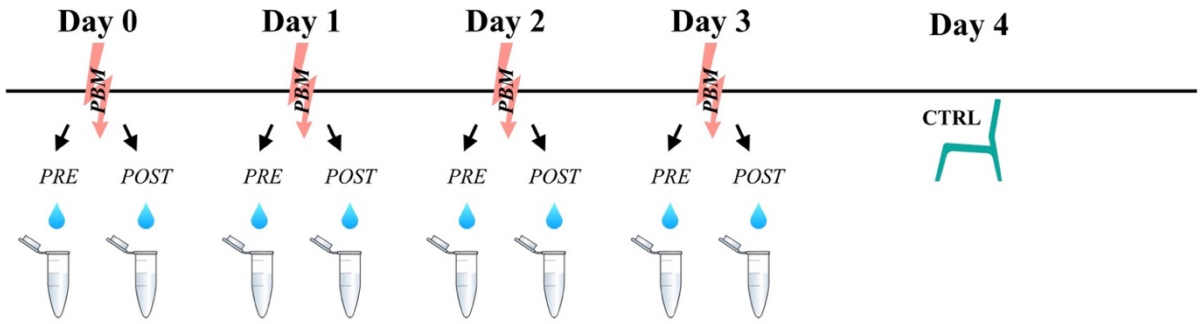

Figure 7. Schematic representation of the study design in oral mucositis patients.

Total Oxidant Status

TOS, as a marker of oxidative stress, was evaluated in saliva from the 10 OM patient enrolled in the study using an already established method by Erel [Erel, 2005].This method is based on the principle that oxidant species present in the saliva oxidize the ferrous ion–o-dianisidine complex to ferric ion, creating a colored complex with xylenol orange in an acidic medium. Briefly, 225 µL of reagent 1 (xylenol orange 150 µM, NaCl 140 mM and glycerol 1.35 M in 25 mM H_2SO_4 solution, pH 1.75), were mixed with 35 µL of saliva, then 11 µL of reagent 2 (ferrous ion 5 mM and o-dianisidine 10 mM in 25 mM H_2SO_4 solution) were added. The solutions were mixed for 5 minutes and then the absorbance was read at 560 nm using a multi-well reader

spectrophotometer (Glomax multi+ detection system, Promega, Madison, Wisconsin, U.S.A.). The absorbance measured before mixing reagent 1 and reagent 2 was used as "blank". The assay was calibrated using standard solutions of hydrogen peroxide (H_2O_2). Each sample was measured in quadruplicate and are expressed as micromolar hydrogen peroxide equivalent per liter (µmol H_2O_2 equivalent/L).

Oral Mucositis Cellular Model

Human keratinocytes (HaCaT) were maintained in DMEM culture medium supplemented with 10% fetal bovine serum, 100 U/ml Penicillin/Streptomycin, 2 mM Glutamine (Euroclone, Pero, Milan, Italy). Cells were seeded one day prior to the experiment (10.000 cells/well in 96 multi-well plates and 50.000 cells/well in 24 multi-well plates). OM was mimicked treating HaCaT cells with 5-FU 0.1 mg/ml for 18 hours then the cells were treated with the following protocol: combined wavelengths λ 660, 800, 905 and 970 nm, peak power 0.25 W, 3 J/cm^2 in CW (λ 660 nm: 0.025 W/ cm^2, λ 800, 905 and 970 nm: 0.075 W/cm^2).

Oxidative Stress Assessment

After 24 hours from irradiation vitality of cells were measured using MTT (3-(4,5-dimethylthiazol-2-yl)-2,5-diphenyltetrazolium bromide) proliferation assay (Trevigen, Gaithersburg, Maryland, U.S.A.) to assess if the irradiation could rescue the viability of cells treated with 5-FU. This assay is based on the conversion of the water soluble MTT to an insoluble formazan that is then solubilized, and the concentration determined spectrophotometrically at 570 nm.

After 30' from irradiation the reactive oxygen species (ROS) production was measured using the using the cell-permeant 2',7'-dichlorodihydrofluorescein diacetate (H2DCFDA) dye (D399, Invitrogen, Thermo Fisher Scientific, Waltham, Massachusetts, U.S.A.) and then the fluorescence normalized on alive cells using the MTT Cell proliferation assay (Trevigen). H2DCFDA is a chemically reduced and acetylated form of fluorescein that is converted in the highly DCF by intracellular esterases and oxidation.

Additionally the transcription levels of two genes (*SOD2* and *HMOX1*) involved in oxidative stress [Miriyala et al., 2011; Wegiel et al., 2014] were measured using Taq-man™ probes (hs01110250_m1 and hs00167309_m1 respectively, Thermo Fisher Scientific) on Applied Biosystems 7900HT Fast Real-Time PCR System (Thermo Fisher Scientific) platform. Raw fluorescent data were collected and converted in fold-increase with the Relative Quantification manager software (Thermo Fisher Scientific) using the ΔΔCt method [Livak, and Schmittgen, 2001]. Untreated cells were used as references for comparisons.

Statistical Analysis

Friedman's test with the Dunn's test for multiple comparison were used to compare the changes over time in CTC score meanwhile Wilcoxon matched-pairs signed rank test was utilized to evaluate the TOS level pre and post PBM session at each day.

In the cellular experiments, Mann-Whitney test was employed to compare cell viability, ROS levels and gene expression between irradiated and not irradiated samples treated or not with 5-FU.

All statistical assessments were two-sided, and a p-value < 0.05 was used for the rejection of the null hypothesis.

Results and Discussion

Demographic and clinical characteristics of the 10 patients suffering OM are reported in table 2. Briefly, there were 2 women and 8 man, the age range was 44-92, 5 patients presented head-neck cancer, 2 gastrointestinal tumor, 2 hematologic malignancies and 1 breast cancer. Six patients were treated with chemotherapy, 2 with radiotherapy and 2 with a combination of the two remedies.

Patient	Age (years)	Sex	Type of tumor	Chemo/Radiotherapy
1	58	M	Gastro-intestinal	Chemotherapy
2	58	F	Breast	Chemotherapy
3	62	M	Head neck	Both
4	92	F	Head neck	Radiotherapy
5	74	M	Hematological	Chemotherapy
6	56	M	Head neck	Chemotherapy
7	65	M	Gastro-intestinal	Chemotherapy
8	44	M	Hematological	Chemotherapy
9	69	M	Head neck	Both
10	71	M	Head neck	Radiotherapy

Table 2. Clinical characteristics of the 10 oral mucositis patients.

PBM treatment improved patient' clinical condition, reducing the CTC scores over time (Friedman's test p-value = 0.003; figure 8 A) and also other subjective parameters (i.e. swallowing, chewing and speaking) (Figure 8 B, C, D).

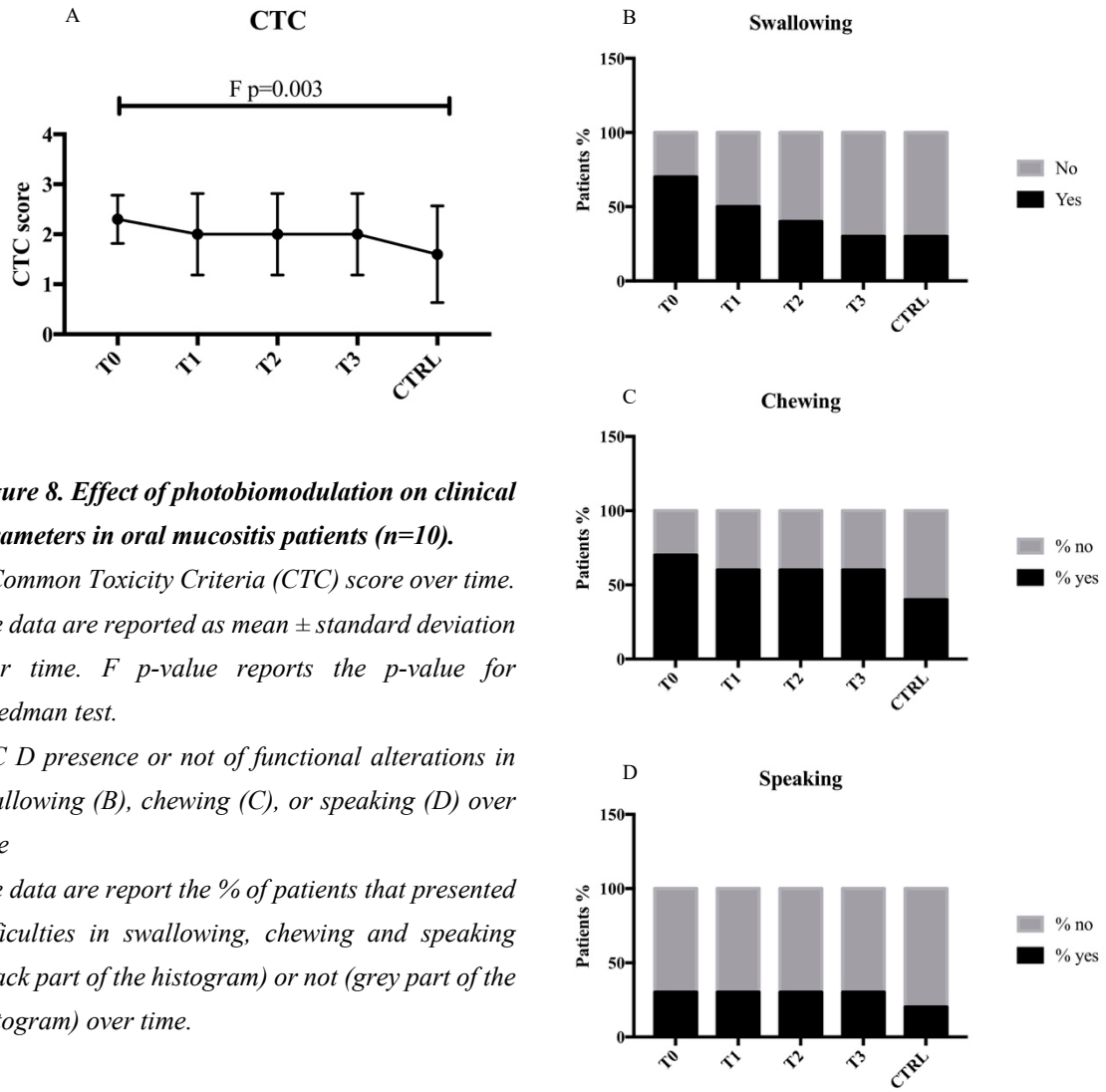

Figure 8. Effect of photobiomodulation on clinical parameters in oral mucositis patients (n=10).

A Common Toxicity Criteria (CTC) score over time. The data are reported as mean ± standard deviation over time. F p-value reports the p-value for Friedman test.

B C D presence or not of functional alterations in swallowing (B), chewing (C), or speaking (D) over time

The data are report the % of patients that presented difficulties in swallowing, chewing and speaking (black part of the histogram) or not (grey part of the histogram) over time.

In figure 9 are reported four examples of OM lesions pre PBM and the outcome at the control day in different oral district in patient number 1, 5, 6 and 7: it was possible to observe a visible improvement of the clinical conditions with the healing of the ulcerations and an amelioration of the inflamed area (characterized by reddening) that reduced significantly at the control day.

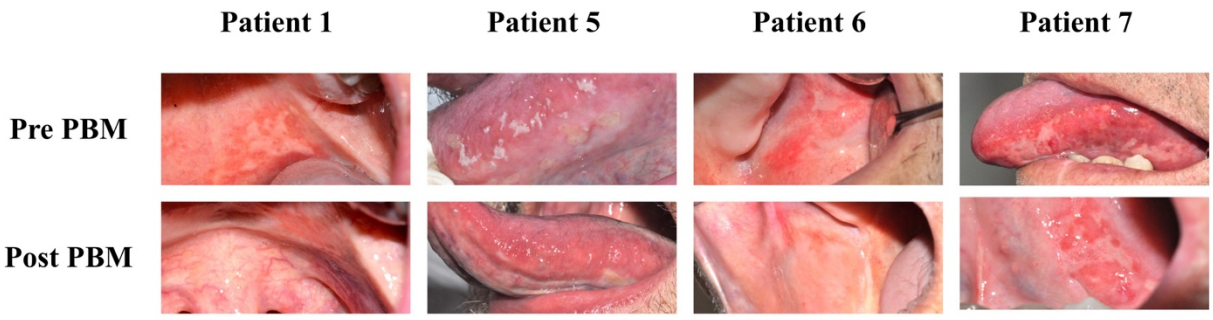

Figure 9. The beneficial effect of photobiomodulation on oral mucositis condition.
Oral mucositis (OM) lesions pre photobiomodulation (PBM) treatment (first line) and post PBM treatment (second line) in four OM patients recruited in the study.

The thermal monitoring was performed initially, during and at the end of the treatment; the temperature registered were 37.0°, 39.5° and 40.2°C respectively: the increased of the temperature was minimal and in the physiologic range not causing thermal injury (figure 10).

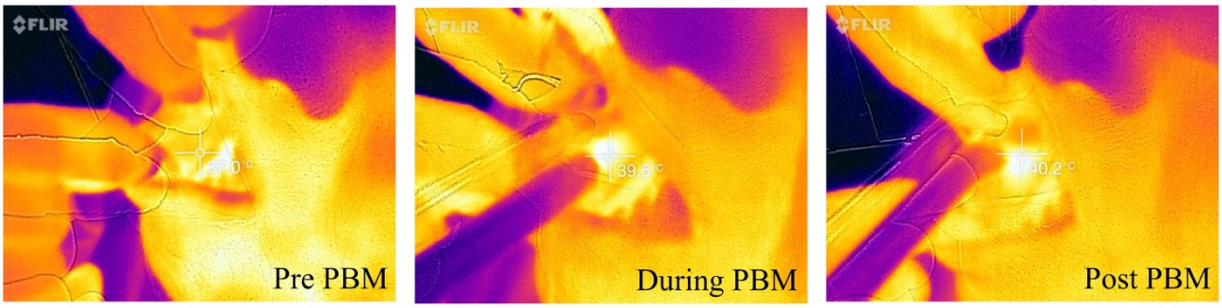

Figure 10. Thermal monitoring during irradiation.
Pretreatment, during irradiation and the end of the photobiomodulation (PBM) therapy.

Our results confirmed and corroborated the previous findings [Ottaviani et al., 2013; Chermetz et al., 2014] regarding the beneficial effect of PBM on OM status, indeed, the improving of patients' condition highlighted the possibility to use PBM also when the lesions manifested. Indeed, in the clinical practice could be sometimes difficult to program the treatment contemporaneously with the cancer therapy or prior to it as the MASCC/ISOO guidelines recommended [Migliorati et al., 2013; Lalla et al., 2014], taken into account also that in some

(although rare) case OM did not happen. Therefore, proving the effectiveness of PBM as a cure and not a prophylaxis is an important goal of our research.

Since as above described, ROS could both initiate the oral damaging and propagate it, a therapy that could partially counteract this event is worthy of consideration.
In our experiments, at day 0, oxidative stress did not change after PBM, meanwhile in the following days, ROS levels decreased after each PBM session (Wilcoxon matched-pairs signed rank test p-value = 0.03 for T1, p-value = 0.006 for T2 and p-value = 0.04 for T3), but increased again during the following 24 hours, as well as at day 5 (CTRL). So, PBM was so able to reduce oxidative stress after each treatment but it did not maintain its effect over time.
Anti-oxidants were not included in the treatment for OM by MASCC/ISOO for inconsistent or conflicting results [Migliorati et al., 2013; Lalla et al., 2014], however, this is the first time that PBM anti-oxidant effect was proven on OM patients and it can endorse its use also for this purpose.

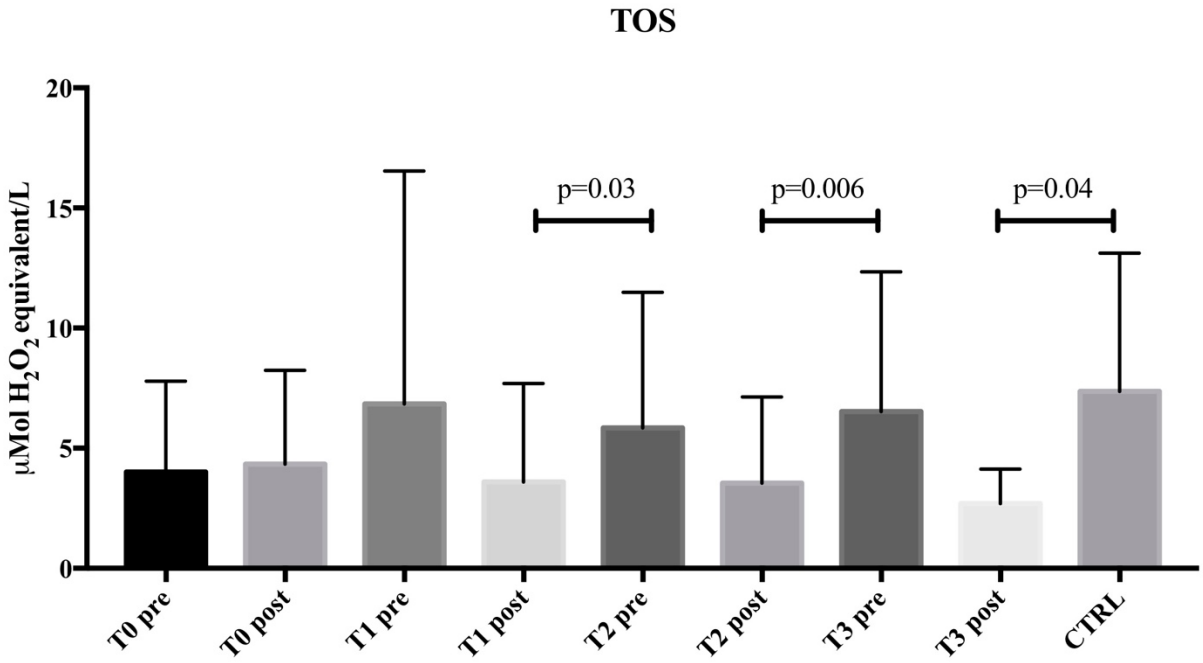

Figure 11. Total Oxidant Status (TOS) levels in the oral mucositis patient saliva during the photobiomodulation (PBM) sessions (n=10).

Data are reported as µMol H_2O_2 equivalent/L and are represented as mean ± standard deviation over time.
P reports the p-value from Wilcoxon matched-pairs signed rank test testing TOS pre PBM versus TOS post PBM each day.

In the *in-vitro* model the 5-FU treatment was chosen to mimic the OM condition, indeed 5-FU is widely used as anti-neoplastic drug, inducing cell apoptosis through different mechanisms such as mitochondria oxidative stress [Bomfin et al., 2017]. After 18 hours, 5-FU treatment dramatically reduced the viability of cells that was recovered by PBM irradiation (from 31% of alive cells to 62%; Mann-Whitney test, p-value = 0.005, figure 12 A).

The ROS production was also increased after the 5-FU treatment and significantly decreased after PBM (Mann-Whitney test, p-value = 0.05, figure 12 B). Moreover, the ROS level in the irradiated cells (without drug administration) was significantly less respect to the not irradiated cells (Mann-Whitney test, p-value = 0.01, figure 12 B).

The pharmacologic treatment increased the gene expression of both *SOD2* and *HMOX1* genes and PBM was able to decrement the mRNA levels of both genes (Mann-Whitney test, p-value = 0.03 for both genes, figure 12 C and D), even in absence of drug administration (Mann-Whitney test, p-value = 0.03 for both genes, figure 12 C and D).

SOD2 and *HMOX1* genes encode for mitochondrial superoxide dismutase 2 and heme oxygenase 1 respectively, two molecules involved in the cellular response to oxidative stress, the first at mitochondrial level [reviewed by [Miriyala et al., 2011]] detoxified O_2^-, the second in the cytosol [reviewed by [Wegiel et al., 2014]].

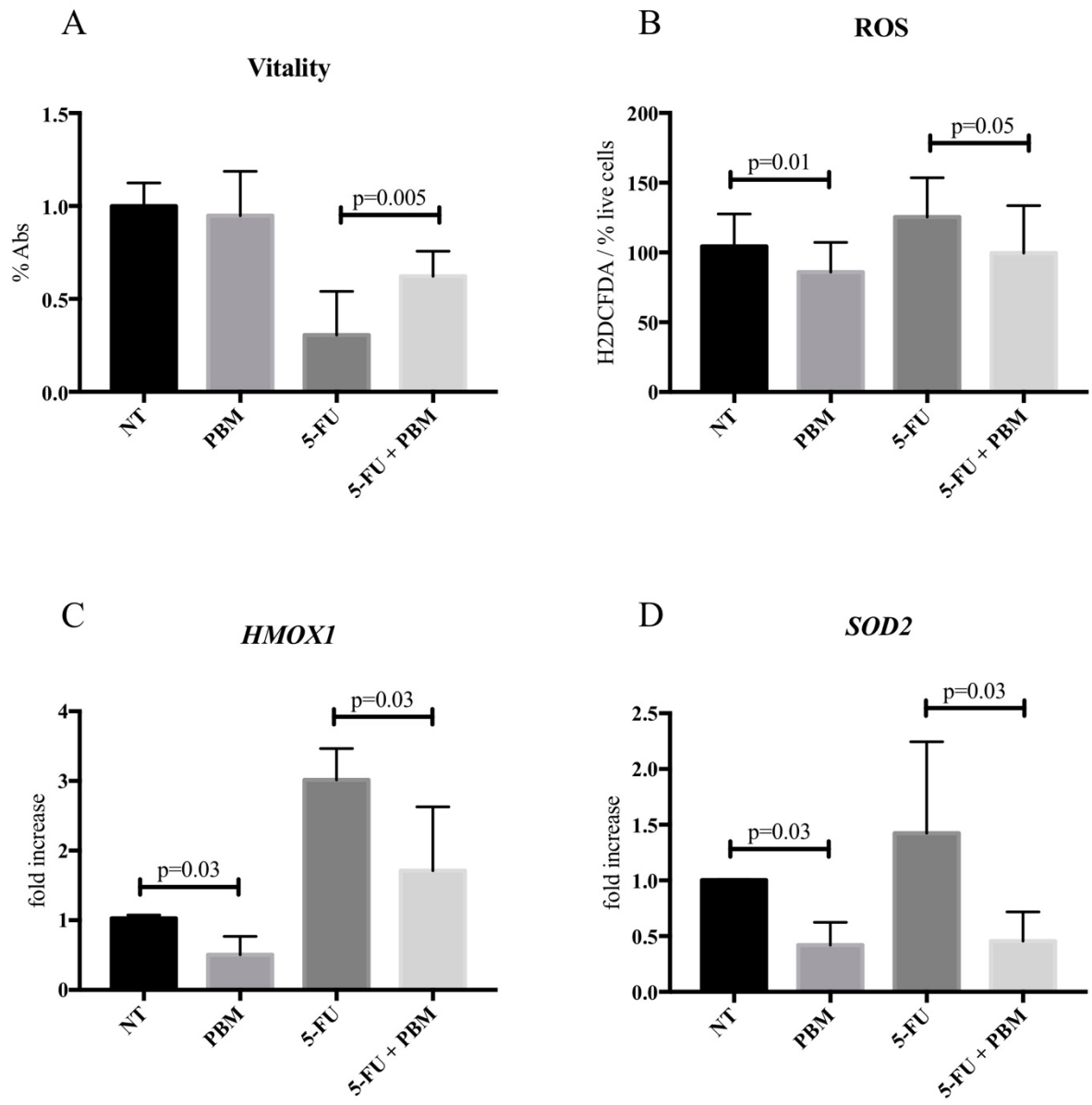

Figure 12. Photobiomodulation (PBM) effect on oxidative stress in an in vitro model of oral mucositis.

A Vitality of cells treated with PBM (designed as PBM), 5-fluorouracil (designed as 5-FU) or 5-fluorouracil plus PBM (designed as 5-FU + PBM) after 24 hours from irradiation. The data are reported as percentage of absorbance respect to not treated cells. The experiments were performed in 8 replicates in two independent days.

B Production of reactive oxygen species in 5-fluorouracil (designed as 5-FU) treated cells and not treated cells (designed as NT) and after laser therapy (PBM) in both 5-FU treated (designed as 5-FU + PBM) and not treated cells (designed as PBM). The results are reported as H2DCFDA fluorescence on percentage of alive cells. The experiments were performed in 16 replicates in two independent days.

C and D gene expression of HMOX1 and SOD2 (respectively) in 5-FU treated (designed as 5-FU) cells and not treated cells (designed as NT) and after laser therapy (PBM) in both 5-FU treated (designed as 5-FU + PBM) and not treated cells (designed as PBM). The results are reported as fold increase respect to NT cells. The experiments were performed in 4 replicates in two independent days

All the results are reported as mean ± standard deviation.

P-value reports the results of Mann-Whitney test.

Our results confirmed previous literature data on the beneficial effects of PBM on induced oxidative stress in different models.

In primary cortical neurons PBM at 810 nm reduced ROS level when the neurons were treated with oxidant reagents [Huang et al., 2013]. On the contrary, other authors showed that PBM at 810 nm could lead to ROS increment through the nuclear factor kappa B (NF-κB) activation in murine embryonic fibroblast [Chen et al., 2011].

PBM at 904 nm was able to reduce thiobarbituric acid reactive substances (TBARS) in the wounded skin of diabetic mice, however the authors observed also an increment in TBARS in irradiated controls respect to not irradiated controls [Tatmatsu-Rocha et al., 2016]. Moreover, PBM at 904 nm reduced the inducible nitric oxide synthase expression and NF-κB pathways, in traumatized murine muscle [Rizzi et al., 2006].

From these data it can be evinced that PBM is more efficacious when the system is under some type of stress respect to normal condition where the PBM effects seemed to be the opposite [reviewed by [Chung et al., 2012]].

Nevertheless, in our *in vitro* model a decrement of markers of oxidative stress (i.e measured through H2DCFDA and *SOD2* and *HMOX1* gene expression) was observed both under normal condition and when 5-FU, an agent capable to promote oxidative stress, was added. This result could be explained with the different cell lines employed in the studies, indeed it has been seen that PBM effect varies a lot in different type of cells, maybe due to the intrinsic cellular characteristics.

This is the first study that observed and confirmed the PBM positive effect on oxidative stress both *in vivo* on patients and *in vitro* on 5-FU treated keratinocytes.

Innate Immunity-Modulatory Effect of Photobiomodulation Therapy on Epithelial Cells

Innate immunity system is considered the first line of defense of human organism, indeed , it is crucial in the fighting against pathogenic microorganisms and for infection eradication, however it is also a regulator of inflammation, so its dysfunctions could be involved in different inflammatory conditions [reviewed by [Turvey, and Broide, 2010]]. The components of innate immunity are commonly activated by microbial molecular structures, called "pathogen associated molecular patterns" (PAMPs) or by molecule released during tissue injury, called "damage-associated molecular patterns" (DAMPs) [reviewed by [Turvey, and Broide, 2010]].

Among the innate immunity members, inflammasomes represent a form of protective response against harmful stimuli, as microorganisms and tissue stressors. Firstly, inflammasome sensor molecules, such as NLRP1 (NACHT, LRR and PYD domains-containing protein) and NLRP3, recognize PAMPs or DAMPs; then, they activate intracellular pathways that lead to the activation of Caspase 1 that in turn cleaves pro Interleukin (IL)-1β, a pro-inflammatory cytokine, activating it [reviewed by [Latz et al., 2013]].

Other innate immune system components are the antimicrobial peptides (AMPs) that can be activated by PAMPs/DAMPs and they support the first line of host defense especially at mucosa level, such as the oral mucosa [reviewed by [da Silva et al., 2012]]. Among them, the β-defensins (hBD) are widely studied; in oral mucosa hBD-1 is constitutively expressed, while hBD-2 and hBD-3, are inducible by pro-inflammatory stimuli and bacteria [reviewed by [Dale, and Fredericks, 2005]]. Another AMP is the Cathelicidin LL-37 that is expressed by neutrophils and epithelial tissues especially in the oral cavity [reviewed by [da Silva et al., 2012]]. AMPs possess antibacterial activity, directly damaging pathogens' membrane but they are also able to stimulate innate and adaptive immunity [reviewed by [da Silva et al., 2012]].

Oral Mucositis (OM) is a pathologic condition driven by the chemo-radiotherapy (CRT) in oncologic patients. It develops in 5 phases: initiation, primary damage response, signal amplification, ulceration and healing [reviewed by [Sonis, 2004]]. It is clinically characterized by inflammatory lesions, specifically in the second OM stage, pro-inflammatory cytokines (e.g. Tumor Necrosis Factor α, IL-1β and IL-6) are produced due to the activation of NF-κB. Then, in the third OM phase, these molecules in turn amplify the original response in a positive-feedback loop leading to ulcerative injuries (i.e. the fourth OM phase) [reviewed by [Sonis, 2004]]. It has been also proposed an inflammasomes activation by CRT in the first phase of OM in parallel with reactive oxygen species (ROS) generation [reviewed by [Sonis, 2004; Sonis, 2007]].

Moreover, an exaggerated innate immune response could play a role as a key factor in the first OM stage, then it continues its contribution in the establishment of the OM condition [reviewed by [Sonis, 2004; Sonis, 2007]].
Possibly, CRT can induce the production of DAMPs yielding an inflammatory cascade that can lead to the mucosal damaging. Successively, the ulcerations can potentiate the sending of DAMPs, while the incoming infections produce PAMPs: these mediators further exacerbate the inflammatory condition [reviewed by [Sonis, 2004; Sonis, 2007]].

Photobiomodulation (PBM) possesses anti-inflammatory properties, enhancing microcirculation, edema re-absorption, lymphatic drainage, lymphocyte activation and macrophage phagocytic activity [Hawkins et al., 2005; Hawkins, and Abrahamse, 2005]. Moreover, it was reported that PBM in human keratinocytes reduced IL-1β and nerve growth factor (NGF) production meanwhile it increased IL-6; in murine macrophages stimulated with lipopolysaccharide (LPS), PBM reduced monocyte chemoattractant protein 1 (MCP-1), IL-1a, IL-1β, IL-6, and IL-10 expression [reviewed by [Peplow et al., 2011]].

In our study we considered the potential action of PBM in modulating mRNA expression of different molecules members of innate immunity system in TR146 epithelial cell line: *DEFB1*, *DEFB4*, *DEFB103, CAMP, CASP1, NRLP3, NLRP1, IL1B* genes encoding for hBD-1, -2, -3, Cathelicidin LL-37, Caspase 1, NRLP3, NLRP1, IL-1β proteins. Moreover, the salivary levels of hBD-1, hBD-2, hBD-3 were measured in OM patients treated with PBM.

Materials and Methods

Salivary Defensins Concentration

The salivary samples from OM patients submitted to PBM were used. Specifically, samples at day 0, before and after PBM, samples at day 3, after the last PBM, and samples at day 4, during patient follow up were analyzed. The specimens were diluted and defensins' salivary concentrations were measured in duplicate using the Human Beta Defensin 1, 2, 3 ELISA kit (Cat. No. 100-240-BD1, 100-250-BD2, 100-260-BD3 Alpha Diagnostic, San Antonio, TX, USA) following manufacturer's instructions. The absorbance was measured with labtech LT 4000 microplate reader (Sorisole, Bergamo, Italy) and the protein concentration was obtained using a standard curve.

TR146 Cellular Model

Cell line TR146 (derived from squamous oral mucosa carcinoma, ECACC catalogue number: 10032305) was used in the experiments [Rupniak et al., 1985].

Cells were irradiated 24 hours after seeding, using the following parameters: λ 660 nm, laser power 0.1 W, irradiance 50 mW/cm^2, fluence 3 J/cm^2, continuous wave (CW); λ 800 nm, 1 W, 0.5 W/cm^2, 20 J/cm^2, CW; λ 970 nm, 0.1 W, 50 mW/cm^2, 3 J/cm^2, CW. Cytotoxicity after PBM was measured using the ATPlite Luminescence Assay System (PerkinElmer, Waltham, Massachusetts, U.S.A.) and the MTT Cell proliferation assay (Trevigen, Gaithersburg, Maryland, U.S.A.) according to manufacturers' instructions.

Gene Expression Analysis

Total cellular RNA was extracted 30 minutes or 24 hours after PBM using RNAqueous®-Micro Kit Micro Scale RNA Isolation Kit (Thermo Fisher Scientific, Waltham, Massachusetts, U.S.A.) and retro-transcribed using High-Capacity cDNA Reverse transcription kit (Thermo Fisher Scientific). To quantify mRNA, Taq-man™ probes for *DEFB1* (Hs00608345_m1), *DEFB4* (Hs00608345_m1), *DEFB103* (Hs00218678_m1), *CAMP* (Hs00189038_m1) *CASP1* (Hs00354836_m1), *NRLP1* (Hs00248187_m1), *NRLP3* (Hs00366465_m1), *IL1B* (Hs01555410_m1) genes expression and β-Actin (as calibrator and reference, *ACTB*: Hs99999903_m1), were employed on Applied Biosystems 7900HT Fast Real-Time PCR System (Thermo Fisher Scientific) platform. Raw fluorescent data were collected and converted in fold-increase with the Relative Quantification manager software (Thermo Fisher Scientific) using the ΔΔCt method [Livak, and Schmittgen, 2001]. Untreated cells were used as references for comparisons.

Statistical Analysis

Kruskal Wallis test with Dunn's test for multiple comparison was used to evaluate the cytotoxicity of PBM irradiation compared to not irradiated cells.

Mann-Whitney test was employed to compare gene expression between irradiated and not irradiated samples treated or not with LPS.

All statistical assessments were two-sided, and a p-value < 0.05 was used for the rejection of the null hypothesis.

Results and Discussion

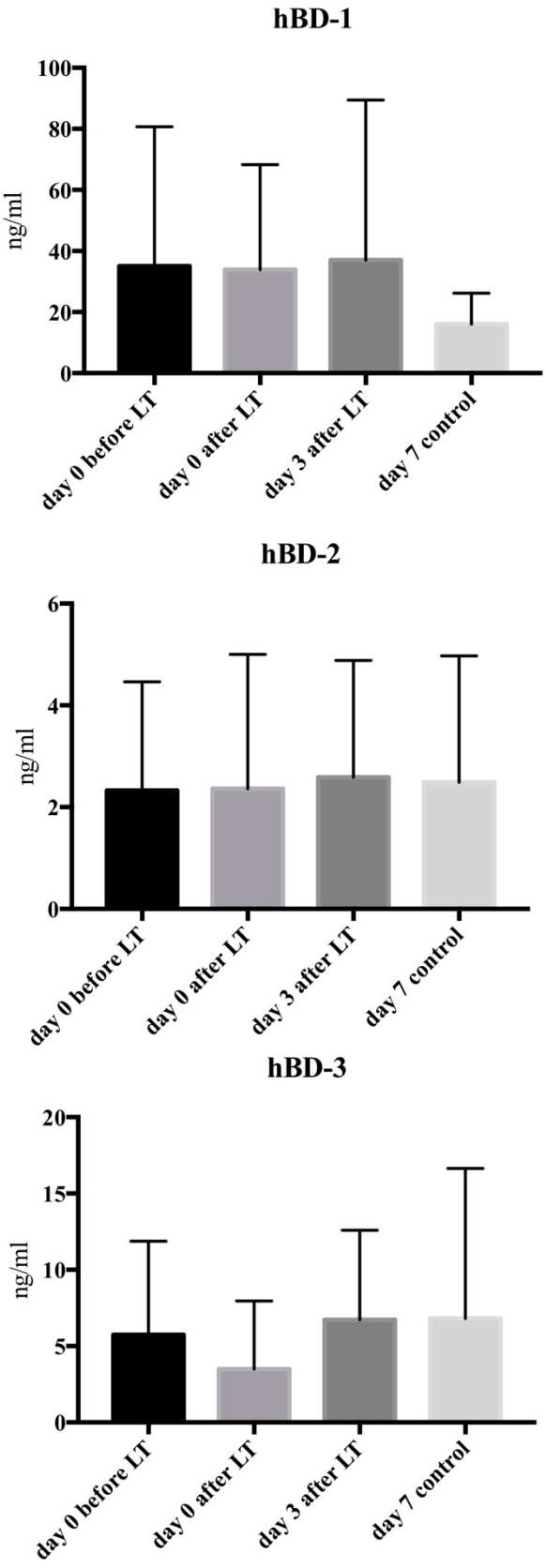

After measuring hBDs in saliva from OM patients, no statistically significant differences were detected comparing the different time points (T0 pre and post PBM, T3 post PBM, and control, figure 13 A, B and C), also when the patients were subdivided according with cancer diagnosis or oncological therapy followed. Considering patients singularly, some of them presented an increment, while others a decrement in defensins concentration suggesting an individual heterogeneous response to PBM.

Figure 13. hBDs concentration in saliva from oral mucositis patients (n=10).

A hBD-1 concentration (ng/ml)

B hBD-2 concentration (ng/ml)

C hBD-3 concentration (ng/ml)

The results are reported as mean concentration ± standard deviation.

Firstly, the cytotoxic effect of PBM was evaluated in the mucosal cell model. It increased the ATP content after 30 minutes from irradiation with all the three protocols (Kruskal Wallis test p-value=0.003; Dunn's test for multiple comparison p-value=0.02 for 970 nm, 0.05 W/cm^2, 3 J/cm^2, CW; p-value=0.03 for 800 nm, 0.05 W/cm^2, 20 J/cm^2, CW; p-value = 0.01 for 660 nm, 0.05 W/cm^2, 3 J/cm^2, CW, figure 14 A). Instead at 24 hours the protocol 800 nm, 0.5 W/cm^2, 20 J/cm^2, CW slightly decreased ATP content but increased MTT assay (ATP assay: Kruskal Wallis test p-value=0.001; Dunn's test for multiple comparison p-value=0.01; MTT assay: Kruskal Wallis test p-value=0.01; Dunn's test for multiple comparison p-value=0.04, figure 14 B and C). These data highlighted a precocious effect of PBM on ATP content after 30 minutes from irradiation, while at 24 hours only the protocol 800 nm, 0.5 W/cm^2, 20 J/cm^2, CW was able to maintain the effect, however the ATP content decremented and MTT assay increased possibly indicating the consumption of ATP caused by cellular metabolism. This was in line with previous article that showed a photochemical activity after illumination [AlGhamdi et al., 2012] and with our study on human keratinocytes [Tricarico et al., 2018].

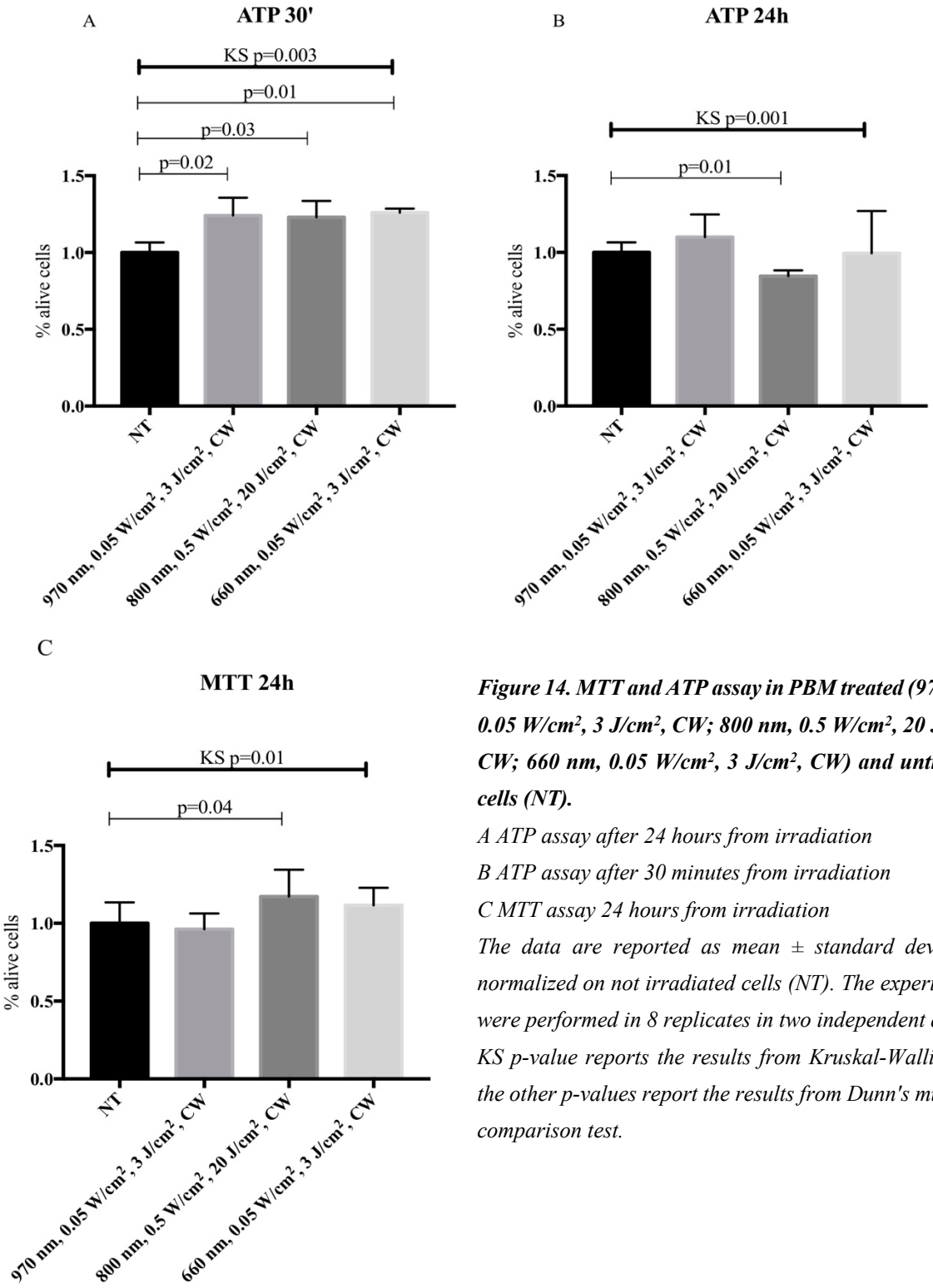

Figure 14. MTT and ATP assay in PBM treated (970 nm, 0.05 W/cm², 3 J/cm², CW; 800 nm, 0.5 W/cm², 20 J/cm², CW; 660 nm, 0.05 W/cm², 3 J/cm², CW) and untreated cells (NT).

A ATP assay after 24 hours from irradiation

B ATP assay after 30 minutes from irradiation

C MTT assay 24 hours from irradiation

The data are reported as mean ± standard deviation normalized on not irradiated cells (NT). The experiments were performed in 8 replicates in two independent days. KS p-value reports the results from Kruskal-Wallis test, the other p-values report the results from Dunn's multiple comparison test.

Then, the gene expression of the genes above cited were analyzed.

CAMP gene expression was not affected by irradiation with all the three protocols (figure 15).

DEFB1, *DEFB4* and *DEFB103* genes' expression after PBM did not present differences between irradiated and not irradiated cells 24 hours after PBM, with the exception of *DEFB103* (figure 16

A, B and C). When comparing the cells LPS-treated with them treated with LPS and irradiated with protocol 660 nm, 0.05 W/cm^2, 3 J/cm^2, CW, it was possible to observe a decrement in *DEFB103* expression (Mann-Whitney test p = 0.01, figure 16 C).
However, it is important to consider that only a little influence of LPS on AMPs gene expression was possible to observe.

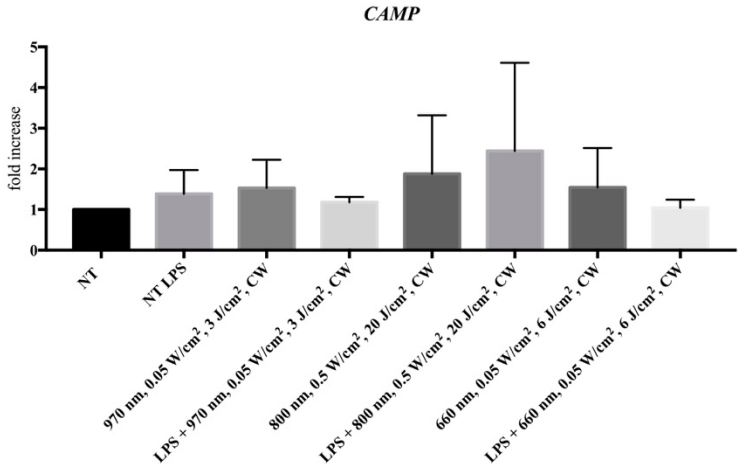

Figure 15. Fold decrease of CAMP gene expression 24 hours after photobiomodulation (PBM) in not irradiated cells (NT), cells treated with LPS (NT LPS), cells irradiated with three different protocols (970 nm, 0.05 W/cm^2, 3 J/cm^2, CW; 800 nm, 0.5 W/cm^2, 20 J/cm^2, CW; 660 nm, 0.05 W/cm^2, 3 J/cm^2, CW).
The data are reported (mean ± standard deviation) as fold increase compared to not irradiated cells. The experiments were performed in 4 replicates in two independent days.

Figure 16. (in the next page). Fold increase of defensins gene expression 24 hours after photobiomodulation (PBM) in not irradiated cells (NT), cells treated with LPS (NT LPS), cells irradiated with three different protocols (970 nm, 0.05 W/cm^2, 3 J/cm^2, CW; 800 nm, 0.5 W/cm^2, 20 J/cm^2, CW; 660 nm, 0.05 W/cm^2, 3 J/cm^2, CW) and cells treated with LPS for 24 hours prior to irradiation (designed as LPS + 970 nm, 0.05 W/cm^2, 3 J/cm^2, CW; LPS + 800 nm, 0.5 W/cm^2, 20 J/cm^2, CW; LPS + 660 nm, 0.05 W/cm^2, 3 J/cm^2, CW).
A DEFB1 gene expression
B DEFB4 gene expression
C DEFB103 gene expression
The data are reported (mean ± standard deviation) as fold increase compared to not irradiated cells. The experiments were performed in 4 replicates in two independent days.
P reports the p-value results from Mann-Whitney test.

A

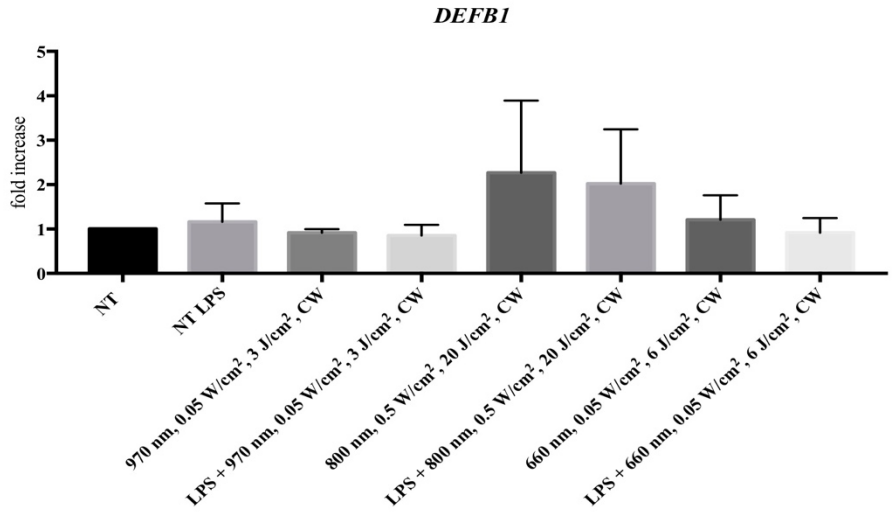
DEFB1
fold increase
0
1
2
3
4
5
NT
NT LPS
970 nm, 0.05 W/cm², 3 J/cm², CW
LPS + 970 nm, 0.05 W/cm², 3 J/cm², CW
800 nm, 0.5 W/cm², 20 J/cm², CW
LPS + 800 nm, 0.5 W/cm², 20 J/cm², CW
660 nm, 0.05 W/cm², 6 J/cm², CW
LPS + 660 nm, 0.05 W/cm², 6 J/cm², CW

B

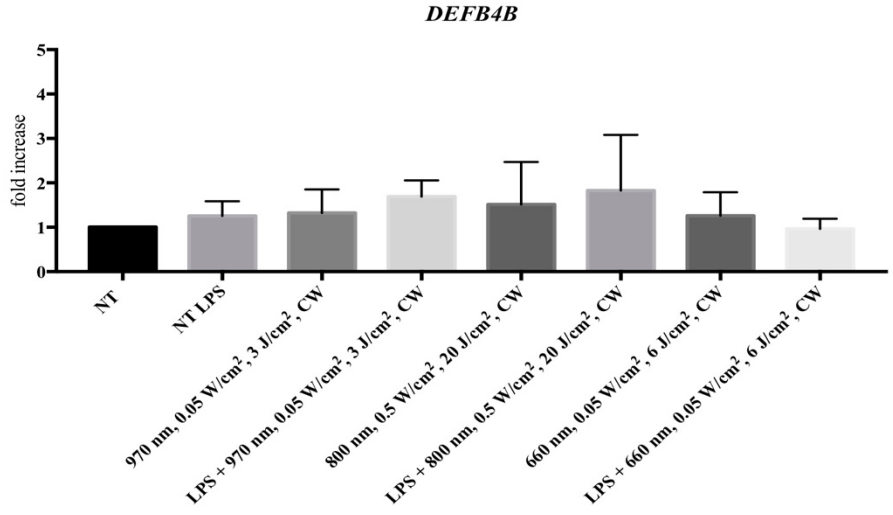
DEFB4B
fold increase
0
1
2
3
4
5
NT
NT LPS
970 nm, 0.05 W/cm², 3 J/cm², CW
LPS + 970 nm, 0.05 W/cm², 3 J/cm², CW
800 nm, 0.5 W/cm², 20 J/cm², CW
LPS + 800 nm, 0.5 W/cm², 20 J/cm², CW
660 nm, 0.05 W/cm², 6 J/cm², CW
LPS + 660 nm, 0.05 W/cm², 6 J/cm², CW

C

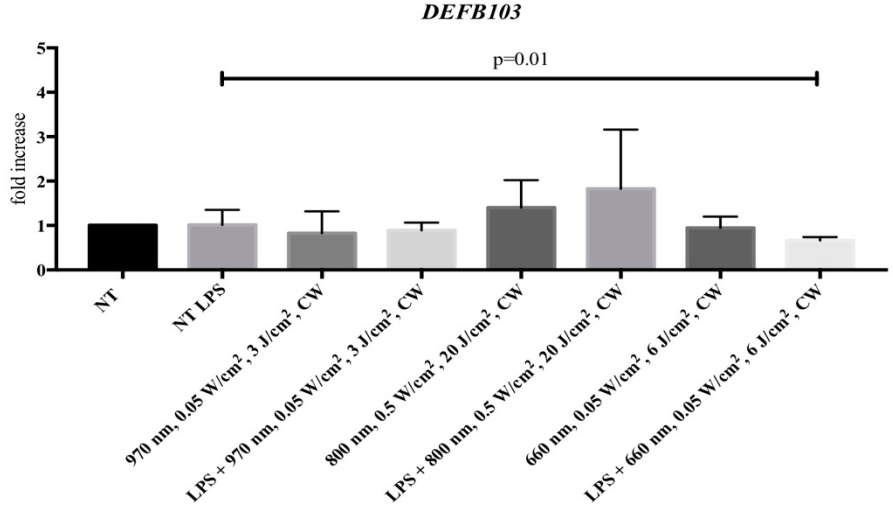
DEFB103
p=0.01
fold increase
0
1
2
3
4
5
NT
NT LPS
970 nm, 0.05 W/cm², 3 J/cm², CW
LPS + 970 nm, 0.05 W/cm², 3 J/cm², CW
800 nm, 0.5 W/cm², 20 J/cm², CW
LPS + 800 nm, 0.5 W/cm², 20 J/cm², CW
660 nm, 0.05 W/cm², 6 J/cm², CW
LPS + 660 nm, 0.05 W/cm², 6 J/cm², CW

However, PBM reduced *DEFB1*, *DEFB4* and *DEFB103* mRNA expression in irradiated cells when compared to the untreated ones 30 minutes after PBM. The protocol 970 nm, 0.05 W/cm^2, 3 J/cm^2, CW diminished *DEFB4* and *DEFB103* mRNA expression (Mann-Whitney test p-value = 0.03 for *DEFB4* and for *DEFB103*, figure B and C). The protocol 800 nm, 0.5 W/cm^2, 20 J/cm^2, CW decremented *DEFB1*, *DEFB4* and *DEFB103* mRNA expression (Mann-Whitney test p-value = 0.03 for all genes, figure 17 A, B and C). The protocol 660 nm, 0.05 W/cm^2, 3 J/cm^2, CW decreased *DEFB1*, *DEFB4* and *DEFB103* mRNA expression (Mann-Whitney test p-value = 0.03 for all genes, figure 17 A, B and C). The timing in our data resulted fundamental, indeed, only a precocious impact of PBM on the gene expression was showed not maintained over time, possibly due to a rapid effect of PBM on the epithelial cells.

The exact mechanism of PBM action on oral mucosa is not completely understood; moreover, little is known regarding PBM effects on innate immune response in oral mucosa [reviewed by [Peplow et al., 2011]] and only one study investigated defensins expression after PBM [Tang et al., 2017]. Tang et al. [Tang et al., 2017] reported an increase in hBD-2 mRNA level 24 hours after PBM in normal human oral keratinocytes using an 810 nm diode laser, differently from our findings, however the different cell lines (primary human oral keratinocytes in the study by Tang et al., neoplastic in our) and PBM protocols employed in the two studies could explained the differences encountered.

Our findings suggest that PBM was able to prevent *DEFB1*, *DEFB4* and *DEFB103* genes over-expression in the immediate phase after PBM, moreover, when LPS was pre-administrated to the cells, PBM at 660 nm decreased *DEFB103* production. So, PBM could possibly avoid higher levels of hBD-1, hBD-2 and hBD-3 that could be detrimental in some conditions for the promotion of inflammation, as already reported in different types of cancer such as lung cancer (characterized by high levels of hBD-1 and hBD-2), renal cell carcinoma (high levels of hBD-1) and oral squamous cell carcinoma (high levels of hBD-3) [Arimura et al., 2004; Kesting et al., 2009]. In the latter case high levels of hBD-3 was correlated to increased expressions of various cytokines: IL-1α, IL-6, IL-8, Chemokine (C-C motif) ligand 18 (CCL18), and tumor necrosis factor-α (TNF-α) expression [Quatromoni, and Eruslanov, 2012].

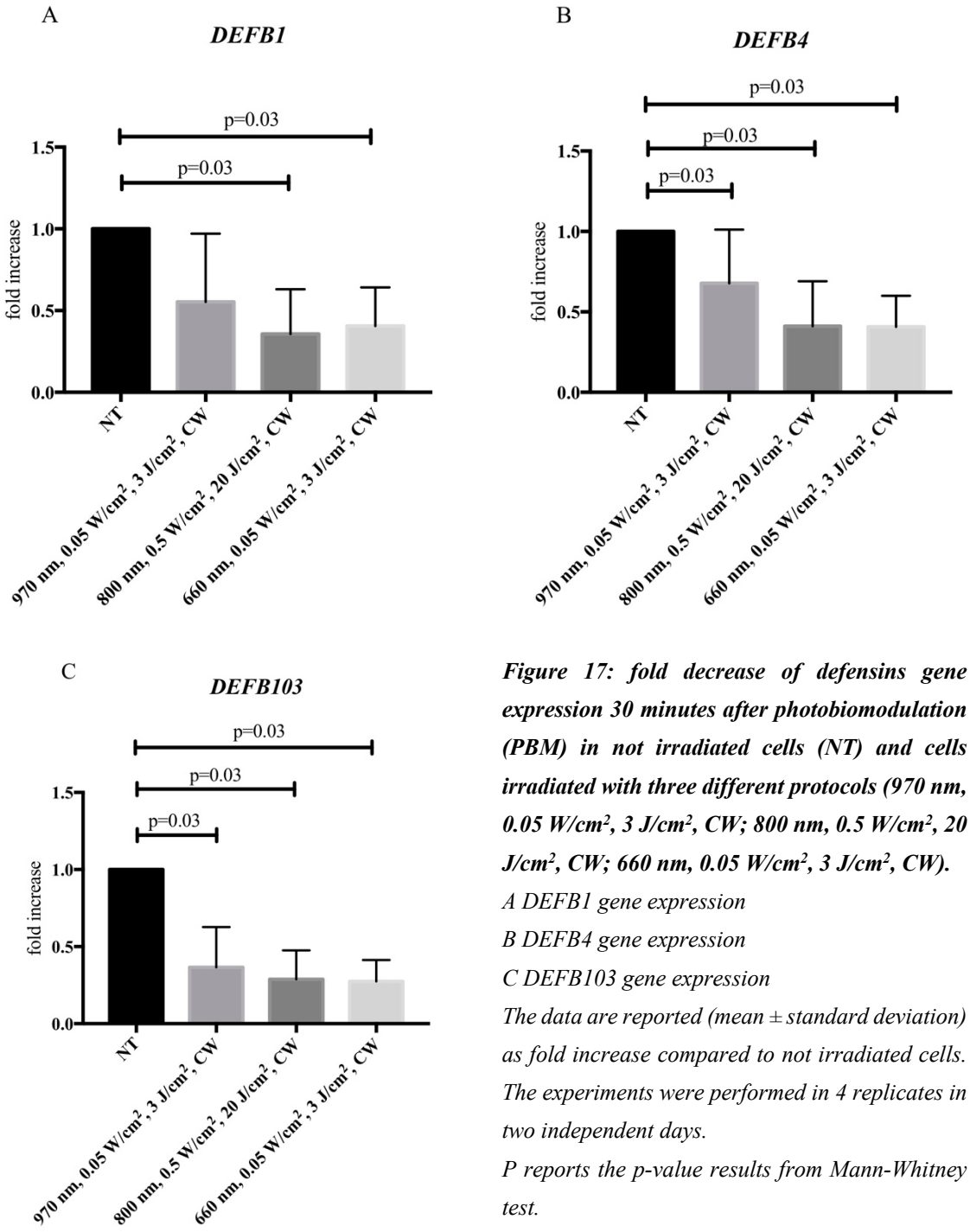

Figure 17: fold decrease of defensins gene expression 30 minutes after photobiomodulation (PBM) in not irradiated cells (NT) and cells irradiated with three different protocols (970 nm, 0.05 W/cm², 3 J/cm², CW; 800 nm, 0.5 W/cm², 20 J/cm², CW; 660 nm, 0.05 W/cm², 3 J/cm², CW).

A DEFB1 gene expression

B DEFB4 gene expression

C DEFB103 gene expression

The data are reported (mean ± standard deviation) as fold increase compared to not irradiated cells. The experiments were performed in 4 replicates in two independent days.

P reports the p-value results from Mann-Whitney test.

Instead, analyzing inflammatory related genes, *IL1B* mRNA increased after 970 nm, 0.05 W/cm^2, 3 J/cm^2, CW laser irradiation (Mann-Whitney test p-value = 0.03, figure 18 A), *NLRP1* increased after PBM with protocol 660 nm, 0.05 W/cm^2, 3 J/cm^2, CW (Mann-Whitney test p-value = 0.03, figure 18 C) finally *NLRP3* decreased following PBM 970 nm, 0.05 W/cm^2, 3 J/cm^2, CW (Mann-Whitney test p-value = 0.03, figure 18 D), meanwhile *CASP1* was not affected (figure 18 B).

PBM at the protocols employed had no effect on the inflammation driven by LPS treatment, on the other hand the wavelength at 970 nm induced slightly *IL1B* gene expression but inhibited *NLRP3* meanwhile the wavelength at 660 nm caused a modest increment of *NLRP1*.

The above cited molecules related to inflammasomes activation was chosen since NLRP3 inflammasome is considered the most versatile and most clinically implicated [reviewed by [Latz et al., 2013]]; however, to note LPS in our *in vitro* model has a minimal effect on inflammasomes molecules.

It could be possible that PBM acting on NF-κB operated the activation of NLRP1 inflammasome with a wavelength, while with the other induced *IL1B* in a NLRP3 inflammasomes independent way. Indeed, in normal cells, the NF-κB activation was well known [Cheng, 2007].

These results could indicate that PBM acted preparing cells to other insult, such as the infection, indeed the metabolism and the viability of cells were not affected by PBM at 660 and 970 nm as possible to observe with the MTT test and ATP level, so a cytotoxic effect can be excluded. Moreover, the increment of *IL1B* was quite moderate and this activation could be counteracted by the decrease in *NLRP3* possibly influenced by PBM in an indirect way. Instead, *NLRP1* increased more, but without influencing pro-inflammatory *IL1B*, in this case another intracellular mechanism perhaps promoted by PBM could possibly block this interaction.

Although preliminary these results could indicate that PBM can act on different pathways possibly influencing the inflammasomes machinery within cells.

Figure 18. (in the next page). Fold increase of mRNA expression of inflammasomes related genes 24 hours after photobiomodulation (PBM) in not irradiated cells (NT), cells treated with LPS (NT LPS), cells irradiated with three different protocols (970 nm, 0.05 W/cm^2, 3 J/cm^2, CW; 660 nm, 0.05 W/cm^2, 6 J/cm^2, CW).

A IL1B gene expression

B CASP1 gene expression

C NLRP1 gene expression

D NLRP3 gene expression

The data are reported (mean ± standard deviation) as fold increase compared to not irradiated cells. The experiments were performed in 4 replicates in two independent days.

P reports the p-value results from Mann-Whitney test.

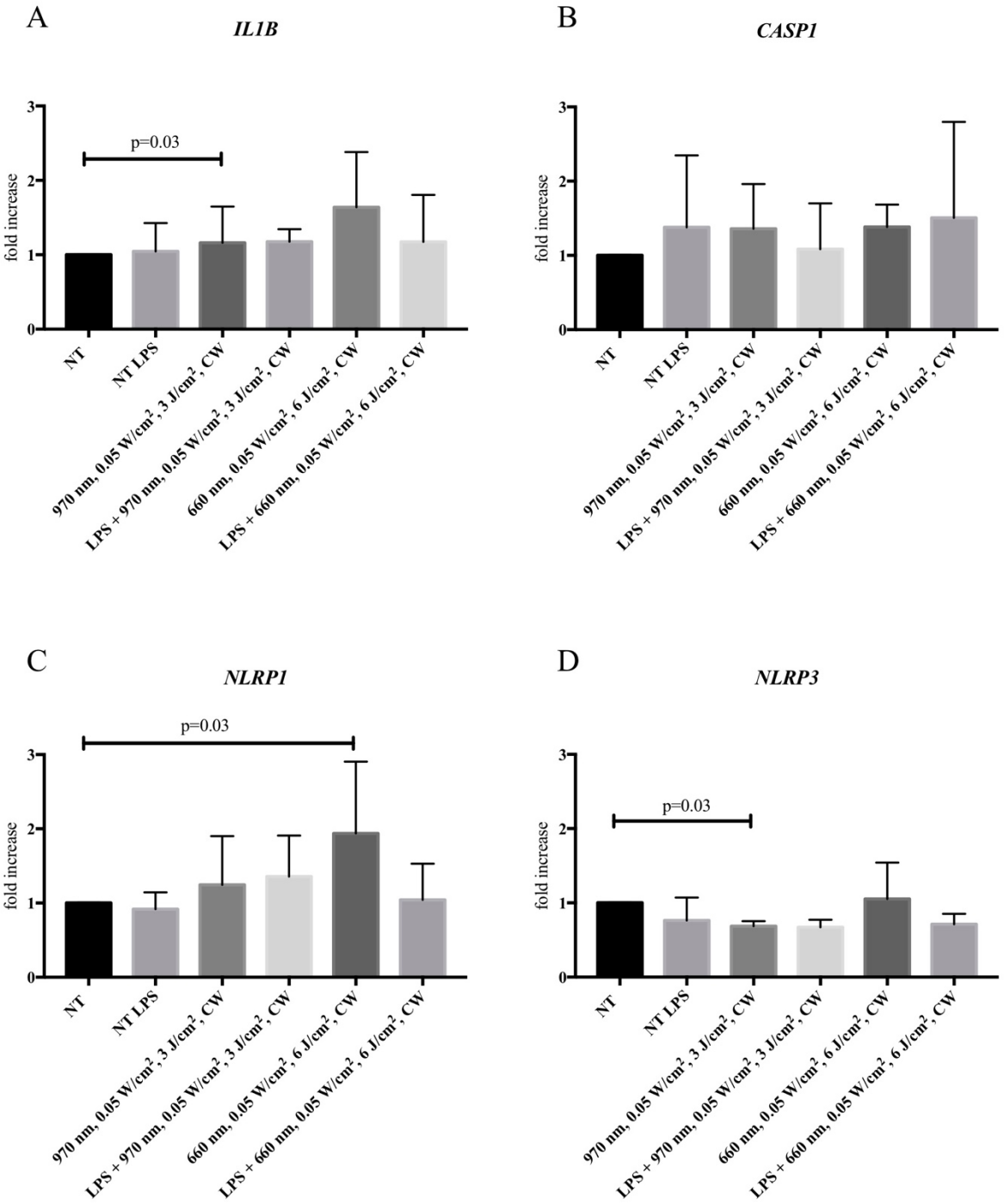
A
IL1B
p=0.03
fold increase
0
1
2
3
NT
NT LPS
970 nm, 0.05 W/cm², 3 J/cm², CW
LPS + 970 nm, 0.05 W/cm², 3 J/cm², CW
660 nm, 0.05 W/cm², 6 J/cm², CW
LPS + 660 nm, 0.05 W/cm², 6 J/cm², CW
B
CASP1
fold increase
0
1
2
3
NT
NT LPS
970 nm, 0.05 W/cm², 3 J/cm², CW
LPS + 970 nm, 0.05 W/cm², 3 J/cm², CW
660 nm, 0.05 W/cm², 6 J/cm², CW
LPS + 660 nm, 0.05 W/cm², 6 J/cm², CW
C
NLRP1
p=0.03
fold increase
0
1
2
3
NT
NT LPS
970 nm, 0.05 W/cm², 3 J/cm², CW
LPS + 970 nm, 0.05 W/cm², 3 J/cm², CW
660 nm, 0.05 W/cm², 6 J/cm², CW
LPS + 660 nm, 0.05 W/cm², 6 J/cm², CW
D
NLRP3
p=0.03
fold increase
0
1
2
3
NT
NT LPS
970 nm, 0.05 W/cm², 3 J/cm², CW
LPS + 970 nm, 0.05 W/cm², 3 J/cm², CW
660 nm, 0.05 W/cm², 6 J/cm², CW
LPS + 660 nm, 0.05 W/cm², 6 J/cm², CW

This is the first study that analyzed mRNA expression of innate immunity genes, such as the AMPs and the actors of inflammasomes machinery: our results showed that PBM impacts also on this type of molecules, confirming its immunomodulatory properties.

Analgesic effect of Photobiomodulation Therapy

Oral mucositis (OM) is generally characterized by erythematous atrophic lesions or in the severe form by ulcerative lesions that penetrate in the mucosa [reviewed by [Sonis, 2004]]. Tissue damaging in the fourth stage of OM development can activate nociceptive pathways, indeed, OM patients refer frequently sore, burning, dull and aching [McGuire et al., 1998] accompanied by pain, oral dysfunction and discomfort [Rose-Ped et al., 2002]. Pain resolves generally at the healing last stage of OM, so it is possible to consider it an acute pain, inflammation related [Harris, 2006]. Pain is the most distressing symptoms reported by the patients, impacting negatively on quality of life, social relationships but also on the compliance to cancer treatment [McGuire et al., 1998].

Pain is defined by the International Association for the Study of Pain as "an unpleasant sensory and emotional experience associated with actual or potential tissue damage, or described in terms of such damage" underlined the physical and emotional multidimensional aspects of pain experience [Loeser, and Treede, 2008].

The pain management is a clinical issue, especially in particular situations such as in pediatric patients who need of special attention since in children the pain is often not accurately recognized and diagnosed [World Health Organization, 2012]. Pain control often requires analgesic assumptions also administrated at systemic level, as acetaminophen, non-steroidal anti-inflammatory drugs and opioids as morphine, however, the reported medications can have adverse effects and present a limited efficacy in some cases [Nalamachu, 2013]. Other compounds with analgesic action have been previously used in the clinical practice, but there is inadequate evidence to include them in the guidelines. The list includes lidocaine, fluconazole, sucralfate, topical sodium hyaluronate, tetracaine, dyclonine, MGI- 209 (with benzocaine), cocaine, amethocaine, capsaicin, methadone, ketamine, nortriptyline, gabapentin and topical coating agents to cover the ulcerations and nerve endings [reviewed by [Saunders et al., 2013]].

So, the study of novel treatments is strongly required to improve the pain conditions and photobiomodulation (PBM) therapy is a promising cure that several groups are employing in pain management with good results in decreasing pain sensation and without complications [Mallick et al., 2016; Oberoi et al., 2014; Spanemberg et al., 2016].

Nevertheless, despite the clinical use, the biological bases of PBM analgesic effect are poorly understood. PBM seemed to be able to slow the nerve conduction in humans but also in rat models exposed to noxious stimuli [reviewed by [Chow et al., 2011]]. *In vitro*, in rat dorsal root ganglia (DRG) neurons, PBM reduced the nociceptors response to various harmful stimuli, like

bradykinin [Jimbo et al., 1998]. Moreover, PBM induced axonal varicosities with microtubules destruction and clustering of mitochondria resulting in a block of the fast axonal flow [Chow et al., 2007; Holanda et al., 2017]: it was proposed that PBM acted on proteins involved in microtubule stability producing a conformational modification [reviewed by [Liebert et al., 2016]].

The transient receptor potential (TRP) calcium channels are potential photoreceptors of light, being light sensitive ion channels. The family comprehends seven subgroups called Canonical (TRPC) Vanilloid (TRPV), Melastatin (TRPM), Polycystin (TRPP), Mucolipin (TRPML), Ankyrin (TRPA) and the NOMPC (TRPN) [reviewed by [Dai, 2016]]. Really, Ryu et al. [Ryu et al., 2010] showed that PBM at 2780 nm in trigeminal DRG reduced the calcium peak induced by capsaicin (activator of TRPV1 channel) in pre-irradiated cells. Analogously, the pre-irradiated neurons presented a reduction of the calcium peak after 4-alpha-phorbol 12,13-didecanoate (a specific TRPV4 activator) treatment. On the other hand, PBM was not able to influence TRPM7, TRPM8, P2X3, native voltage-gated channels, native P2Y, histamine, and muscarinic receptors. These results indicated that laser light could directly and specifically act on TRPV functionality [Ryu et al., 2010].

On the other end, PBM could produce cytosolic alkalinization so inducing TRPV opening and calcium ion influx from extracellular environment [Nilius et al., 2005].

The aim of the present study was to analyze the analgesic action of PBM in OM patients and then to try to describe the molecular basis of this effect. For this purpose, the potential action of PBM on mitochondria of murine sensory neurons isolated from dorsal root ganglia (DRG) was investigated. Moreover, a murine model of nociception, through the use of capsaicin as stimulus of pain, was developed to observe the effect of laser light on the whole organism in a behavioral test.

Materials and Methods

OM Patients Visual Analogue scale

The visual analogue scale (VAS) was employed to evaluate patients' referring painful sensation, at the 4 PBM sessions and at the control day [Hawker et al., 2011].

Primary Dorsal Root Ganglia Sensory Neuron Culture

Dorsal Root Ganglia (DRG) sensory neurons were isolated from mice: animal care and treatment were conducted in conformity with institutional guidelines in compliance with Italian national (Decreto Legislativo 26/2014, Italian Ministry of Health) and international (European Union Directive 2010/63/EU) laws and policies.

DRG were manually dissected from CD1 mice at 6-8 weeks of age and maintained in Hank's Balanced Salt Solution until processing (HBSS, H6648, Sigma Aldrich, Saint Louis, Missouri, U.S.A.).

DRG sensory neurons isolation was performed accordingly with already established protocols with slight modifications [Malin et al., 2007]. Briefly, DRG were digested using 60 units of papain (000020 10108014001, Roche, Basel, Switzerland) and 0.66 mg/ml of L- Cysteine in HBSS at 37°C for 10 minutes, then with 12 mg of collagenase type II (LS004176, Worthington Biochemical Corporation, Lakewood, New Jersey, U.S.A.) and 14 mg of dispase type II (D4693, Sigma Aldrich) in HBSS at 37°C for 10 minutes. DRG were triturated using a pipette and seeded in Ham's F12 culture medium supplemented with 10% fetal bovine serum, 100 U/ml Penicillin/Streptomycin, 2 mM Glutamine (Euroclone, Pero, Milan, Italy) in 96 or 24 multi-wells plates previously coated with 1 mg/ml of extracellular matrix (ECM) gel from Engelbreth-Holm-Swarm mouse sarcoma (E1270, Sigma Aldrich) at cell density of 2 x 10^4 cells/ml. The medium was changed every two days and the DRG culture were used for the experiments after 72 hours from the seeding to permit neurons branching and at this time the glial cells did not proliferate [Malin et al., 2007].

Sensory neurons characterization

The cells were seeded on 12 mm round coverslips coated with ECM gel. After 72 hours they were characterized using immunofluorescence staining for β-Tubulin III, a known neuronal marker of the peripheral nervous system [Jiang, and Oblinger, 1992]. Cells were fixed in 4% paraformaldehyde (PFA) in phosphate buffer saline (PBS) for 20 minutes, then after washing, permeabilized (glycine 0.1 M in PBS) and aspecific sites blocked (10% normal goat serum – NGS– in PBS with 0.1% TritonX100 – PBS-T), the cells were incubated overnight with an anti β-Tubulin III antibody (dilution 1:100 in PBS-T plus 10% NGS, TU2020, Cell Signaling Technologies, Danvers, Massachusetts, U.S.A.) and subsequently for 1 hour with an anti-mouse Alexa Fluor 488 secondary antibody (1:500, A11029, Thermo-Fisher Scientific, Waltham, Massachusetts, U.S.A.) and with DyLight™ 554 Phalloidin for the staining of cytoskeleton F-actin (1:250, 13054S, Cell Signaling Technologies, Danvers, Massachusetts, U.S.A.), finally the coverslips were sealed on glass slides (Superfrost, 10143560, Thermo Fisher Scientific) with a

mounting compound containing DAPI for the staining of nucleic acid (H-1300, Vectashield, Burlingame, California, U.S.A.).

Laser Irradiation protocols

Two protocols were selected 970 nm, 0.1 W/cm^2, 6 J/cm^2, 5 Hz and 800 nm, 0.1 W/cm^2, 6 J/cm^2, 5 Hz based on the clinical experience of our colleagues from the Division of Oral Medicine and Pathology of "Maggiore" Hospital in Trieste.

Mitochondria visualization

Immediately after irradiation, mitochondria were stained with Mito red (5 nM, 53271, Sigma Aldrich) for 30 minutes at 37°C, then fixed for 20 minutes with 4% PFA and further stained for cytochrome C oxidase (diluted at 1:250, 7H8, sc-13560, Santa Cruz Biotechonology, Dallas, Texas, U.S.A.) a mitochondrial enzyme, to see the localization of this protein respect to mitochondria.

Adenosine triphosphate determination

Neurons were irradiated in 24 multiwells plate, then 30 minutes, or 2, 4, 24 hours after PBM they were lysed using 100 µl of phosphate buffer saline (PBS) with 0.5% of TritonX100 (Sigma Aldrich): Adenosine triphosphate (ATP) was measured using the ATP determination kit (A22066, Invitrogen, Thermo Fisher Scientific) in 10 µl of the lysates and the luminescence was read at the multimode plate reading - PerkinElmer Envision (PerkinElmer, Waltham, Massachusetts, U.S.A.) and expressed as ATP concentration using the standard provided by the kit. ATP level was normalized on protein concentration quantified testing 5 µl of the lysates with the Bradford protein assay (Bio-Rad, Hercules, California, U.S.A.) using Bovine Serum Albumin (BSA) as standard.

Oxidative stress measurement

Reactive oxygen species (ROS) production was measured using the cell-permeant 2',7'-dichlorodihydrofluorescein diacetate (H2DCFDA) dye (D399, Invitrogen, Thermo Fisher Scientific) 30 minutes after PBM: cells were loaded with 10 µM of dye for 30 minutes at 37°C, then the fluorescence was read and normalized on protein concentration lysing the cells with 50 µl (PBS) with 0.5% of TritonX100 and testing 5 µl of the lysates with Bradford protein assay (Bio-Rad).

The mitochondrial superoxide was measured using the MitoSOX fluorescent probe (M36008, Invitrogen, Thermo Fisher Scientific): after irradiation cells were loaded with 5 µM of the dye

for 10 minutes at 37°C, then the fluorescence was read. The fluorescence was normalized on protein concentration lysing the cells with 50 µl (PBS) with 0.5% of TritonX100 for 5 minutes and testing 5 µl of the lysates with Bradford protein assay (Bio-Rad).

Mitochondrial membrane potential measurement

Mitochondrial membrane potential (MMP) was measured using the JC-1 probe (Invitrogen, Thermo Fisher Scientific), loading cells with probe (5 µM) for 30 minutes at 37°C, then cells were irradiated, and the fluorescence read immediately after irradiation. The results were expressed as green (525 nm) to red (590 nm) fluorescence intensity ratio; normalized on not irradiated cells (NT).

Calcium flow analysis

Fluo-4, AM, cell permeant dye (F10472, Invitrogen, Thermo Fisher Scientific) was used to observe intracellular calcium flow. The cells were loaded with the dye for 30' at 37°C and then they were irradiated. Twenty µl of capsaicin (M2028, Sigma Aldrich) at 10 µM was dispensed in each well and at the same time the fluorescence excited at 494 nm and emitted at 516 nm was read at the multimode plate reading - PerkinElmer Envision (PerkinElmer): 130 time points were read for each well at intervals of 0.2 seconds. The baseline fluorescence was obtained as an average normalized fluorescence emitted during the initial first 10 time points (F_0). The ratio between the mean initial fluorescence (F_0) and the fluorescent emitted at each time point (F/F_0) was used in the analysis [Simpson, 2006].

Murine model of nociception

For the behavioral experiment, 60 CD1 female mice at 8 weeks of age were employed. Animal care and treatment were conducted in conformity with institutional guidelines in compliance with Italian national (Decreto Legislativo 26/2014) and international laws and policies (European Union Directive 2010/63/EU). Animals were housed under controlled environmental conditions with a 12 hours light/dark cycle.

The animals were divided in 6 groups with 10 animals in each group: 1) vehicle injection without PBM, 2) PBM 970 nm, 0.1 W/cm^2, 6 J/cm^2, 5 Hz with vehicle injection, 3) PBM 800 nm, 0.1 W/cm^2, 6 J/cm^2, 5 Hz with vehicle injection, 4) capsaicin injection without PBM, 5) PBM 970 nm, 0.1 W/cm^2, 6 J/cm^2, 5 Hz with capsaicin injection, 6) PBM 800 nm, 0.1 W/cm^2, 6 J/cm^2, 5 Hz with capsaicin injection. After an acclimation period of 30 minutes, the mice were submitted to sedation with 5% isoflurane concomitant or not with PBM, then, 20 µl of vehicle (PBS) or capsaicin (4 µg in PBS) were injected subplantarly and mice behavior digitally recorded for 5

minutes in a plexiglass box: the time spent in licking, biting and shaking the paw was recorded and used as a measure of nociception [Simone et al., 1989; Ryu et al., 2010; De Prá et al., 2017]. At the end of the experimental day the groups were randomly assorted and the next week tested on the other paw, after 2 weeks the procedure was repeated (first a paw and the next week the other): this setting was chosen since capsaicin does not produce permanent damage at the site of injection and also to reduce the number of animals employed [De Prá et al., 2017]. Analysis of the time spent licking/biting the injected paw was performed by two trained researchers blinded to the experimental group and the median of the recorded time was used for statistical analysis.

Statistical Analysis

Friedman's test with the Dunn's test for multiple comparison were used to compare the changes over time in VAS score.

Kruskal Wallis test with Dunn's test for multiple comparison was used to evaluate the effect of PBM on irradiated compared to not irradiated cells.

All statistical assessments were two-sided, and a p-value < 0.05 was used for the rejection of the null hypothesis.

Results and Discussion

PBM treatment improved patients' clinical condition, reducing the VAS score over time (Friedman's test p-value = 0.0003 for VAS, Dunn's test for multiple comparison, p-value = 0.01 for T0 versus T3 and p-value = 0.01 for T0 versus CTRL, figure 19).

This result was in agreement with previous literature [Ottaviani et al., 2013] regarding a reduction of patients' referred pain with PBM.

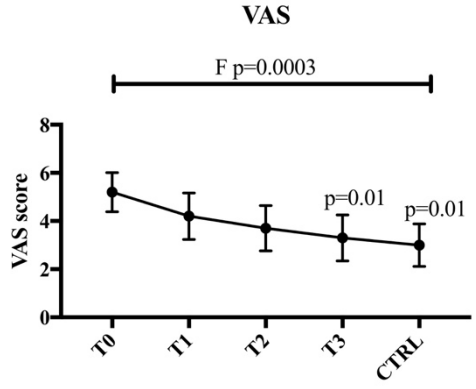

Figure 19. VAS in the oral mucositis patients treated with photobiomodulation therapy (n=10).

F p-value reports the p-value for Friedman test, the other p-values report the results from Dunn's multiple comparison test.

To explore and to try to understand the molecular basis of this effect, the *in vitro* model of sensory neurons was exploited.

To confirm the isolation of the DRG sensory neurons immunocytochemistry using β-tubulin III as neuronal marker was performed [Katsetos et al., 2003].

Figure 20 displays a typical preparation 72 h after isolation.

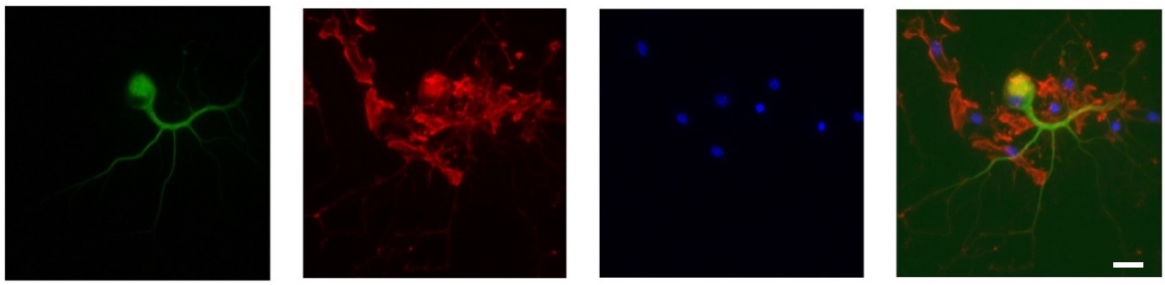

Figure 20. Immunocytochemical characterization of DRG neurons 72 h after isolation.
β-Tubulin III (green) Phalloidin (red) Dapi (blue) and merge of the channels. Scale bar 20 µm.

In order to see if PBM could damage the cells, a double staining for mitochondria and cytochrome C oxidase was performed after irradiation with the two protocols: if the two do not co-localize that indicates a release of the enzyme from the mitochondria and a situation of cellular damage with initiation of the apoptotic pathway [Gogvadze et al., 2006]. In our experiments mitochondria and cytochrome C oxidase displayed a similar pattern between irradiated and not irradiated cells: the two co-localized together, indicating that the cytochrome C was not released from mitochondria, sign of a healthy condition (figure 21 A, B and C); so, it is possible to affirm that the treatments were not toxic for the cells.

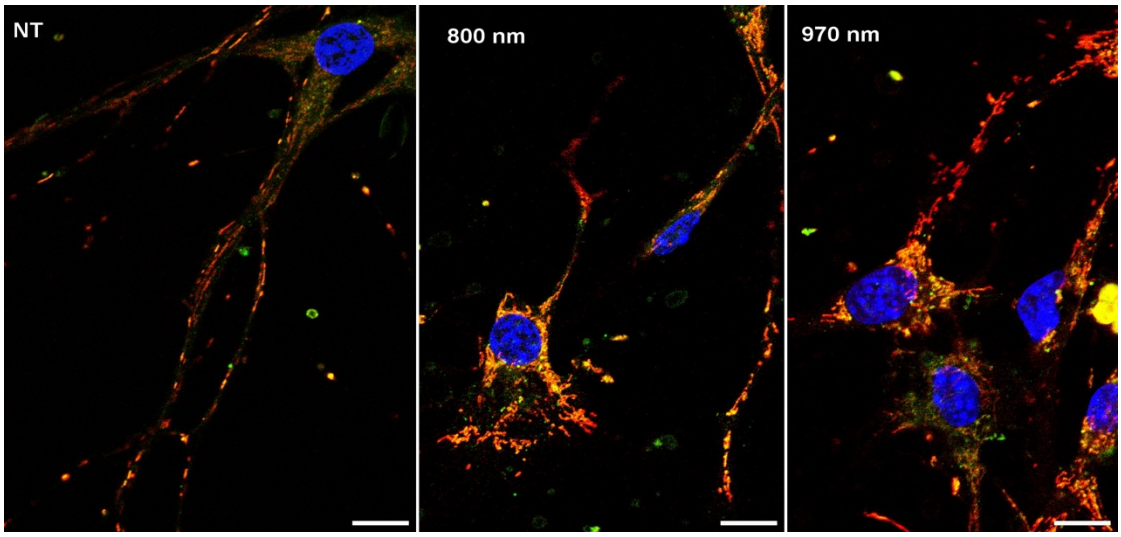

Figure 21.Morphological analysis of mitochondria in irradiated and not irradiated DRG neurons.
DAPI (blue), Mitored (red), (green).
A DRG neurons not irradiated. Red and green signal mainly colocalized, indicating healthy cells.
B DRG neurons treated with λ 800 nm, 0.1 W/cm², 6 J/cm², 5 Hz.
C DRG neurons treated with λ 970 nm, 0.1 W/cm², 6 J/cm², 5 Hz.
Scale bar 20 μm

Both laser protocols were able to reduce ATP levels after 15 minutes from irradiation respect to not treated cells (Kruskal Wallis test p-value=0.001; Dunn's test for multiple comparison p-value=0.01 for 970 nm 0.1 W/cm^2, 6 J/cm^2, 5 Hz and p-value=0.001 for 800 nm, 0.1 W/cm^2, 6 J/cm^2, 5 Hz; figure 22), but not 2, 4 and 24 hours from irradiation (data not shown). A reduced availability of ATP should lead to failure in generation of action potentials, since the Na^+-K^+-ATPase, responsible of action potential generation, requires ATP for its functionality [Albers, and Siegel, 1999]. So, its inhibition could lead to the block of pain signaling transmission to brain through sensory neurons, confirming the analgesic effect of PBM. These results were in agreement with the study of Holanda et al., that observed a decrement in mitochondrial metabolism after 808 nm laser treatment using the MTS assay [Holanda et al., 2017] and with the work of Wang et al. that showed a decrement of extracellular ATP in DRG culture with a 645 nm irradiation, hypothesizing a suppressive effect of PBM on ecto-ATPase (that was confirmed only partially by the researchers using an ecto-ATPase inhibitor) [Wang et al., 2015].

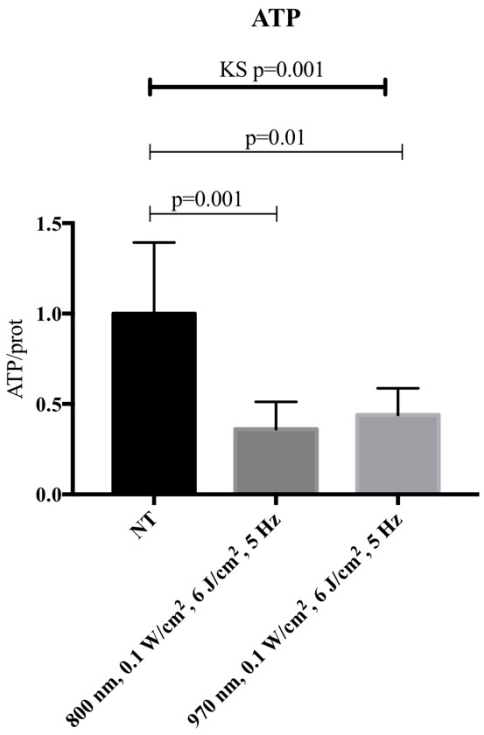

Figure 22. ATP levels normalized on total protein content in irradiated (λ 970 nm, 0.1 W/cm², 6 J/cm², 5 Hz, and λ 800 nm 0.1 W/cm², 6 J/cm², 5 Hz) and not irradiated DRG neurons (NT).

The data are reported as mean ± standard deviation.

KS p-value reports the results from Kruskal-Wallis test, the other p-values report the results from Dunn's multiple comparison test.

The experiments were performed in 16 replicates in two independent days.

An increase of ROS production was also observed with both protocols respect to not treated cells (Kruskal Wallis test p-value=0.0005; Dunn's test for multiple comparison p-value=0.003 for 970 nm 0.1 W/cm^2, 6 J/cm^2, 5 Hz and p-value=0.001 for 800 nm, 0.1 W/cm^2, 6 J/cm^2, 5 Hz; figure 23 A), interestingly, a selective increment in mitochondrial specific anion superoxide specie was found only with the 800 nm λ (Kruskal Wallis test p-value=0.001; Dunn's test for multiple comparison p-value=0.04 for 800 nm, 0.1 W/cm^2, 6 J/cm^2, 5 Hz; figure 23 B). Mitosox is a selective indicator of only superoxide that has a mitochondrial origin [Batandier et al., 2002] and it is not influenced by other ROS or reactive nitrogen species. This result could be expected since the principal target of the NIR wavelength is Cu_A redox center of the cytochrome C oxidase that has its maximum absorption at 835 nm [Mason et al., 2014]. This leads to intracellular redox state changes that accounted for our results about wavelength at 800 nm [Mason et al., 2014]. ROS production could cause axonal varicosities with the formation of mitochondria cluster. The varicosities were β-tubulin positive, a sign of microtubule disruption, leading to the block of ATP transport along the neurites [reviewed by [Liebert et al., 2016]]. The final effect was the block of fast axonal flow (FAF): this effect impacted on nerve conduction, since it was specific for small diameter fibers, Aγ and C , both significant for pain alleviation [reviewed by [Chow et al., 2011]]. FAF block in turn could affect the anterograde transport of ATP-rich mitochondria leading to ATPase impairment [reviewed by [Chow et al., 2011]]. Moreover, the varicosities formation with the consequent negative impact on axonal flow, mitochondrial metabolism, nerve conduction and

signal transduction has been proposed as physiologically adaptive neuro-protective mechanisms [reviewed by [Liebert et al., 2016]].

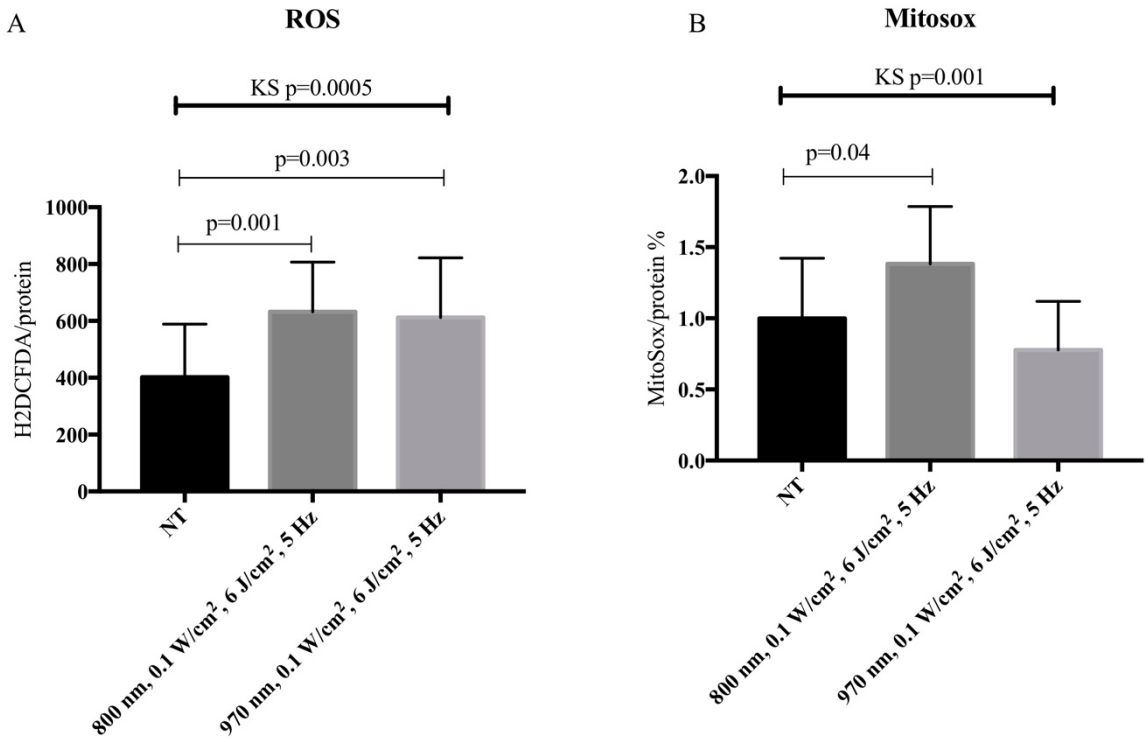

Figure 23. ROS and superoxide levels in irradiated (λ 970 nm, 0.1 W/cm², 6 J/cm², 5 Hz; and λ 800 nm 0.1 W/cm², 6 J/cm², 5 Hz) and not irradiated DRG neurons (NT).

A H2DCFDA fluorescent intensity levels normalized to total protein content.

B MitoSox fluorescent intensity levels normalized to total protein content and to NT.

The data are reported as mean ± standard deviation. The experiments were performed in 16 replicates, in two independent days.

KS p-value reports the results from Kruskal-Wallis test, the other p-values report the results from Dunn's multiple comparison test.

Increased ROS could influence the mitochondrial membrane potential (MMP) or could be the cause of MMP imbalance. MMP was measured with JC-1, a membrane-permeant cationic probe exhibiting accumulation in the mitochondria which is potential-dependent. It is able to shift its fluorescent emission from green (monomers in the cytosol) to red range (aggregates inside mitochondria). The red/green fluorescence intensity ratio can be used as a measurement of MMP since this ratio is dependent on MMP and not on other factors: a decrement indicates a mitochondrial depolarization, meanwhile an increment a hyperpolarization. In our experiments the red/green ratio was normalized on not treated cells: the protocol λ 800 nm 0.1 W/cm^2, 6 J/cm^2,

5 Hz produced a significant slight hyperpolarization (Kruskal-Wallis test, p-value = 0.05; Dunn's multiple comparison test p-value = 0.04 for λ 800 nm 0.1 W/cm^2, 6 J/cm^2, 5 Hz; figure 24).
These findings well correlated with MitoSox results, possibly indicating that λ 800 nm 0.1 W/cm^2, 6 J/cm^2, 5 Hz drove a dysregulation in mitochondrial activity.
Our results were not in agreement with the study of Chow et al. [Chow et al., 2007], that found a depolarization of neurons, however, the irradiation protocols were different from our study specially in the power density utilized, higher in the Chow et al. [Chow et al., 2007] study respect to ours and in the modality, continuous wave respect to 5 Hz: these different settings could account for the deviations encountered.

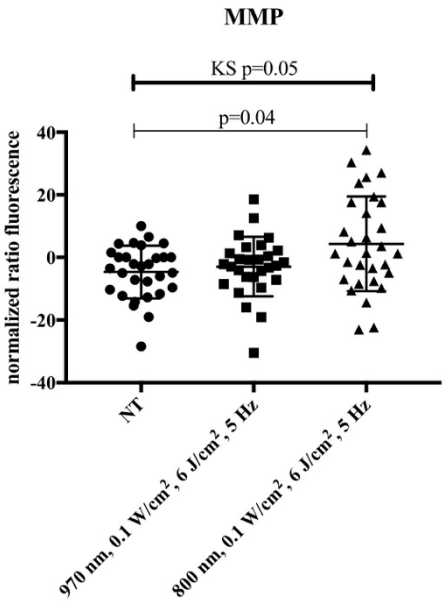

Figure 24. Mitochondrial Membrane Potential (MMP) in irradiated (λ 970 nm, 0.1 W/cm^2, 6 J/cm^2, 5 Hz; and λ 800 nm 0.1 W/cm^2, 6 J/cm^2, 5 Hz) and not irradiated DRG neurons (NT).
Ratio between Red/Green fluorescence emission of JC1 probe (measuring MMP) are normalized toward NT condition.
The bars indicate mean ± standard deviation. The experiments were performed in 16 replicates, in two independent days.
KS p-value reports the results from Kruskal-Wallis test, the other p-value reports the result from Dunn's multiple comparison test.

The analysis of nitric oxide (NO) content showed that NO was reduced by both PBM protocols respect to not treated cells (Kruskal-Wallis test, p-value = 0.0002; Dunn's multiple comparison test p-value = 0.0003 for λ 970 nm 0.1 W/cm^2, 6 J/cm^2, 5 Hz and p-value = 0.002 for λ 800 nm 0.1 W/cm^2, 6 J/cm^2, 5 Hz, figure 25). NO was detected with the DA-FM probe that is non-fluorescent until it diffuses inside the cells, it is deacetylated and reacts with NO forming a fluorescent benzotraizole. Different studies revealed that PBM could activate the release of NO from cytochrome C oxidase increasing the respiratory rate and the level of NO [reviewed by [Hamblin, 2008]]. On the other hand, when NO was pathologically increased, such as inflammatory condition, PBM reduced it. No previous studies reported the effect of NO on DRG sensory neurons, however, NO is also an agonist of TRPV1, possibly mediating nociception; it

could be considered as a neurotransmitter, improving the sensory perception [reviewed by [Dai, 2016]]. In this view, a decrement of NO after PBM could be useful to decrease the nociceptive pathways.

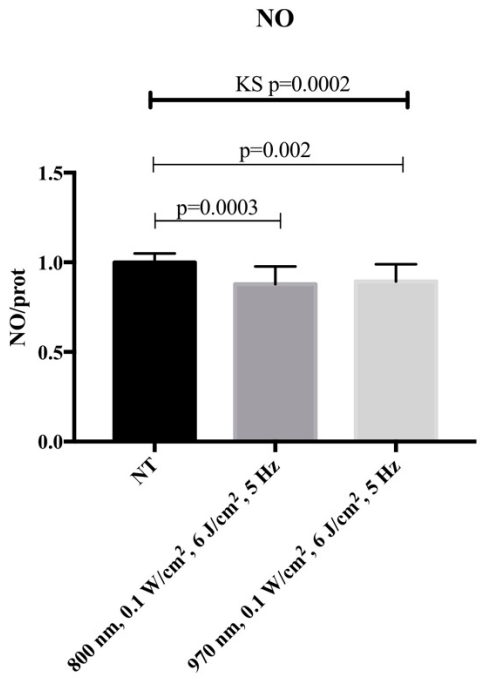

Figure 25. Nitric Oxide (NO) production in irradiated (λ 970 nm, 0.1 W/cm², 6 J/cm², 5 Hz; λ 800 nm 0.1 W/cm², 6 J/cm², 5 Hz) and not irradiated DRG neurons (NT).

The data are reported as mean ± standard deviation. The experiments were performed in 16 replicates, in two independent days.

KS p-value reports the result from Kruskal-Wallis test, the other p-values report the results from Dunn's multiple comparison test.

Since PBM was reported as able to influence the intracellular calcium flow [Yan et al., 2017], and considering that calcium is a neurotransmitter also in nociception pathways [reviewed by [Prado, 2001]], calcium flow was measured in DRG neurons after PBM and stimulus (capsaicin). The fluctuation in concentration of this ion following capsaicin stimulation was registered using a dye (fluo-4) that increments fluorescent emission upon calcium binding. Capsaicin is a endogenous agonist of TRPV1, a non-selective cation channel that normally converts heat and pain sensation into electric stimuli that are then transmitted to the spinal cord, thalamus, and the cerebral cortex [reviewed by [Dai, 2016]]. TRPV1 is widely expressed in the peripheral nervous system, specifically in the nociceptive neurons and in small C- and Aδ fibers [reviewed by [Jara-Oseguera et al., 2008]]. Mean peak intensity diminished significantly for the cells treated with λ 970 nm 0.1 W/cm^2, 6 J/cm^2, 5 Hz (Kruskal-Wallis test, p-value = 0.003; Dunn's multiple comparison test p-value = 0.01 for λ 970 nm 0.1 W/cm^2, 6 J/cm^2, 5 Hz, figure 26 A). In figure 26 B are showed representative traces of fluo-4 emission with or without PBM.

Our results suggested a decreased signaling towards an external nociceptive stimulus.

In primary neurons from spinal cord PBM at 632 nm caused the calcium released from inositol triphosphate receptor (IP3R)-sensitive calcium stores but did not act on calcium influx through cell membrane [Yan et al., 2017]. In murine primary cortical neurons PBM at 810 nm induced an increment of calcium levels with fluency 0-10 J/cm^2 but a decline was noted when PBM was increased to 30 J/cm^2 [Sharma et al., 2011], nevertheless, when excitotoxins were added PBM reduced calcium concentration [Huang et al., 2014]. Intriguingly, in our model 800 nm wavelength did not influence intracellular calcium response to capsaicin, thus suggesting different mechanism of action in different type of cells.

In another non neural cellular model, the adipose-derived stem cells, 980 nm wavelength could elicit a thermal response, with TRPV1 activation [Wang et al., 2017a]. Although irradiation setting was slightly different in the two works (3 J/cm^2 versus 6 J/cm^2 and continuous wave versus pulsed wave in Wang et al. and in this research respectively) a small, localized temperature increase could be not excluded, indicating a possible TRPV1 desensitization: increased temperature of intracellular water could open TRPV1 bringing it to be less susceptible toward another stimulus, like capsaicin.

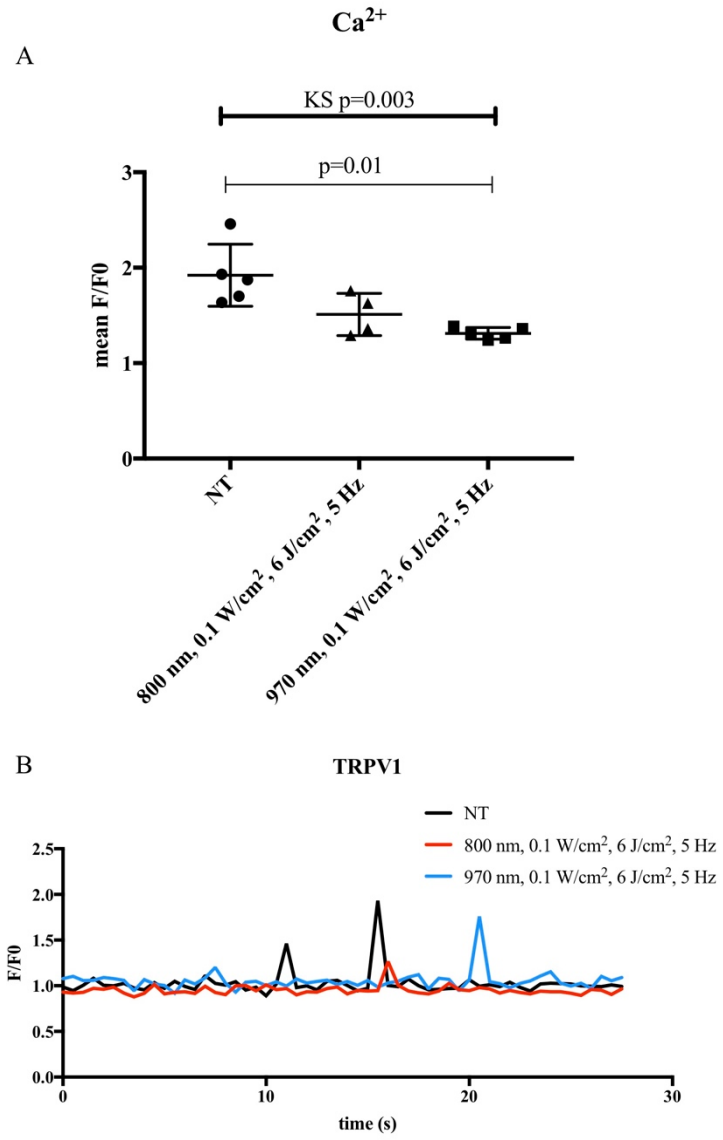

Figure 26. Calcium flow analysis of irradiated (λ 970 nm, 0.1 W/cm², 6 J/cm², 5 Hz; and λ 800 nm 0.1 W/cm², 6 J/cm², 5 Hz) and not irradiated DRG neurons (NT).

A Mean peak normalized fluorescent after capsaicin-induction.

The bars indicate mean ± standard deviation. The experiments were performed in 5 replicates, in two independent days.

KS p-value reports the result from Kruskal-Wallis test, the other p-values report the results from Dunn's multiple comparison test.

B Typical traces of normalized fluoresce emission (F/F_0 = mean initial fluorescence / fluorescent emitted at each time point) of NT and irradiated neurons. Each trace represents emission from a single well of a 96 well plate, being thus the mean fluorescent emission of approximately 10000 cells.

Finally, a clear analgesic effect was detected also in the animal model of nociception: the administration of capsaicin induced an evident pain-related response characterized by licking, biting, and shaking of the paw tested, that was significantly reduced by the PBM pre-treatment with the protocol λ 970 nm 0.1 W/cm^2, 6 J/cm^2, 5 Hz (figure 27 A), but not with the λ 800 nm 0.1 W/cm^2, 6 J/cm^2, 5 Hz one (figure 27 B) that although reduced the pain-related behavior, it was not able to achieve the statistical significance. This outcome reflected previous research that underlined the analgesic effect of PBM *in vivo* in different models, such as inflammation related pain [Hagiwara et al., 2007], neuropathic pain [Hsieh et al., 2012] and post-operative pain [Cidral-Filho et al., 2014]. However, no previous study evinced the effect of PBM on capsaicin treatment as in ours: this test was selected because capsaicin provokes an acute, intense but transient painful sensation without causing permanent damage [De Prá et al., 2017]; it is also a substance worldwide accepted as an inductor of thermal and mechanical hyperalgesia [Gregory et al., 2013].

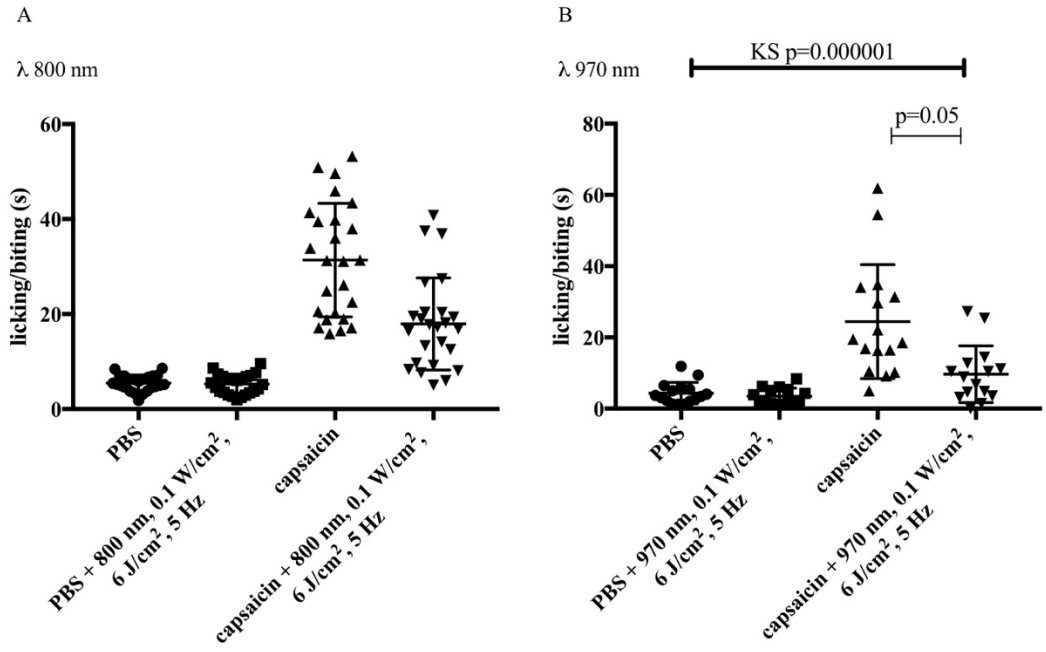

Figure 27. Results from the in vivo model of nociception

Mice were subplantarly injected with capsaicin or vehicle (PBS). Half of the animals were subsequently irradiated with PBM protocols λ 800 nm 0.1 W/cm^2, 6 J/cm^2, 5 Hz (panel A) or λ 970 nm, 0.1 W/cm^2, 6 J/cm^2, 5 Hz (panel B). The time spent in licking and/or biting the paw treated was recorded as seconds. The experiments were performed with 10 animals in each subgroup, and the test were performed twice on each animal (alternating the two paws in different days).

KS p-value report the result from Kruskal-Wallis test, the other p-value reports the result from Dunn's multiple comparison test.

Also, in this *in vivo* model, a differential effect of 800 nm and 970 nm wavelength was observed, suggesting a different PBM mechanism of action: λ 800 nm seemed to act on mitochondria, with less influence on calcium flux; λ 970 nm instead, reduced TRPV1 activity possibly impacting on pain-response signaling.

Our data suggested a significant repercussion of PBM on DRG sensory neurons, with a wavelength dependent response, possibly acting on different cellular target in fact, λ 970 nm appeared to possess stronger analgesic activity respect to λ 800 nm, data corroborated by the findings observed in the murine behavioral model.

Antimicrobial action of Blue Laser Light

Pseudomonas Aeruginosa is a Gram negative bacteria, ubiquitous in soil and aqueous environments and it is, among the *pseudomonas* genera, the most frequent found in human infections [Streeter et al., 2016]. It shows a very high adaptability at growing in different moist conditions and in setting both natural and artificial, requiring simple nutritional needs. It presents several virulence factor, such as adhesins (i.e. pili, flagella), lipopolysaccharide, type III secretion system through which *P. Aeruginosa* injects ExoS, ExoU, ExoT, ExoY in phagocytic cells, secreted toxins i.e. ExoA, leucocidin, elastase, phospholipases, rhamnolipids, pyocyanin, hydrocyanic acid [Ramphal, 2012] and the capacity of forming biofilm [McDougald et al., 2008]. It is an opportunistic pathogen and infects only humans with impairment of immune system, mucosal damages or antibiotic suppression of normal microbiome; thus, the most common infections are nosocomial urinary tract infections, skin infections in burn patients, airways infection in fibrosis cystic subjects [Ramphal, 2012]; moreover, in oral mucositis (OM) oncologic patients *P. Aeruginosa* was correlated with oral infections [reviewed by [Wong, 2014]] and with bacteremia [reviewed by [Donnelly et al., 2003]].
Furthermore, in the recent years *P. Aeruginosa* developed resistance to different types of antibiotics, leading to the worldwide issue of bacterial eradication [reviewed by [El Zowalaty et al., 2015]]. So, there is a global necessity of discover novel strategies to fight *P. Aeruginosa* infections.

Photobiomodulation Therapy (PBM) employing the blue spectrum of light (400-500 nm) is a promising treatment that has demonstrated its antibacterial action against a wide spectrum of bacteria as for example *Staphylococcus aureus, Streptococcus pneumoniae, Escherichia coli, and P. aeruginosa* [reviewed by [Wang et al., 2017b]]. There are also some recent studies that attested the efficacy of blue light also on *in vivo* models of infection and on patients [reviewed by [Wang et al., 2017b]]. The main bacterial endogenous chromophores that absorb the blue laser light are probable the porphyrins, in fact, bacteria presenting higher levels of these photosensitizers are more susceptible to laser light [reviewed by [Wang et al., 2017b]]. Probably the excitation of porphyrins increases reactive oxygen species (ROS) to a high lethal level that bacteria cannot counteract leading to cell death [reviewed by [Lubart et al., 2011]].

In the present study the anti-bacterial effect of blue laser light was investigated in *P. Aeruginosa* culture *in vitro* (both in solid agar surface, in planktonic conditions and visualizing the culture on microscopy) and in a murine *in vivo* model of infected abrasion. Moreover, with the aim of

disclosing the mechanism at the basis of antimicrobial properties, the oxidative stress was also evaluated. Finally, *P. Aeruginosa* mutants for enzymes of the porphyrin biosynthetic pathway (involved probably in the adsorption of blue light) were tested.

Materials and Methods

Pseudomonas Aeruginosa

Pseudomonas Aeruginosa (ATCC 27853) were cultured in Luria-Bertani (LB) broth at 37°C overnight in agitation overnight prior to experiments; moreover, the bacteria were also seeded on LB agar to check the morphology of colonies and the presence of eventual contamination. The day of experiments *P. Aeruginosa* culture were diluted in LB broth at a concentration of 10^8 CFU (colony forming unit) / ml (Optical Density O.D. = 0.1) and then prepared for the different experiments.

Growth on LB agar

P. Aeruginosa was inoculated on 45 mm petri dishes using a sterile cotton swab; afterwards, the plates were irradiated in specific areas, marked on the plastic. The following protocols were tested in blue, red and near infrared wavelengths (445 nm, 660 nm, and 970 nm): 0.2 W/cm^2 40 J/cm^2, 0.3 W/cm^2 40 J/cm^2, 0.4 W/cm^2 40 J/cm^2, 0.5 W/cm^2 40 J/cm^2, 1 W/cm^2 40 J/cm^2; all in CW. Subsequently the plates were incubated at 37°C and checked after 24 hours.

Growth on LB broth

P. Aeruginosa was inoculated in 96 multi-wells plates with a final concentration of 10^5 CFU for well in LB broth (100 µl). Instantly after seeding bacteria were irradiated with the following protocols: 445 nm, 660 nm, and 970 nm) with the power densities 0.2 W/cm^2, 0.5 W/cm^2, 0.7 W/cm^2, 1 W/cm^2, 1,5 W/cm^2, 2 W/cm^2 and energy fluency 60 J/cm^2, 60 J/cm^2 plus 60 J/cm^2 in two applications, 120 J/cm^2. The optical density at 600 nm of the multi-wells plate was measured at the multimode plate reading - PerkinElmer Envision (PerkinElmer, Waltham, Massachusetts, U.S.A.) immediately after irradiation and after 6, 12, 18 and 24 hours.

Bacteria Visualization

To investigate the effect of blue laser on bacteria, the irradiated cultures were observed on a high resolution Scanning Electron Microscope (SEM, Quanta250 SEM; FEI, Hillsboro, Oregon, U.S.A.). The specimens were prepared seeding *P. Aeruginosa* (100 µl of 10^5 CFU) bacterial

suspension on sterile a 13 mm diameter cover glasses on the bottom of plastic wells in LB growth medium. After 1 hour, the plates were irradiated with the laser at 445 nm or 970 nm (1 W/cm^2, 75 J/cm^2 or 150 J/cm^2). Subsequently the glasses were washed, fixed in paraformaldehyde 4% in Phosphate Buffered Saline for 1 hour, dehydrated with graded ethanol series (30, 50, 70, 95 (twice), 100 (twice) % V/V ethanol/water; 30' in each solution) and 1,1,1,3,3,3-hexamethyldisilazane (HMDS; Acros Organics, Springfield, NJ, U.S.A.) for 90 minutes. The coverslips were then mounted on metallic stubs, sputter-coated with gold and SEM images were obtained using different magnifications (300x, 2400x, 20.000x). The working distance and the accelerating voltage were adjusted to obtain the suitable magnification. The 300x magnification images taken from quadruplicates were analyzed using the ImageJ software to calculate the density of the remaining bacteria: every image was binarized and the quantity of white pixels, corresponding to the surface covered by bacteria, was obtained.

Blue LED light irradiation

To test if also another type of light, the blue LED, could have the same antimicrobial activities, a LED device providing 380-490 nm light (VALO LED curing light, Ultradent Products, Inc., South Jordan, Utah, U.S.A.) was tested on *P. aeruginosa*.

One hundred µl of *P. aeruginosa* (10^5 CFU) were inoculated in 96-well plates and irradiated (0.3 W/cm^2 combined with 60 J/cm^2 120 J/cm^2, CW). The OD_{600} of the wells was measured using a spectrophotometer at several time points: immediately after irradiation, and after 6, 12, 18 and 24 hours.

***Pseudomonas aeruginosa* knock-out for porphyrins**

Three *P. aeruginosa* knock out mutants were purchased from a PAO1 transposon mutant library [Kesting et al., 2009; Held et al., 2012] (Manoil Lab, UW Genome Sciences, University of Washington, Seattle, Washington, U.S.A.). The *P. aeruginosa* are knock out for the enzymes that convert glutanate-1-semialdehyde in 2-amino-levulinate in the porphyrin biosynthesis pathway [Hungerer et al., 1995] (figure 28, based on KEGG pathway at URL https://www.genome.jp/kegg-bin/show_pathway?pae00860). There are three different enzymes that could alternatively operate in this point of the pathway, PA3977 (PW7732, glutamate-1-semialdehyde 2,1-amino aminotransferase, gene *hemL*), PA4088 (PW7917, aminotransferase), PA5523 (PW10358, aminotransferase). Thus, these mutants should produce less uroporphyrinogen and protoporphyrin IX (figure 28), resulting less susceptible to laser light. One hundred µl of *P. aeruginosa* (10^5 CFU) were inoculated in 96-well plates and irradiated (power

0.3 W irradiance 0.18W/cm^2 fluence 60 J/cm^2, CW). After 24 hours, bacterial viability was checked spectrophotometrically.

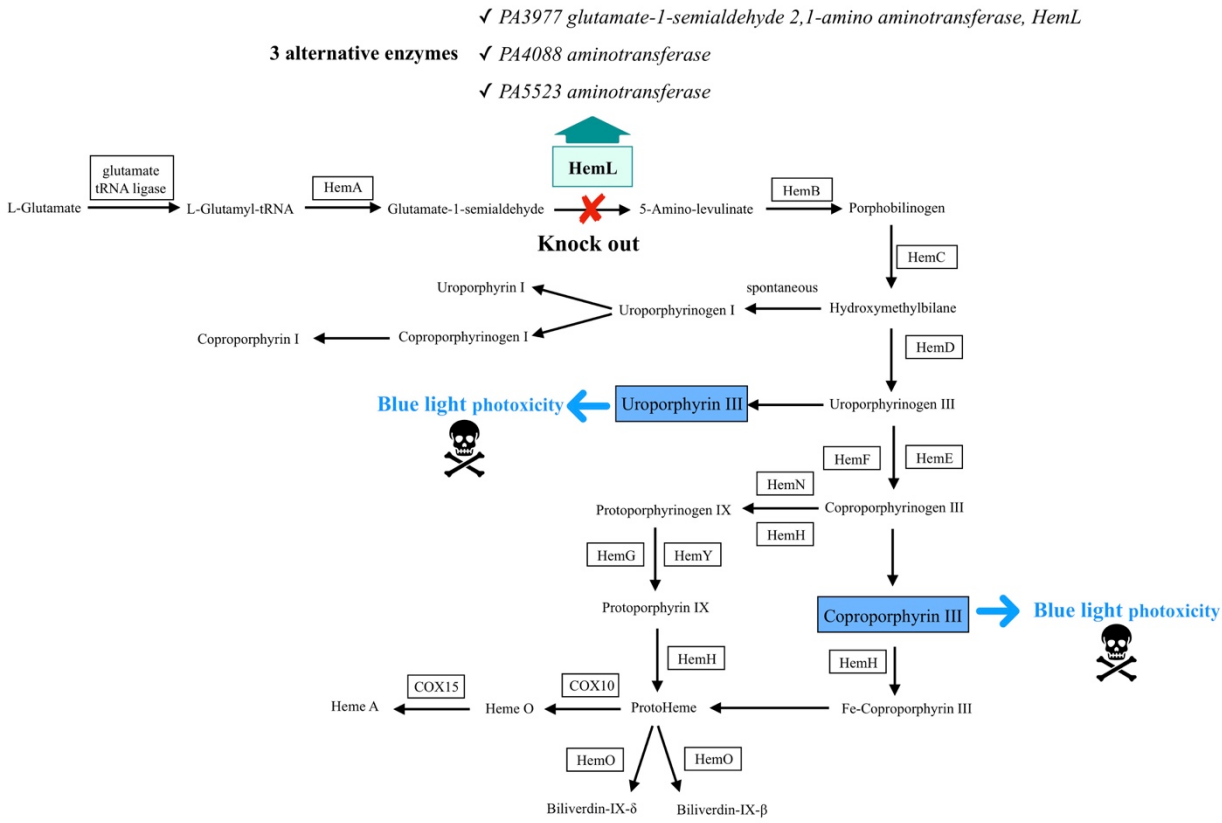

Figure 28. Porphyrin pathway in Pseudomonas aeruginosa.
In green the hemL gene that was knocked out in our bacteria is highlighted
In blue the two molecules involved in blue light photo-reception are highlighted

Total Oxidant Status

Since it has been postulated that the oxidative stress generation after PBM is the mechanism through which laser light exploits its action [reviewed by [Lubart et al., 2011]], total oxidant status, as a marker of oxidative stress, of bacteria was measured.

One hundred µL of bacterial suspension (10^5 CFU) were inoculated to a 96-well sterile plate and irradiated using the blue laser protocol 0.3 W/cm^2, 60 J/cm^2, CW. One hour after irradiation, the Total Oxidant Status (TOS) assay was performed [Erel, 2005]. Thirty-five µL of bacterial suspension were added to Reagent 1 (Reagent 1: xylenol orange 150 µM, NaCl 140 mM and glycerol 1.35 M in 25 mM H_2SO_4 solution, pH 1.75). The absorbance of the mixture was then read spectrophotometrically at OD_{560}. Subsequently, 11 µL of Reagent 2 (ferrous ion 5 mM and

o-dianisidine 10 mM in 25 mM H_2SO_4 solution) was added. After 5 minutes the solutions were gently mixed and a second end-point absorbance measurement at OD_{560} was performed.

Antioxidant compound addition

The antimicrobial activities of PBM was also evaluated after the addition of an antioxidant molecule to investigate if the presence of ascorbic acid could preserve the bacteria from the damaging.

One hundred µL with 10^5 CFU of bacterial suspension were inoculate in each well of a 96 wells plate and the bacteria were divided into four groups:

1) Not treated bacteria
2) Not treated bacteria with the addition of ascorbic acid (40 µM)
3) PBM (0.3 W/cm^2, 120 J/cm^2, CW) treated bacteria
4) PBM (0.3 W/cm^2, 120 J/cm^2, CW) treated bacteria with the addition of ascorbic acid (40 µM)

The optical density of the wells was measured at OD_{600} immediately after irradiation and after 24 hours. The experiment was performed in triplicate.

Blue Photobiomodulation Cytotoxicity

Human oral mucosa epithelial cells (TR146) were employed. TR146 was maintained in Ham's F12 culture medium with 10% fetal bovine serum, 100 U/ml Penicillin/Streptomycin, 2 mM Glutamine (Euroclone, Pero, Milan, Italy). Cells were seeded one day prior to experiment (50.000 cells/well in 24 multi-wells plate).

To test cell viability after 24 hours from blue laser (445 nm) irradiation, ATP production was assessed using the ATPlite luciferase assay (PerkinElmer, Waltham, Massachusetts, U.S.A.) accordingly with manufacturer's instruction.

***In vivo* Murine Skin Abrasion Infection Model**

P. Aeruginosa in vivo infection was examined developing a murine model of abrasion. *P. Aeruginosa* overnight culture was washed in PBS and diluted at 10^8 CFU/ml. Briefly, 15 C57BL/6 mice at 8 weeks of age were anesthetized peritoneally with xylazine/ketamine, shaved at the dorsal surface and the abrasions (about 13 mm x 13 mm) were performed with a sterile scalpel on the back of the animals. Immediately after the mice were infected topically with 20 µl of the bacterial suspension and randomly assigned at the treated (n=8) or not treated (n=7) group. After 30 minutes from infection, the animals of the laser group were treated with 0.3 W/cm^2, 60 J/cm^2, CW, on the infected abrasion (figure 29).

The mice were housed under controlled environmental conditions with food and water ad libitum for 24 hours, after which they were sacrificed for cervical dislocation and a skin biopsy (10 mm x 10 mm) was taken from each animal. Half tissue was placed in 2 ml of 10% buffered formalin to perform hematoxylin/eosin staining and histopathological examination. Half tissue was placed in in 2 ml of LB broth and vortexed for 1 minute: 10 µl were seeded on LB agar petri dishes for CFU counting and the rest maintained in broth for 24 hours and then the OD_{600} was read at the multimode plate reading - PerkinElmer Envision.

Animal care and treatment were conducted in conformity with institutional guidelines in compliance with Italian national (Decreto Legislativo 26/2014) and international laws and policies (European Union Directive 2010/63/EU). Animals were housed under controlled environmental conditions with a 12 hours light/dark cycle.

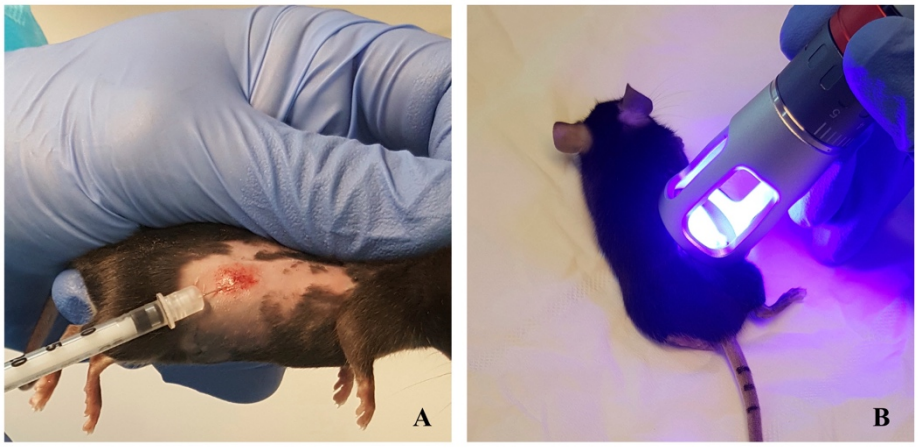

Figure 29. The experimental procedure performed in the in vivo model of infection.

A Skin abrasion infected applying 10^6 CFU of bacteria.

B Blue Photobiomodulation treatment.

Statistical Analysis

Kruskal Wallis test with Dunn's test for multiple comparison (for more than 2 groups) and Mann-Whitney test (for 2 groups) were used to evaluate the effect of PBM on irradiated compared to not irradiated bacteria or cells.

All statistical assessments were two-sided, and a p-value < 0.05 was used for the rejection of the null hypothesis.

Results and Discussion

The growing incidence of bacteria resistance to common antibiotics is still a problem for health care. It is also linked to higher cost for public service, for more expensive and toxic drugs that impact on patients increasing the days of recovery and possibly causing adverse effect. Thus, the research of novel antimicrobial therapy is urgently needed [reviewed by [Jasovský et al., 2016]]. To this end, the use of the antimicrobial properties of blue light emerges as a possible treatment, alone or in combination with photosensitizers or antibiotics, and it is worthy of consideration.
In our research we were able to show the strong laser blue activity against a gram negative bacteria, *P. aeruginosa* that in recent years developed resistance to various antibiotics [reviewed by [El Zowalaty et al., 2015]].

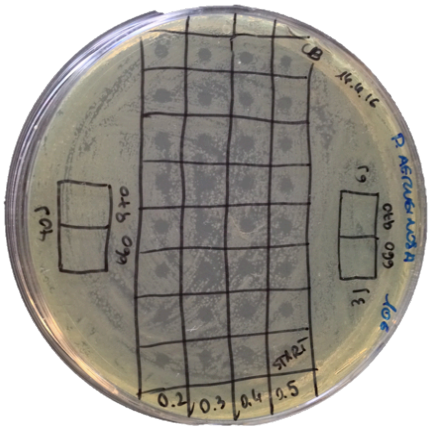

Only blue laser protocols at 445 nm exerted antimicrobial activity on agar plates causing a complete inhibition of bacterial growth on the area of irradiation, surrounded by a homogeneous layer of grown bacteria. Instead, the wavelengths at 660 and 970 nm did not exert any inhibition (figure 30).
To observe if the effect could be in somehow related to a degrading effect on the medium, the agar plates were irradiated before the seeding, but a uniform growth of bacteria was detected.

Figure 30. Representation of Blue Photobiomodulation effect on Pseudomonas aeruginosa on agar plate.
The experiments were performed in 3 replicates in 2 independent days.

The possible increment of temperature that could be related to bacterial damaging, was checked with the infrared camera: the maximum thermal increase registered was 33.7°C (figure 31).

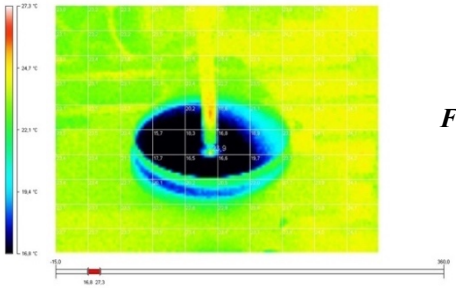

Figure 31. Thermal monitoring during irradiation

The protocols effective in eradicating planktonic bacteria were those involving blue laser light with λ at 445 nm. Specifically, all the protocols that employs 60 J/cm^2 were efficacious in reducing the bacterial growth over time. The use of 0.2 W/cm^2, 0.5 W/cm^2 and 0.7 W/cm^2 exerted stronger antimicrobial effect respect to 1 W/cm^2, 1.5 W/cm^2 and 2 W/cm^2. The 0.2 W/cm^2 protocol was the less effective, since at 24 hours the bacteria completely recovered (figure 32 A). The use of laser setting with 120 J/cm^2 in one dose or in two equal close doses were the most efficacious: all the test protocols exploited a complete inhibition of bacterial survival at 24 hours (figure 32 B and C). The use of alternative wavelength 660 and 970 nm did not show any antimicrobial effect (data not shown).

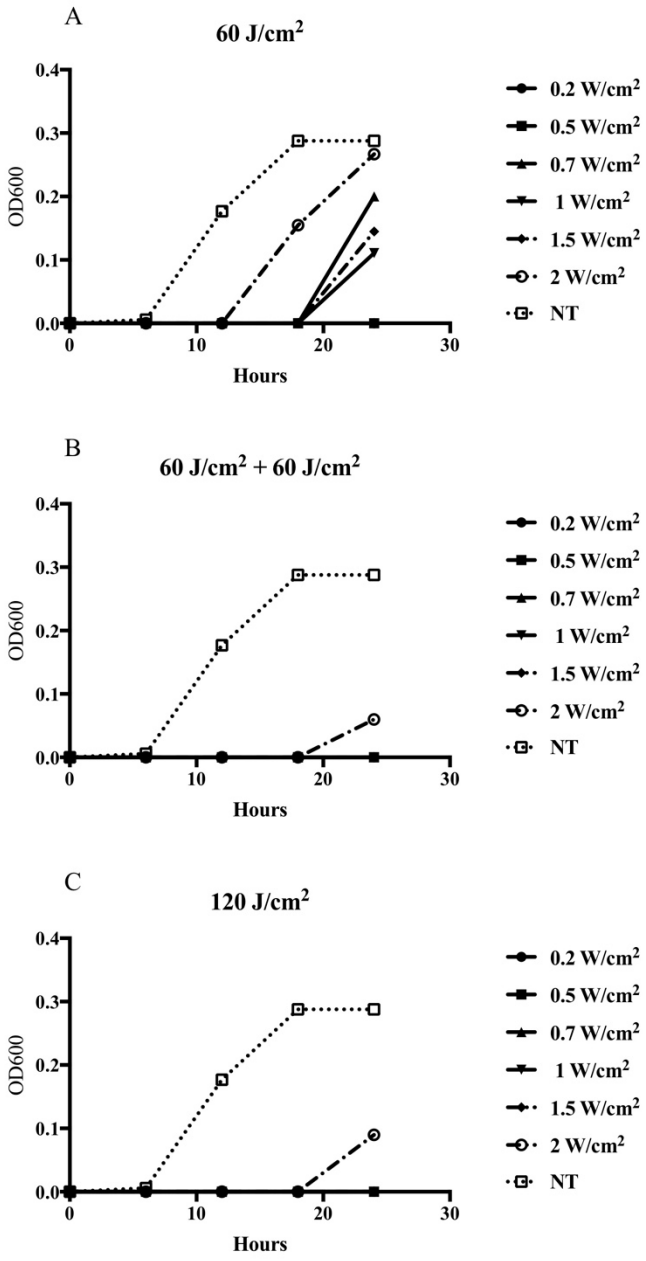

Figure 32. Pseudomonas aeruginosa growth in broth, after 0, 6, 12, 18, 24 hours from irradiation.

A Protocols with 0.2 W/cm^2, 0.5 W/cm^2, 0.7 W/cm^2, 1 W/cm^2, 1.5 W/cm^2, 2 W/cm^2 and 60 J/cm^2

B Protocols with 0.2 W/cm^2, 0.5 W/cm^2, 0.7 W/cm^2, 1 W/cm^2, 1.5 W/cm^2, 2 W/cm^2 and two doses of 60 J/cm^2

C Protocols with 0.2 W/cm^2, 0.5 W/cm^2, 0.7 W/cm^2, 1 W/cm^2, 1.5 W/cm^2, 2 W/cm^2 and 120 J/cm^2.

Bacterial visualization at the SEM showed a marked reduction in density after irradiation (Mann-Whitney test, p-value=0.03, figure 33 B), whereas the NIR wavelength did not present any effect. AT higher magnification (20000X), a higher frequency of damaged bacteria was seen: multiple blebs on the outer membrane and perturbed membrane morphology were visible (Figure 33 A).

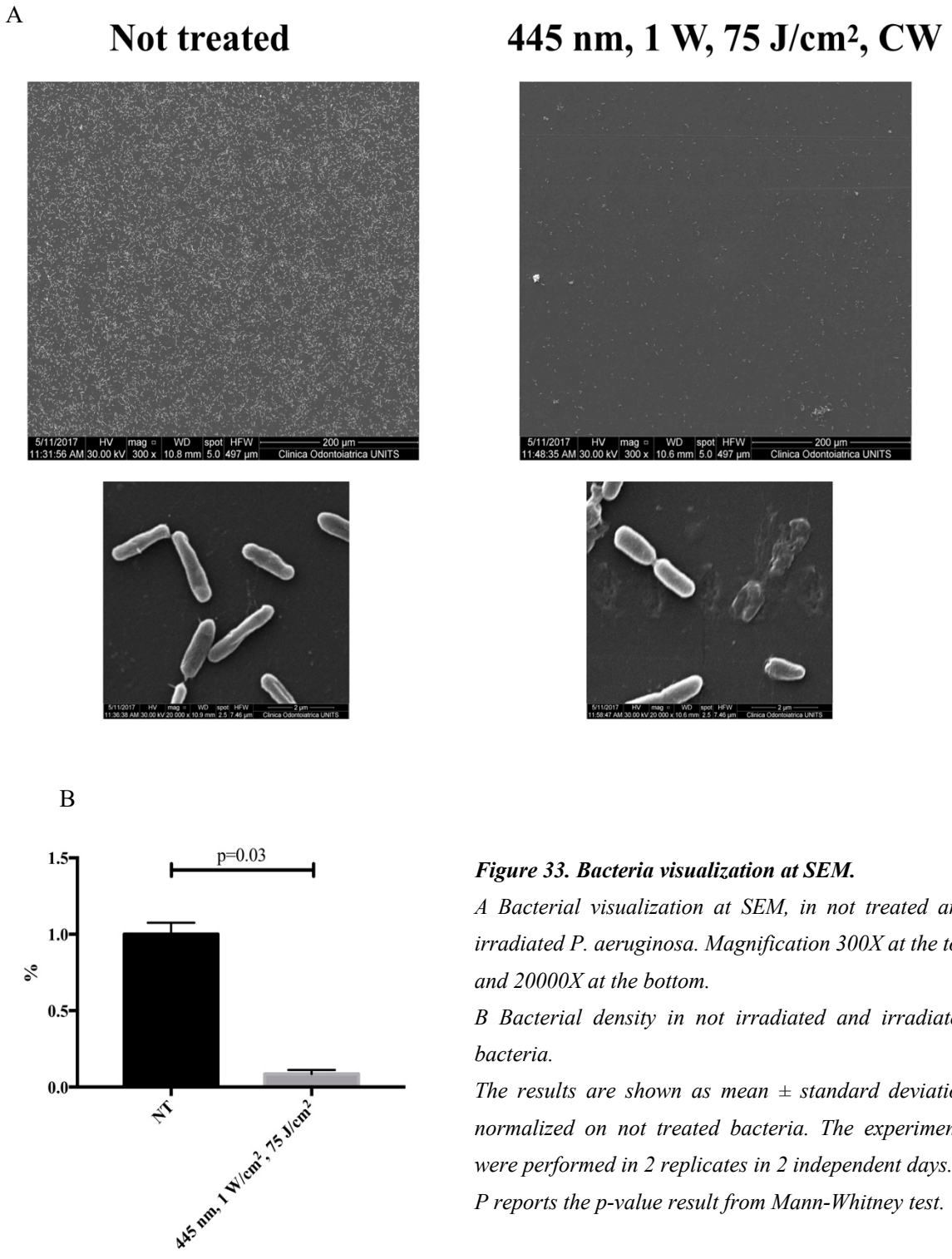

Figure 33. Bacteria visualization at SEM.

A Bacterial visualization at SEM, in not treated and irradiated P. aeruginosa. Magnification 300X at the top and 20000X at the bottom.

B Bacterial density in not irradiated and irradiated bacteria.

The results are shown as mean ± standard deviation normalized on not treated bacteria. The experiments were performed in 2 replicates in 2 independent days.

P reports the p-value result from Mann-Whitney test.

To test if the antimicrobial properties were due to the wavelength used and if another source of blue light could exert the same effect, thus confirming the photochemical effect, a planktonic growth curve assay was repeated using a blue LED light device. All the three blue LED light protocols (0.2 W/cm^2, 0.3 W/cm^2 and 0.5 W/cm^2) with 60 J/cm^2 inhibited bacterial growth with an initial rescue at 24 hours (Figure 34 A); similarly blue LED light protocols (0.2 W/cm^2, 0.3 W/cm^2 and 0.5 W/cm^2) with 120 J/cm^2 prevented bacterial survival, even if a slight increase in bacterial density with the protocols with 0.2 W/cm^2 was observed (Figure 34 B).

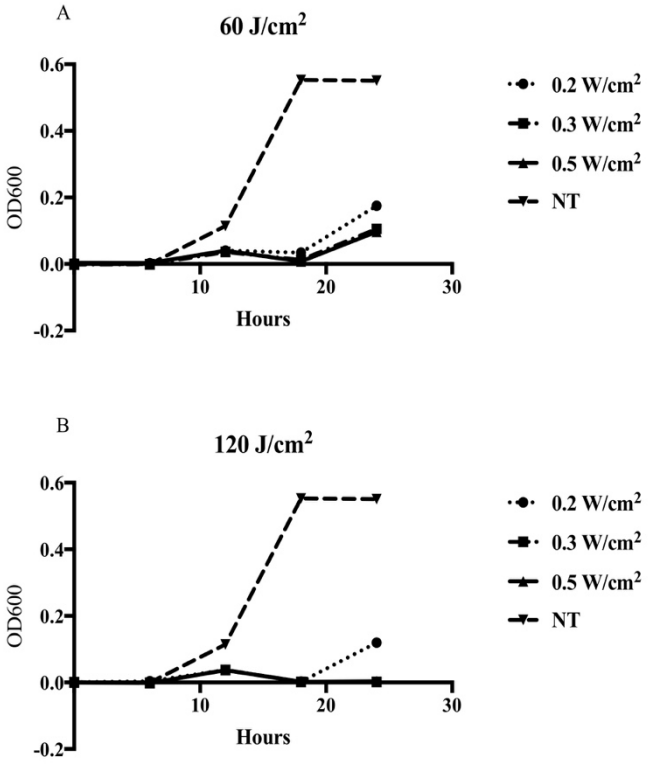

Figure 34. Pseudomonas aeruginosa growth after treatment with LED device

A P. aeruginosa growth after blue LED treatment with 0.2 W/cm^2, 0.3 W/cm^2, 0.5 W/cm^2 and with 60 J/cm^2

B P. aeruginosa growth after blue LED treatment with 0.2 W/cm^2, 0.3 W/cm^2, 0.5 W/cm^2 and with 120 J/cm^2

These results were comparable to those obtained with the diode laser device, although the diode laser was more effective in inhibiting completely the bacterial growth over time.

Prior to our results other works analyzed the effect of blue light on *P. aeruginosa*, although the most of research studies were conducted with LED instrument and not with diode laser machine. Our results partially disagreed the study by Amin et al. [Amin et al., 2016] that observed only a partial inhibition of bacterial growth after 40 minutes of LED treatment with 48 J/cm^2 and 0.02 W/cm^2. Similarly, de Sousa et al. [de Sousa et al., 2015], using lower fluence (6 J/cm^2, 12 J/cm^2, 18 J/cm^2, and 24 J/cm^2) respect to our experiments, reported a partial block of *P. aeruginosa*

growth. Instead, Fila et al. [Fila et al., 2017] showed a bacterial density under the limit of detection with 50 J/cm^2 and 0.009 W/cm^2.
The mean difference between diode laser and LED is the type of light that they emit: monochromatic wavelength for diode laser and polychromatic for LED. Moreover, diode laser possesses coherence and unidirectionality that LED lacks [Moskvin, 2017].

It has been hypothesized that intracellular bacterial photoreceptors for blue light should be endogenous porphyrins, in fact, for example *Propionibacterium acnes,* producing high level of these molecules, can be easily affected by visible light [Ashkenazi et al., 2003]. When endogenous porphyrins are excited by blue light and converted to their triplet state, they may generate free radicals from hydrogen or electron transfer (Type I), and/or they can produce singlet oxygen (Type II) [Foote, 1991]. The free radicals generation could react with cellular components damaging them and it could lead to cell death [Foote, 1991]. Specifically in *P. aeruginosa,* coproporphyrin III and uroporphyrin III should be the two main molecules produced that are excited by blue wavelength (about 405 nm) [Dai et al., 2013; Amin et al., 2016].
Thus, in our study, three different mutants for the enzymes that convert glutanate-1-semialdehyde in 2-amino-levulinate in the porphyrin biosynthesis pathway [Hungerer et al., 1995] (KEGG pathway at URL https://www.genome.jp/kegg-bin/show_pathway?pae00860) were employed: PA3977 (glutamate-1-semialdehyde 2,1-amino aminotransferase, gene *hemL*), PA4088 (aminotransferase), PA5523 (aminotransferase).
Thus, these mutants should produce less uroporphyrinogen (and so coproporphyrin III and uroporphyrin III), and protoporphyrin IX, being less susceptible to blue laser light, indeed, all the three mutants were more viable after PBM treatment respect to the wild-type (WT) *P. aeruginosa* (Kruskal-Wallis test p-value = 0.0000001, Dunn's multiple comparison test p-value = 0.01 for WT vs. PW5523; Mann-Whitney test WT vs. PA3977 p-value = 0.0002, WT vs. PA4088 p-value = 0.001, WT vs. PA5523 p-value= 0.001, figure 35), confirming the involvement of endogenous porphyrins in the blue light antimicrobial activity.

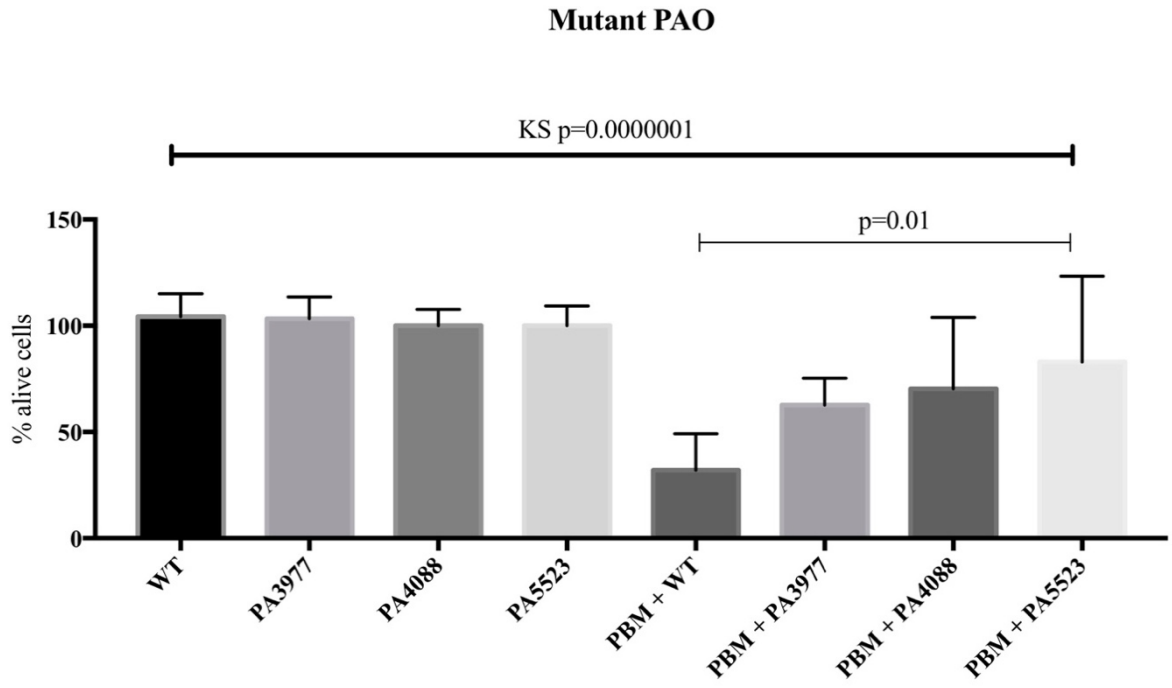

Figure 35. Survival of mutant Pseudomonas aeruginosa and wild type bacteria after blue laser treatment.
The results of irradiated cells are reported as % of alive cells ± standard deviation respect to the respective not treated strains. The experiments were performed in 12 replicates in 2 independent days.
KS p reports the p-value result from Kruskal-Wallis test, the other p reports the p-value result from Dunn's multiple comparison test.

Endogenous porphyrin are essential to elicit the photo-toxicity of blue light, but also the oxygen presence is required for the antimicrobial activity, indeed, the increment of oxygen in the bacterial culture during the irradiation increased the killing of *Staphylococcus aureus* [Maclean et al., 2008]. Comparably, *Porphyromonas gingivalis* and *Fusobacterium nucleatum* in anaerobic environment did not present susceptibility to light and the supplement of scavengers of ROS reduced photo-toxicity [Feuerstein et al., 2005].
Thus, the photo-toxicity could be oxygen dependent and could be related to ROS production at high level that are lethal for the bacteria.
In our study the oxidative stress was assessed by the TOS method. TOS was measured after irradiation, and an increase of TOS was observed in treated respect to not treated bacteria (Mann-Whitney test p-value=0.004, figure 36 A).

A second experiment was performed to see if the administration of ascorbic acid (a ROS scavenger) could revert the antimicrobial effect: the PBM treatment significantly reduced the *P. aeruginosa* viability (Kruskal Wallis test p-value=0.000007, Dunn's multiple comparison test p-value=0.0002, figure 36 B), but when the ascorbic acid was added, a rescue of *P. aeruginosa*

survival was obtained (Kruskal Wallis test p-value=0.000007, Dunn's multiple comparison test p-value=0.0004, figure 36 B).

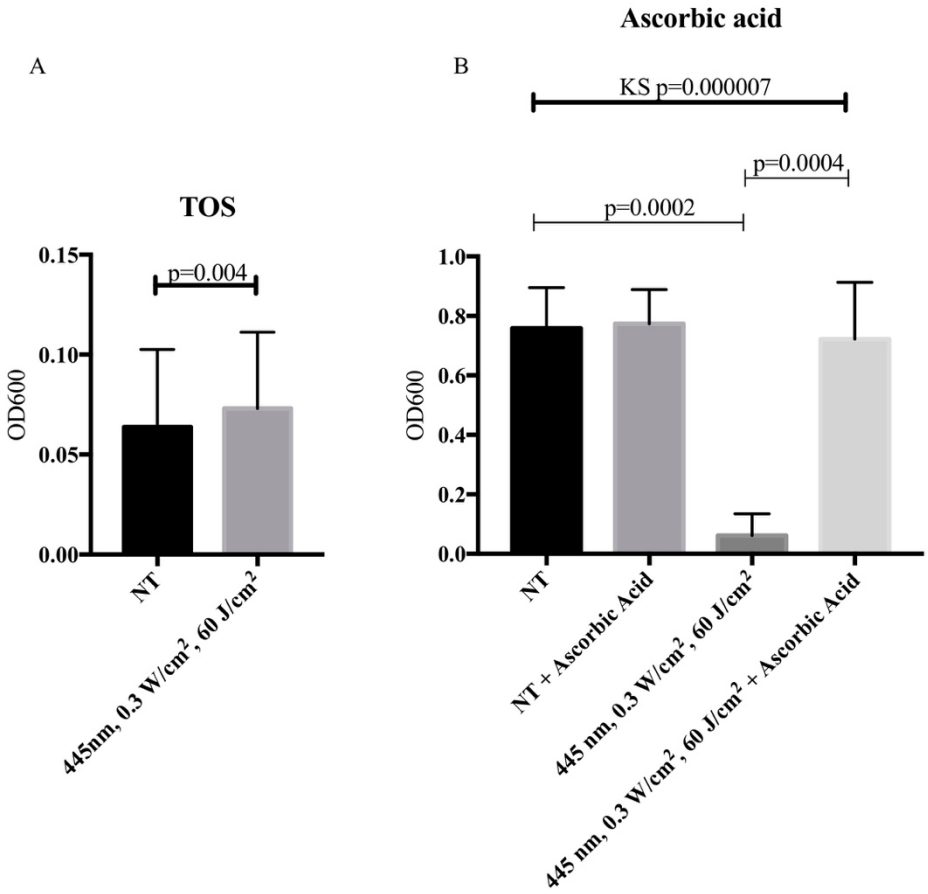

Figure 36.Oxidative stress in irradiated and not irradiated bacteria.

A Total oxidant status (TOS) measured in treated and not treated bacteria.

The results are reported as mean ± standard deviation.

P reports the p-value result from Mann-Whitney test.

B Bacterial survival after the treatment with ascorbic acid (a ROS scavenger) in irradiated and not irradiated bacteria.

The results are reported as mean ± standard deviation. The experiments were performed in 24 replicates in 2 independent days.

KS p reported the p-value result from Kruskal Wallis test, the other p the p-value results from Dunn's multiple comparison test.

Our results confirmed the previous literature reporting an increased amount of ROS production after blue light irradiation in *Escherichia Coli* and *Staphylococcus aureus* [reviewed by [Lubart et al., 2011]].

However, the ROS involvement in *P. Aeruginosa* was never assessed. Our results highlighted the higher production of ROS after PBM treatment confirmed the prior data on other type of bacteria [reviewed by [Lubart et al., 2011]]. Moreover, the addition of ascorbic acid, a scavenger of ROS, rescued the survival of the bacteria, corroborating the hypothesis that oxidative stress induced by PBM was lethal for the cells.

To assess if the protocols employed were specific for bacteria species but not toxic for eukaryotic cells, the viability of TR146 epithelial cells (model of oral buccal epithelium derived from well-differentiated keratinizing squamous cell carcinoma) was assessed. At 24 hours or 30 minutes from irradiation, ATP production was not affected by blue light (figure 37 A and B), never the metabolism tested using MTT assay (figure 37 C), so confirming the specificity of blue laser antimicrobial action.

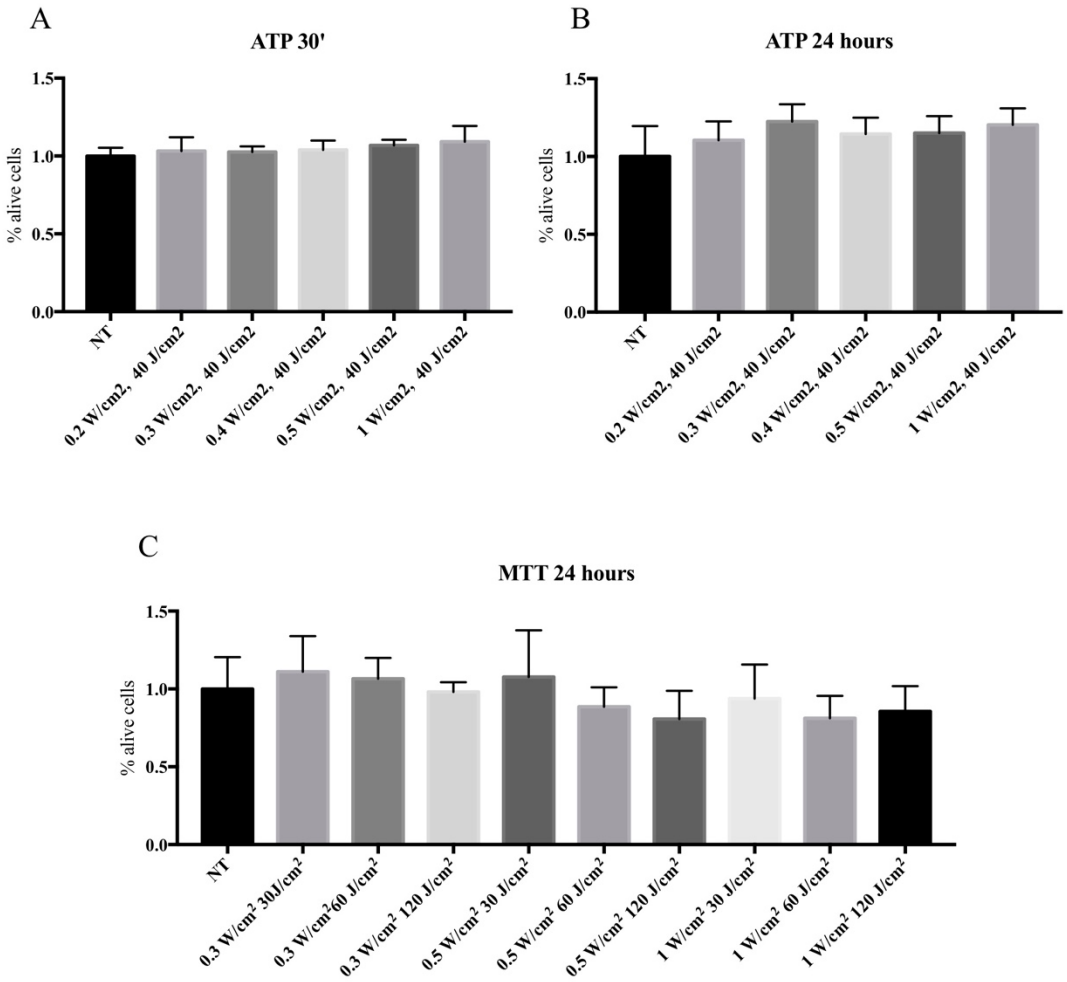

Figure 37. Cellular metabolism after Blue Photobiomodulation Therapy.

A ATP production after 30' from irradiation.

B ATP production after 24 hours from irradiation.

C Metabolism assessment using MTT test after 24 ours from irradiation. The experiments were performed in 4 replicates in 2 independent days.

The results are reported as percentage ± standard deviation of alive cells respect to the not treated group.

The *in vitro* experiments on cells were also helpful for assaying that blue PBM can be applied also on keratinocytes *in vivo* without causing skin damage; on the other hand, all the experiments performed on *P. aeruginosa* were needed for select the best protocol in term of antimicrobial activity. Therefore, the last experiment was performed *in vivo* developing a murine model of skin abrasion infected with *P. aeruginosa* that was irradiated with the protocol 0.3 W/cm^2, 60 J/cm^2, CW. After 24 hours from irradiation the skin abrasions were processed and after another 24 hours bacterial growth was checked.

P. aeruginosa viability decreased both in agar plate, counting the colonies and in broth, measuring well turbidity spectrophotometrically (Mann-Whitney test p-value = 0.003 and p-value = 0.03 for count in agar and in broth respectively; figure 38 A and B). All laser treated samples remained below 3 x 10^3 CFU/ml (with only one complete eradication of bacteria), while in not treated samples, the results were heterogeneous but always higher than 2 x 10^3 CFU/ml.

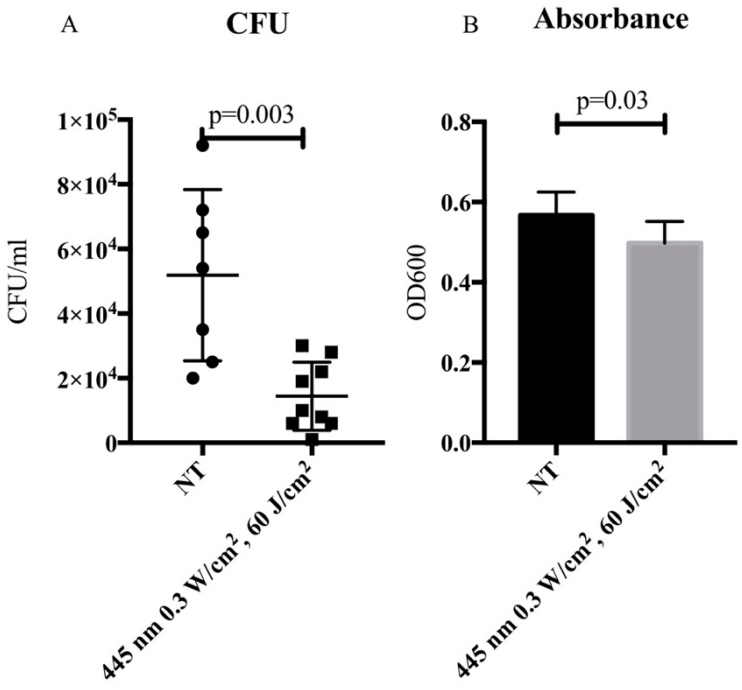

Figure 38. In vivo murine model of skin abrasion infection.

Mice were infected with P. aeruginosa, half animals were irradiated. After 24 hours the skin abrasions were collected and maintained in LB broth for other 24 hours, moreover, 10 µl of broth were seeded on agar plate and checked after 24 hours for colonies growth.

A. CFU count in treated and not treated samples

B. Absorbance at OD600 of LB broth in treated and not treated samples.

The results are reported as mean ± standard deviation. The experiments were performed on 15 animals, 8 treated and 7 not treated in 2 independent days.

P reported the p-value results from Mann-Whitney test.

The histological examination of the skin samples showed that epithelium thickness was reduced in all samples. Three samples (PBM 1, PBM 3 and PBM 4) presented thermal damage that remained always in the external half of the epithelium layer (28.6 µm, 40.9 µm and 117.8 µm respectively; mean depth of thermal damage = 23.4 ± 41.4 µm). In samples PBM 1 and PBM 3, there were a visible purulent inflammatory infiltrate/abscess. In the other treated samples, there were modest inflammatory infiltrations throughout dermal and hypodermal layers (figure 39).

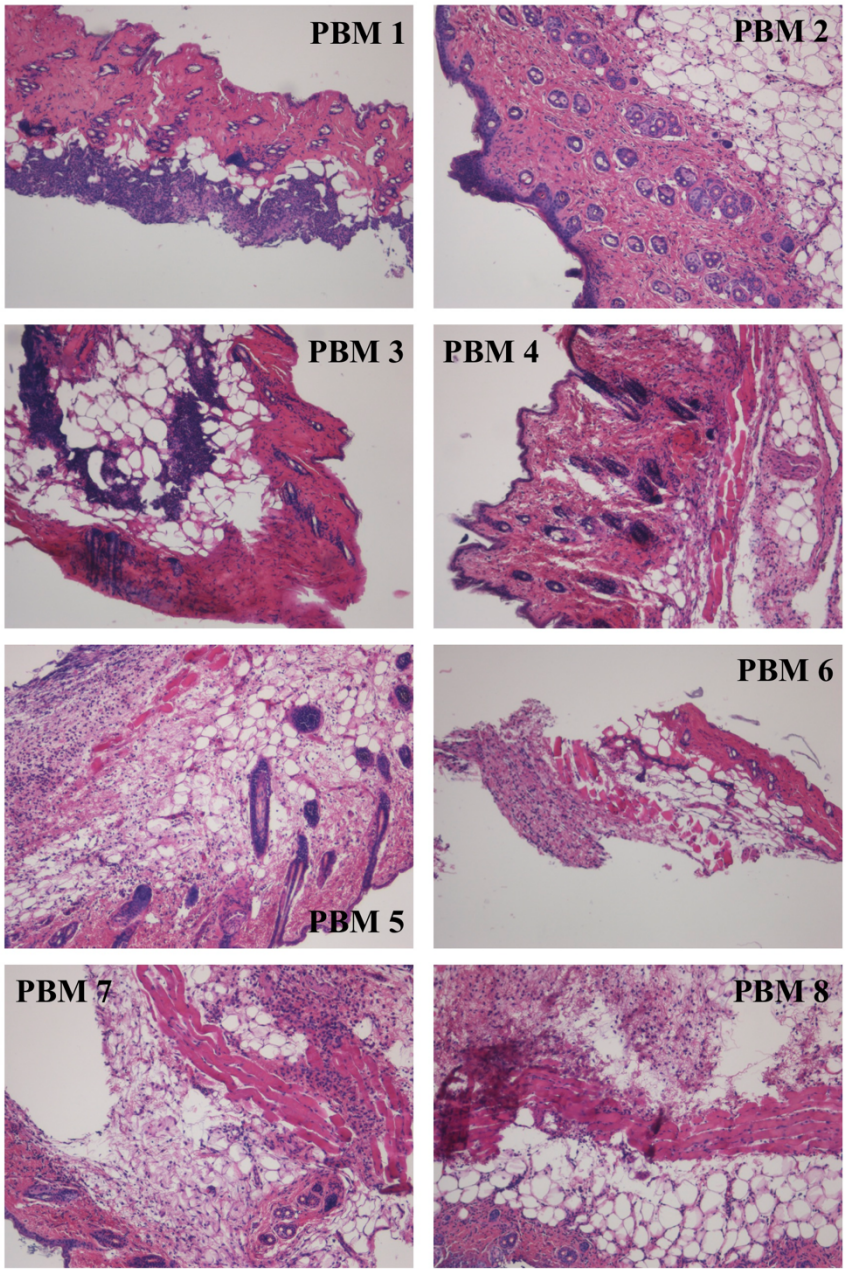

Figure 39. Epidermal, dermal and muscular tissues stained with hematoxylin and eosin in laser treated animals. (10x magnification) (n=8)

In all not treated samples, the epidermal layer was visibly and importantly permeated by inflammatory infiltrate with inflammation rate increased respect laser treated animals. In sample NT 1, inflammation was extended to the muscle. In samples NT 2, NT 3, NT 4, NT 5, NT 6, NT 7, inflammation was extended to the hypodermal layer (figure 40).

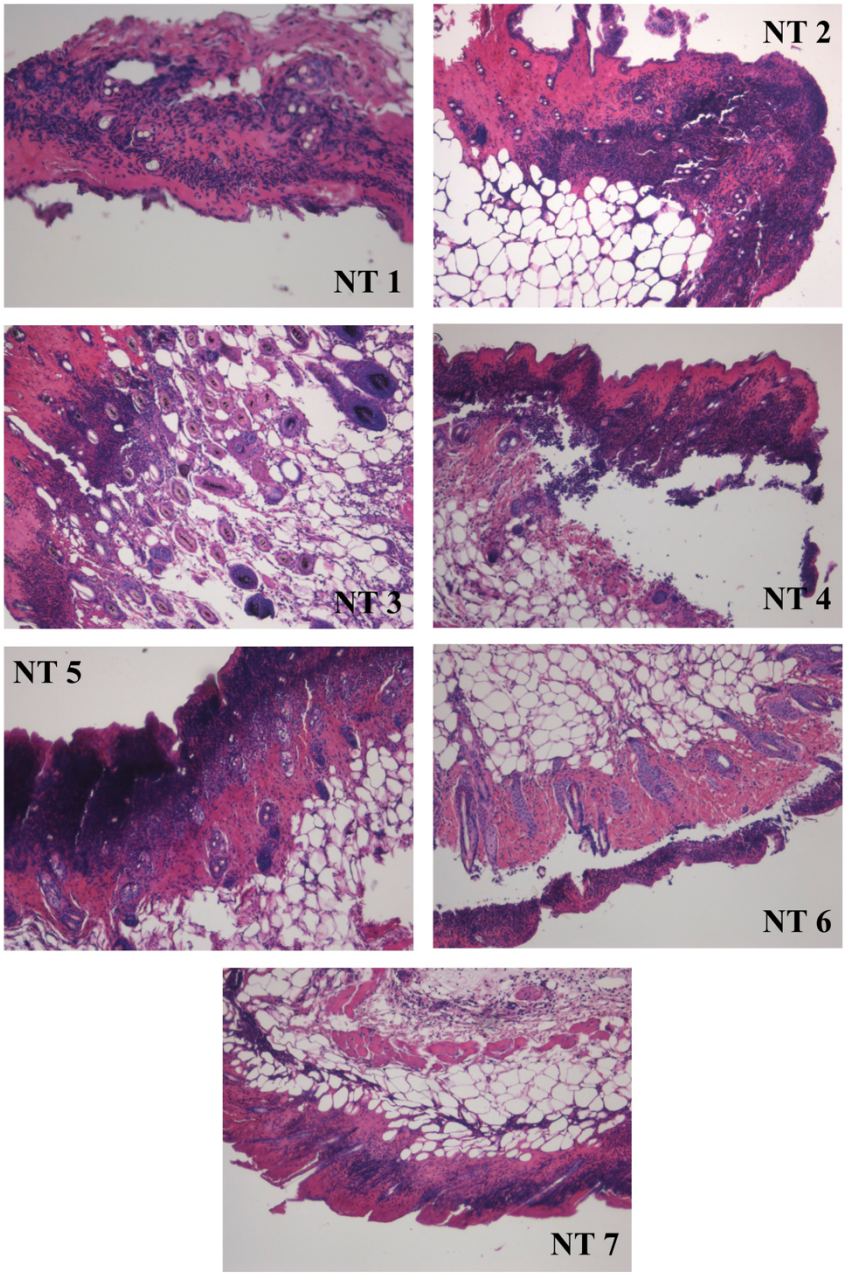

Figure 40. Epidermal, dermal and muscular tissues stained with hematoxylin and eosin in not treated animals. (10x magnification) (n=7)

Our results agreed with previous studies performed on *P. aeruginosa* murine skin infection performed through abrasion [Amin et al., 2016] and burn wounds [Dai et al., 2013] with lasers protocols similar to ours.
Other than the antimicrobial effect, an important achievement was related to the skin histology investigation. A very low thermal damage was detectable in only 3 samples, but the great difference was correlated to the inflammation rate: all not irradiated samples presented the dermal and epidermal layers permeated with a huge inflammatory infiltrate, while in laser treated specimens the epidermal layer was free from inflammatory infiltrate.
To date one study investigated the outcome of blue light irradiation on normal skin of healthy volunteers reporting no burn lesions on treated areas [Kleinpenning et al., 2010].
To note, few studies tested the clinical application of blue laser light. Blue LED light inhibited the growth of oral bacteria on teeth of gingivitis patients [Genina et al., 2015] and the growing of *Porphyromonas gingivalis* and *Prevotella intermedia* in healthy volunteers [Soukos et al., 2015] with reduction of dental plaques [Genina et al., 2015; Soukos et al., 2015]. Blue light decremented also the concentration of *Helicobacter pylori* in the stomach [reviewed by [Dai et al., 2012]]. Finally, blue PBM therapy is currently used for the topical treatment of acne vulgaris, although the real impact on microbial load was not reported by the studies [reviewed by [Dai et al., 2012; Ablon, 2018]].

Our results highlighted the strong antibacterial property of blue PBM, both *in vitro* and *in vivo*, determining also the mechanisms at the basis of the activity, the ROS production, and confirming the involvement of porphyrins in the photoreception of blue light.

Blue Laser antiviral action on Herpes Simplex Virus type 1

Herpes simplex virus type 1 (HSV-1) is a double strand DNA virus member of the *Herpeviridae* virus family, a known viral agent able to cause lifelong infections in the human species. The HSV-1 infection occurs through oral mucosa or damaged skin, then, in the epidermis and in the dermis, the virus begins its replication [Corey, 2012]. After this first infection, HSV-1 is able to infect peripheral sensory nerve endings and establishes latency in the neuronal cell body in the trigeminal ganglia; from here HSV-1 reactivation can lead to the viral spreading to muco-cutaneous surfaces [Corey, 2012]. The first infection is clinically characterized by gingivostomatitis and pharyngitis, meanwhile the virus reactivation causes the recurrent herpes labialis, a condition that presents intraoral mucosal ulcerations, or blisters on the mouth or on external facial skin, often designated as "cold sores" that are painful and uncomfortable for the people affected [Corey, 2012].

It is estimated that about 90% of the population under the age of 50 presented immunoglobulin against HSV-1 but only in the 67% of them the virus causes the recurrent infective episodes [World Health Organization, 2017].

Patients are normally treated with anti-viral drugs, like acyclovir, famciclovir or valacyclovir, however it has been reported cases of acyclovir resistant strains; moreover, some patients are unable to follow the treatment, (e.g. for allergy), and in immuno-compromised individuals, (for example due to radio-chemotherapy in oncologic patients both adult and pediatric), the problem of HSV-1 infection prevention remains a main issue, and anti-viral drugs are administered as prophylaxis [Corey, 2012; World Health Organization, 2017]. To note, the current anti-viral treatments show only a reduced effect in decreasing the occurrence of infections [reviewed by [Opstelten et al., 2008]].

So, the study of novel treatments for HSV-1 infection worldwide is an interesting and important topic, especially in the pediatric oncologic field where the management of immunocompromised patients requires special attention by clinicians [Carrega et al., 1994; Glenny et al., 2010].

The Photobiomodulation (PBM) therapy is a promising treatment that in the recent years has been used in HSV-1 infections, using red, near infrared (NIR) or infrared (IR) wavelengths. The previous studies reported that PBM was able to lead to a significantly reduction in herpes labialis recurrence, in the duration of herpetic sores, in painful sensations; moreover, no study reported side effects [reviewed by [de Paula Eduardo et al., 2013]].

Although we and other authors reported [reviewed by [Wang et al., 2017b]] the antimicrobial action of blue PBM, until today, this laser was not tested on viruses.

The possible antiviral effects of the blue laser light was tested irradiating HSV-1 alone and transferring it to keratinocyte cells to discover if PBM could reduce virus infectivity; irradiating keratinocyte cell culture already infected with HSV-1 to investigate the possible action on virus spreading and replication in a model more similar to the *in vivo* situation; moreover, the laser was delivered on keratinocyte cell culture prior to infection to see if the irradiation was able to render the cells more resistant to infection.

Materials and Methods

HSV-1 culture infection

HaCaT (human skin keratinocytes spontaneously immortalized) were used to mimic the HSV-1 skin infection. Cells were culture in DMEM (with 4.5 gr/L glucose, without L-Glutamine and Phenol Red, 12-917F, Lonza, Basel, Switzerland) culture medium supplemented with 10% fetal bovine serum, 100 U/ml Penicillin/Streptomycin, 2 mM Glutamine (Euroclone, Pero, Milan, Italy) and seeded in 96 multi-wells plates in 100 µl of final volume per well at cells density of 10^4 cells/well.

After 24 hours they reached a confluence of 70 - 80% and they were infected with different concentration of HSV-1 and incubated for 24 hours at 37°C and 5% CO_2. After 24 or 48 hours the cells vitality was measured using the MTT cell proliferation colorimetric assay (Trevigen) following manufacturer's instructions and the absorbances were read at a GloMax®-Multi Detection System (Promega, Fitchburg, Wisconsin, U.S.A.). At the same time point the supernatants were collected to determine HSV-1 viral load. Briefly HSV-1 nucleic acids were extracted from supernatants using the ZR Viral DNA/RNA Kit™ (Zymo Research, Murphy Ave., Irvine, CA 92614, U.S.A.). Five µl of DNA was then quantified in Real Time PCR amplifying viral glycoprotein B with a probe (forward primer GCATCGTCGAGGAGGTGGAC, reverse primer TTGAAGCGGTCGGCGGCGTA, probe FAM CGACCCCTCCCGGTAGCCGT, (Sigma, St. Louis, Missouri, U.S.A.) [Frobert et al., 2008] and the Kapa Probe Fast Universal One-step qRT-PCR kit (Kapa Biosystems, Inc. Wilmington, Massachusetts U.S.A.) on LightCycler® 480 Instrument II (Roche Molecular Diagnostics, F. Hoffmann-La Roche AG, Basel, Switzerland).

The HSV-1 viral load quantification was performed using a home-made standard derived from initial virus expansion on HaCaT cells quantified by the diagnostic kit HSV1 Q – PCR Alert Kit (ELItechgroup, Puteaux, France).

Laser cytotoxicity

Cells and virus were irradiated with protocols of λ 445, 0.1-1 W/cm^2, fluency 10-120 J/cm^2, in continuous (CW) or pulsed waves.

The PBM was tested on HaCaT cell culture to detect the maximum dose tolerated by the cells: cells vitality was measured 24 hours after irradiation using MTT Cell proliferation assay (Trevigen).

Antiviral effect of PBM

To test the antiviral effect of PBM, five different experimental setting were chosen:

Setting 1. Irradiation of HSV-1 virus alone: the virus kept in DMEM without phenol red and irradiated with the protocol 445 nm, 0.30 W/cm^2, 60 J/cm^2, CW in a final volume of 150 µl, after 30' from irradiation the virus was transferred to cells and maintained in incubator for 24 hours.

Setting 2. Irradiation of HSV-1 virus alone: the virus kept in DMEM without phenol red and irradiated with the protocol 445 nm, 0.15 W/cm^2, 30 J/cm^2, 5 Hz in a final volume of 150 µl, after 30' from irradiation the virus was transferred to cells and maintained in incubator for 24 hours.

Setting 3. Irradiation of culture then infected with HSV-1: cells were irradiated with the protocol 445 nm, 0.15 W/cm^2, 30 J/cm^2, 5 Hz and then infected for 24 hours with HSV-1 in incubator.

Setting 4. Irradiation of established HSV-1 infected culture: the cells were infected for 24 hours, after this time the wells were irradiated with the protocol 445 nm, 0.15 W/cm^2, 30 J/cm^2, 5 Hz and then kept in incubator for 24 hours.

Setting 5. Irradiation of HSV-1 infected culture: the cells were infected for 1 hour, after this time the wells were irradiated with the protocol 445 nm, 0.15 W/cm^2, 30 J/cm^2, 5 Hz and then kept in incubator for 24 hours.

At the end of the experiments, for each setting, cells vitality was tested using the MTT Cell proliferation assay (Trevigen), while the HSV-1 viral load was measured using Real Time PCR as described above.

Moreover the plaque forming unit (PFU) assay was performed, since it is a method allowing to quantify the real infectivity of HSV-1 [Baer, and Kehn-Hall, 2014]: after 24 hours from irradiation, 200 µl of the supernatant at different dilution were used to infect monolayers of Vero cells in 24 multi-wells plate for 2 days, after which the plates were fixed with paraformaldehyde 4% in Phosphate Buffered Saline for 30 minutes and colored with crystal violet (Merck KGaA, Darmstadt, Germany).

Figure 41 represents schematically the setting employed.

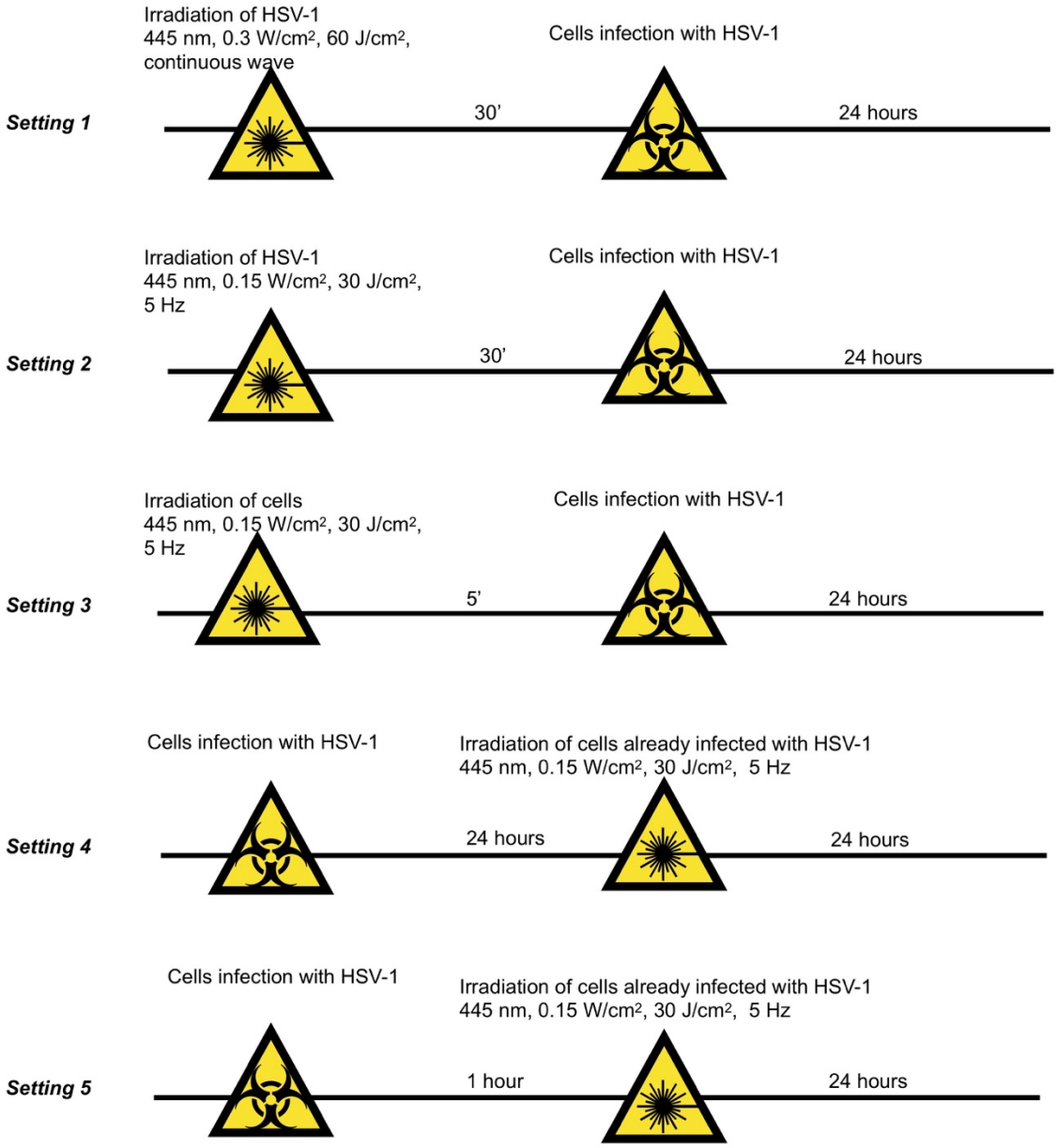

Figure 41. Schematic representation of experimental settings employed.

Statistical Analysis

Mann-Whitney test were used to evaluate the effect of PBM on viral load of irradiated compared to not irradiated virus and the cells viability between the treatments.

All statistical assessments were two-sided, and a p-value < 0.05 was used for the rejection of the null hypothesis.

Results and Discussion

To choose the better concentration of HSV-1, five different concentration of HSV-1 were tested in order to obtain the condition in which it is possible to see a medium mortality of the cells (about 50%): therefore, the viral concentration of 540000 viral copies/µl was chosen (data not shown). The HSV-1 employed for the experiments derived from a clinical isolate of HSV-1 showing a 99% identity with the TG3 strain (sequence ID: HQ686001) in a 300 base pair region of the thymidine kinase gene.

Instead, to determine the laser doses tolerated by the cells, different protocols were tested: λ 445, irradiance 0.1, 0.15, 0.2, 0.3, 0.5, 0.8, 1 W/cm^2, fluency 10, 20, 30, 60, 120 J/cm^2 for each irradiance, both in continuous (CW) and pulsed (frequency = 5 Hz) waves. Irradiance 0.15 W/cm^2, fluency 30 J/cm^2, 5 Hz was the higher protocol that did not present cytotoxic effects.

HSV-1 was diluted to a concentration of 540000 viral copies/µl from stock and irradiated with the following protocol: 0.3 W/cm^2, 60 J/ cm^2, CW. This protocol was chosen since its bactericidal efficacy was previously tested on *Pseudomonas aeruginosa*.
After 24 hours from irradiation it was possible to see a statistically significant decrease in viral load in the samples that were infected with irradiated virus respect to not irradiated ones (Mann-Whitney test, p-value = 0.001, figure 42 A). Confirming this result, vitality of cells infected with irradiated virus increased respect to the cells infected with not irradiated virus (Mann-Whitney test, p-value = 0.0001, figure 42 B).
To test the same experimental setting, but with a protocol that was not cytotoxic, HSV-1 was also irradiated with protocol 0.15 W/cm^2, fluency 30 J/cm^2, 5 Hz.
An analogue result was observed: there was a statistically significant decrease in viral load in the samples infected with irradiated virus respect to not treated (Mann-Whitney test, p-value = 0.03, figure 42 C) but the viability of the cells was not affected (figure 42 D).

These results suggested that PBM was probably able to act directly on the virion, possibly altering some vital structure of the microorganism. Prior to this study, no other work reported the antiviral activity of blue laser light, so we can only hypothesize what is the mechanism of action causing viral inactivation. It was reported that ultra pulsed laser treatment could act on enveloped virus producing selective aggregation of viral capsid and tegument proteins leading to virus inactivation without affecting the global structure or the nucleic acid. The aggregation was

probably due to disruption of hydrogen bonds and/or hydrophobic interactions inducing unfolding of proteins [Tsen et al., 2012].

A similar mechanism could be induced by blue laser light, but this was only a speculation and further studies in this field are needed to elucidate this issue.

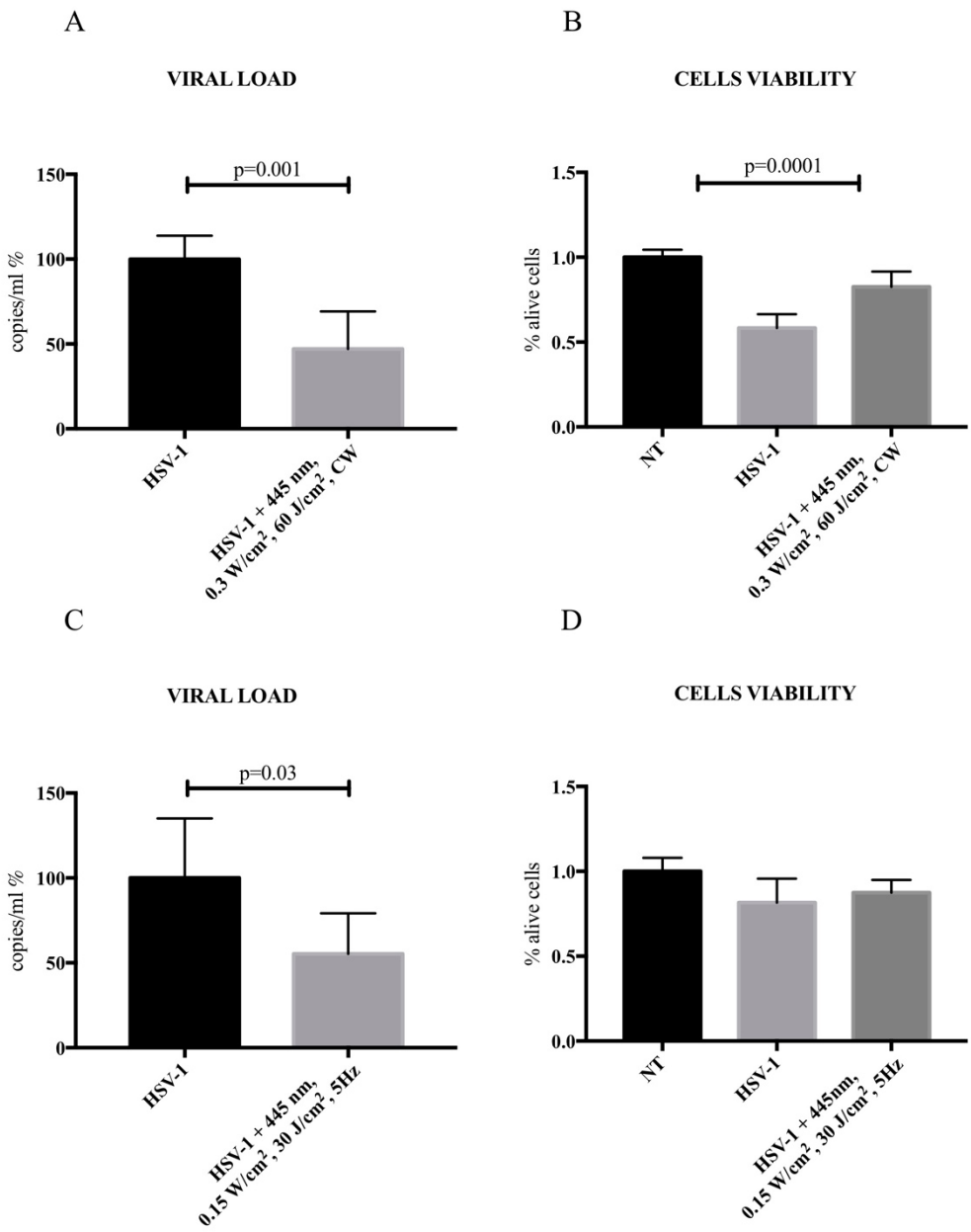

Figure 42. Antiviral effect of Blue Photobiomodulation Therapy

A HSV-1 quantification after 24 hours from laser irradiation (445 nm, 0.30 W/cm^2, 60 J/cm^2, CW) of virus alone (setting 1) normalized on not irradiated virus (designed as HSV-1).

B Cells vitality after 24 hours of infection with irradiated (HSV-1 + 445 nm, 0.30 W/cm^2, 60 J/cm^2, CW) or not irradiated virus (HSV-1) (setting 1) normalized on not treated cells (NT).

C HSV-1 quantification after 24 hours from laser irradiation (445 nm, 0.15 W/cm^2, 30 J/cm^2, 5 Hz) of virus alone (setting 2) normalized on not irradiated virus (designed as HSV-1).

D Cells vitality after 24 hours of infection with irradiated (HSV-1 + 445 nm, 0.15 W/cm^2, 30 J/cm^2, 5 Hz) or not irradiated virus (HSV-1) (setting 2) normalized on not treated cells (NT.)

The results are reported as percentage respect to untreated cells (NT), mean ± standard deviation. The experiments were performed in 6 replicates for viral load quantification and in 16 replicates for cellular viability in two independent days.

P report the p-value results from Mann-Whitney test.

To test if the laser light could render irradiated cells more resistant to infection, cells were submitted to PBM prior to the infection, but no change in vitality or viral load was detected (data not shown).
To test if PBM could be efficacious also in the situation of an already established infection, cells infected for 24 hours or 1 hour were irradiated but also in these conditions PBM was not able to modify viral load or cell vitality: only a trend of decrement of viral load in cells infected by 1 hour was possible to notice, but the statistically significance was not achieved (data not shown). These data indicated that PBM was less effective when the virus was inside the cells where it was in some way protected by cell membrane.

The experiment of plaque assay instead showed a decrease of PFU with setting 1, 2, 3 and 5 (figure 43). The Real Time PCR techniques is commonly used to quantify the viral load, however, the PFU assay allow to detect the real infectious particles. With this test it was possible to recognize a marked reduction of PFU with the PBM treatment, more significant respect to PCR. Maybe, since the genome was replicate before virion assembly [Corey, 2012], PBM could act mainly on virus formation or infectivity in the last phases of virus cycle inside the cells.

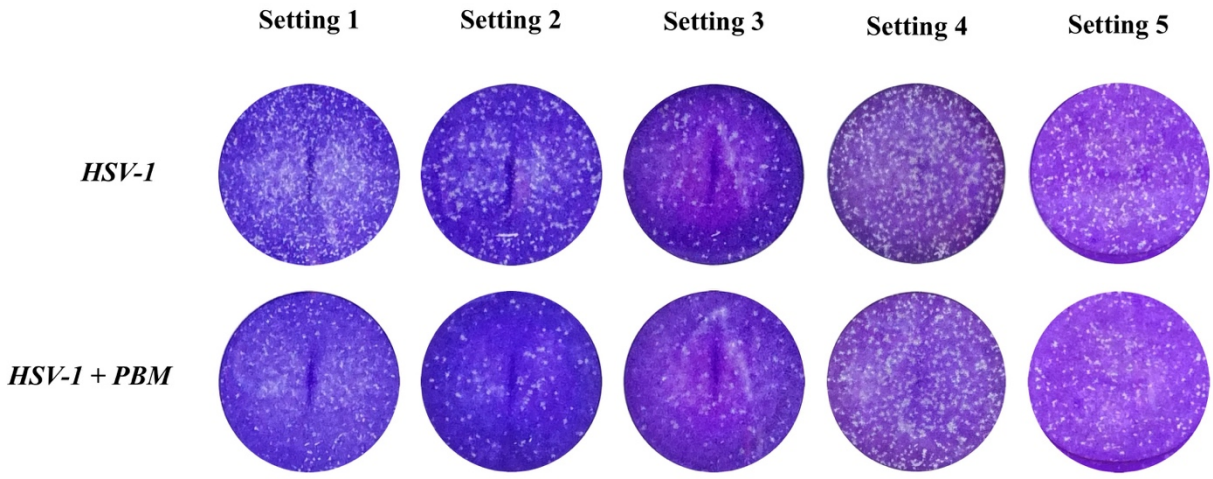

Figure 43. Representative images of PFU assay, performed using the five settings.
The experiments were performed in 3 replicates in two independent days.

Finally, the effect is not linked to thermal increment, since the temperature measured during irradiation is 25°C (figure 44).

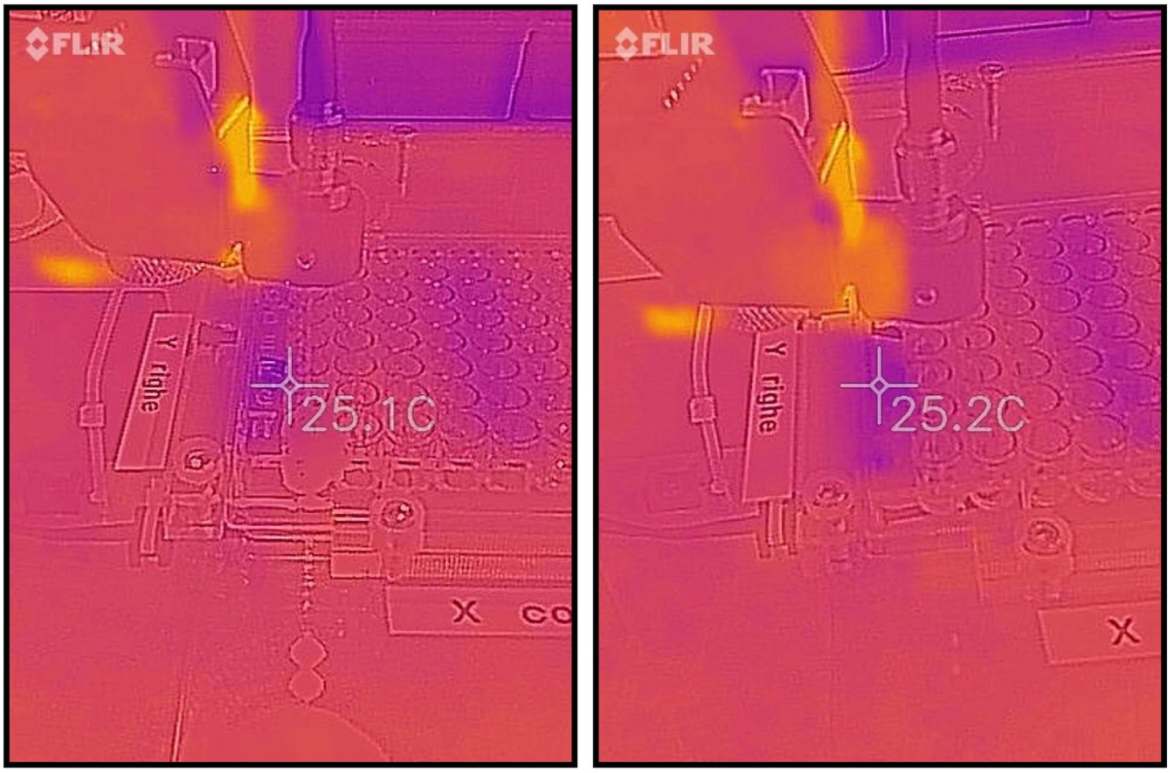

Figure 44. Thermal monitoring during irradiation

Different works reported the power of PBM in reducing the recurrence of infectious episodes *in vivo* on patients and in helping the healing of the HSV-1 oral vesicles [reviewed by [de Paula Eduardo et al., 2013]]. Interestingly, Eduardo et al. submitted patients to multiple PBM sessions on oral and perioral area in the prodromic phase, where the virus was latent, and the patients did not have clinical signs of the infection. The outcomes at 3 years showed a decreased frequency of herpetic manifestations, with rapid healing and milder symptoms [Eduardo et al., 2012]. However, the wavelengths employed were different from the blue one, since this study employed the red, near infrared and infrared wavelengths.

Moreover, several works utilized an antimicrobial photodynamic approach: an exogenous photosensitizer, a dye specific for targeting microorganisms and not eukaryotic cells, were used to elicit a high production of reactive oxygen species, leading to lethal outcomes [reviewed by [Wainwright, 2003]].

Only the work of Donnarumma et al. tried to understand the effect of laser therapy on HSV-1, developing an *in vitro* model [Donnarumma et al., 2010]. The researchers observed that irradiated (λ 830 nm) HSV-1 infecting HaCaT cells presented a reduction in viral replication with a decrease

level of VP16, a tegument viral protein necessary for virus replication. Moreover, they found an increase of pro-inflammatory cytokines and proteins, normally suppressed by the accumulation of progeny virus. So, they speculated that PBM activated immune anti-viral response and acted on final stage of HSV-1, instead our results showed at the contrary an inhibitory PBM effect on the virus itself.

This is the first work reporting the antiviral activities of blue PBM, indicating a possible direct effect on the virus itself: theses data could lead to a new potential application of blue PBM for antiviral purpose.

Conclusion

Despite its use is increasing year by year, Photobiomodulation (PBM) is still a treatment elicited by few centers and professionals in the medical field considering the almost infinite possible applications of laser light.

Certainly, PBM should not be considered the panacea for all human ailments, as one could imagine reading the previous literature, but it should be esteemed as a useful adjuvant intervention that can support the healing of lots of pathologic conditions.

Indeed, varying the wavelengths and the dosimetry it is possible to achieve a plethora of beneficial effects; this should not surprise considering the fundamental properties that sunlight has in the life on earth [Rapf, and Vaida, 2016].

Really, PBM was initially used in an empirical mode, observing some therapeutic effects and applying the laser light to enhance wound healing [Mester et al., 1968]. Fifty years have passed, a lot a research was conducted, and much effort was made, nevertheless, today, many aspects are not completely understood regarding "how PBM really works".

Moreover, the irradiation protocols reported in the literature are very different from one study to another in terms of wavelength, power, irradiance, energy, fluence, modality, but also considering the treatment schedule and the intervals between sessions. Also, the different patient's conditions or the various cell lines employed in the *in vitro* experiments enlarges the possibility of treatments.

Obviously, this makes very difficult to compare the research and probably for this reason, few meta-analyses were published so far. Therefore, obtaining a universal consensus about the best protocol is hard, considering also that each center tends to optimize the protocols on its own experience.

Despite this, PBM works and laser devices are spreading around the world thanks to technology progression that renders this instrument cheaper and more compact respect to the past.

This research project tries to depict a picture, although incomplete, of PBM properties and applications.

During the three years of PhD, two sets of experiments were performed, utilizing the red and near-infrared (NIR) wavelengths or the blue wavelength, the firsts for achieving bio-stimulation of eukaryotic cells the second to test the antibacterial and antiviral effects.

Firstly, the laser effect on oxidative stress was inquired.

The study performed on oral mucositis (OM) patients treated with PBM at 970 nm gave some important achievements. The patients were treated for 4 consecutively days and the clinical parameters ameliorated with the healing of oral ulcerations, with the improvement of the CTC score and of subjective parameters as swallowing, chewing, speaking.

Although the PBM effects on OM was largely described, the majority of works reported its beneficial effect as prophylaxis [Oberoi et al., 2014; He et al., 2018] and only the 660 nm wavelength was recommended by MASCC/ISOO [Lalla et al., 2014; Migliorati et al., 2013], meanwhile the current work presented its use when OM lesions were manifested and using another wavelength, at 970 nm, showing the effectiveness of PBM also in the fourth phase of OM and with NIR wavelength. Additionally, PBM was able to reduce salivary total oxidant status (TOS) immediately after the second, third and fourth session of PBM, but did not maintain its effect over time, since each day after PBM the TOS increased newly, possibly indicating an immediate but transient reaction.

Then, the *in vitro* effect of PBM was tested on a model of skin keratinocytes treated with 5-fluorouracil (5-FU), a known mucotoxic drug causing oxidative stress, to mimic the OM condition. In this case a combination of 4 different wavelength at 970, 905, 800 and 660 nm was employed with the aim of proposing a new PBM protocol. PBM was able to increment the viability of 5-FU treated cells after 24 hours from the irradiation, and to reduce the level of ROS and the gene expression of two antioxidant enzymes (*SOD2* and *HMOX1*) in 5-FU treated cells after 30 minutes from PBM.

These results were emblematic for the immediate impact of PBM on ROS, both *in vivo* and *in vitro*. Although the antioxidant activities of PBM was previously reported [Rai, 2016] this is the first study that proves PBM effectiveness on OM patients and in an *in vitro* model of OM, suggesting also a protocol based on the combination of 4 different wavelengths.

Secondly, PBM was tested for its immuno-regulatory actions.

Specifically, PBM effect on members of innate immune system was tested.

The possible PBM (at 970 nm) impact on β-defensins concentration in saliva from OM patients was tested, but the level of the hBD-1, hBD-2, hBD-3 varied considerably inter-individually and so a PBM effect was not individuated.

To have a more reproducible system, an oral mucosa epithelial cell line was employed: in this model the mRNA expression of genes encoding for antimicrobial peptides and inflammasomes related molecules were considered. PBM at 970 nm, 800 nm and 660 nm reduced the mRNA expression of *DEFB1*, *DEFB4* and *DEFB103* genes (encoding for hBD-1, hBD-2 and hBD-3) 30 minutes from irradiation, but not 24 hours later, confirming a precocious effect of PBM also in

this model. Too see if PBM could reduce the response to a pro-inflammatory stimulus, the cells were pre-treated with lipopolysaccharide for 24 hours, then PBM was applied: PBM at 660 nm reduced the expression of *DEFB103* gene after 24 hours from irradiation. Regarding inflammasomes related genes, PBM at 970 nm increased slightly *IL1B* but inhibited *NLRP3*, meanwhile PBM at 660 nm increased *NLRP1* after 24 hours from irradiation.
These results suggested that PBM prevented hBD-1, hBD-2 and hBD-3 high expression which could be harmful in some pathologic conditions for the induction of inflammation [Arimura et al., 2004; Kesting et al., 2009]. Besides, 24 hours from treatment, PBM at 970 nm increased *IL1B* production, contrasted through the decrement of *NLRP3* meanwhile PBM at 660 incremented *NLRP1* expression, without influencing pro-inflammatory *IL1B.* A complex balance between pro and anti inflammatory pathways seemed to be possible influenced by PBM.

Thirdly, the analgesic activities of PBM were investigated.
PBM at 970 nm was able to decrease the painful subjective sensation referred by the patients through the VAS score and this effect was particularly evident at the last PBM treatment and at the control day. This result is particularly interesting since PBM at 970 nm was not largely employed in the clinical practice and considering also that OM lesions are extremely painful for the OM patients often requiring analgesic drugs [Sonis, 2004].
Then, with the aim of describing the molecular effect at the basis of analgesia, an *in vitro* model of nociception was tested, employing primary murine sensory neurons from dorsal root ganglia. NIR PBM at 970 and 800 nm reduced ATP production, possibly leading to the block of action potential, decremented NO secretion, a neurotransmitter, and increased ROS, with the plausible formation of axon varicosities. These effects could impact on transmission of nociceptive signaling to the brain, inhibiting it.
PBM at 800 nm increased also superoxide anion (another type of ROS, generated by mitochondria) and incremented slightly mitochondrial membrane potential, so acting primarily on mitochondria. Instead, PBM at 970 nm decreased the calcium flow after administration of capsaicin, an agonist of TRPV1 ion channel, that was used as an inducer of nociceptive pathways. This effect was confirmed also in a murine *in vivo* behavioral model of nociception where capsaicin was subplantarly injected and the pain related response monitored. PBM at 970 nm reduced the licking, biting and shaking of the paw injected.
All these results were obtained very early after irradiation, confirming the immediate PBM effect, indeed the analgesia was the first benefit the patients reported.
PBM showed also a differential effect that was wavelength dependent, suggesting also a different PBM mechanism of action: PBM at 800 nm seemed to act on mitochondria, meanwhile at 970

nm impacted on TRPV1 activity and confirmed its effect on OM patients and in the *in vivo* murine model.

Fourthly, the blue wavelength at 445 nm was studied for its antibacterial properties.
Blue laser light was tested on *Pseudomonas aeruginosa*, a bacterium that was implicated in opportunistic infection in OM patients both in the oral cavity [Wong, 2014] and systemically causing bacteremia [Donnelly et al., 2003]. PBM inhibited bacterial growth on agar plate and in broth, inducing also bacterial wall damaging at the SEM imaging.
To try to understand the antibacterial mechanism of action different approaches were applied: blue light caused an increment of ROS that could be lethal for the cells, this outcome was rescued through a pre-treatment with ascorbic acid, a ROS scavenger. The possible chromophores receptive of blue laser light were identified in the porphyrin biosynthetic pathway: *P. aeruginosa* mutant for enzymes of this pathway, producing less porphyrins, resulted less susceptible to irradiation.
Blue PBM did not cause an increment in temperature, so excluding a thermal damaging. Red (at 660 nm) and NIR wavelength (at 970 nm) was also utilized to assess if the antimicrobial activity is specific of blue wavelength: PBM at 660 and 970 nm did not impact on bacterial survival. Moreover, A LED device emitting blue wavelengths was tested to prove the specificity of antibacterial properties of blue light: the results were comparable to laser instrument although LED was less efficacious than diode laser.
Last, blue light was not toxic for eukaryotic cells, so being safe for the consecutively experiment conducted *in vivo*.
A murine *in vivo* model of skin abrasion infected by *P. aeruginosa* was developed: PBM was able to inhibit bacterial replication also in this case. Intriguingly, blue PBM reduced the inflammatory infiltrate in the murine skin.
These results highlighted the efficacy of blue laser light as a potent antibacterial device both *in vitro* and *in vivo*; moreover, the antibacterial mechanism of action was identified in porphyrin excitation and ROS generation, proving also the specificity of blue light for this purpose.

Lastly, blue light was examined for its possible antiviral activities.
Blue PBM was tested on Herpes simplex virus type 1 (HSV-1), a viral agent able to cause infections in immunocompromised OM patients [Corey, 2012; World Health Organization, 2017]. For this experiment, an *in vitro* model of HSV-1 was developed infecting human skin keratinocytes with the virus.

The virus was irradiated alone and then the cells were infected: PBM decremented the viral load and increased the viability of the cells infected with irradiated virus. When the cells already infected by 1 hour were irradiated only a trend of antiviral effect was possible to observe, meanwhile when cells presenting 24 hours of previous infection were irradiated no PBM impact was detected. The irradiation of cells prior to infection was also not effective and it did not render them more resistant to HSV-1. These results were confirmed through the plaque forming unit assay showing the less infectivity capacity of irradiated HSV-1, moreover this test evidenced a reduction in the plaque forming units also in the setting where the cells were infected by 1 hours prior to PBM and where the cells were irradiated prior to infections.

These findings suggested a new potential application of blue laser light for antiviral purpose, PBM seemed to have direct effect on the virus itself and it could be less efficacious when the virus penetrated inside the cells. Only other wavelengths were reported to be efficacious on relieving symptoms on patients [reviewed by [de Paula Eduardo et al., 2013]], meanwhile this is the first report of the antiviral action of blue light on HSV-1.

The main findings of the research are reported in figure 45 (red and NIR λ) and 46 (blue λ).

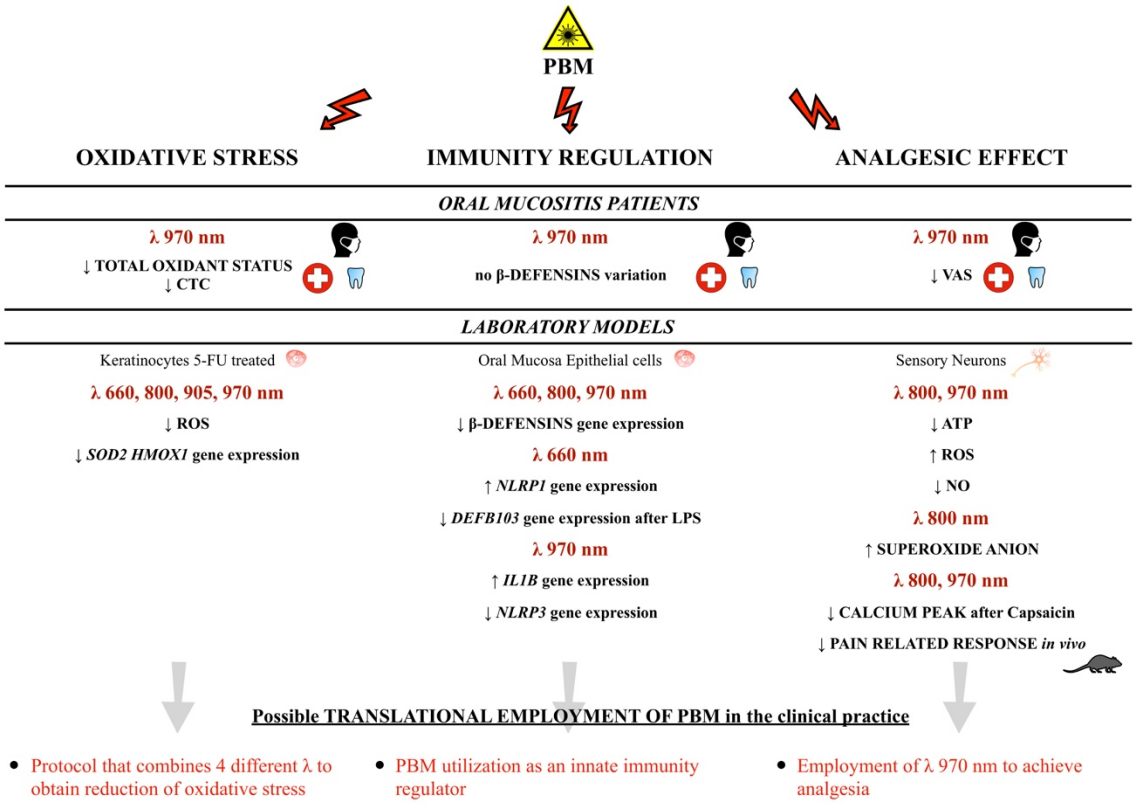

Figure 45. Schematic representation of the main findings regarding red and near-infrared λ.

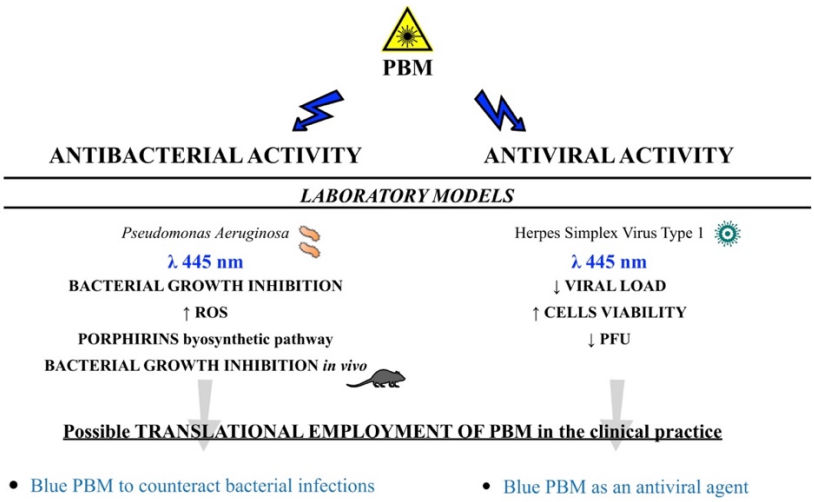

Figure 46. Schematic representation of the main findings regarding blue λ.

So, our results highlighted a pleiotropic action of PBM dependent on the wavelength and dosimetry used: PBM acts as anti-oxidant, immunoregulatory, analgesic, antibacterial and antiviral. In figure 47 a possible algorithm for clinicians is proposed.

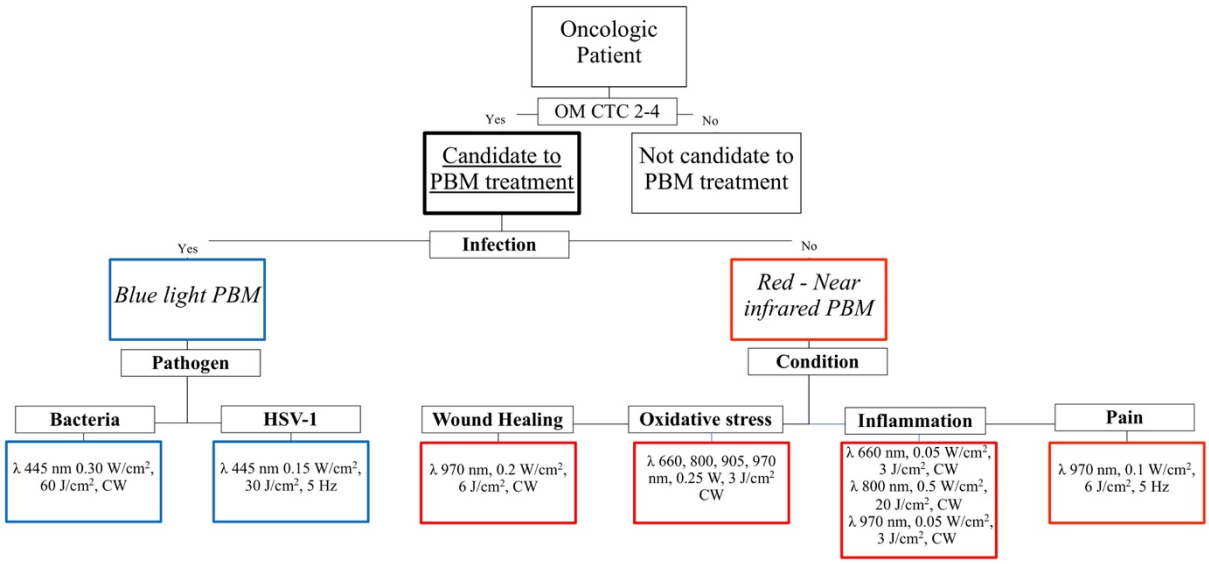

Figure 47. Algorithm for photobiomodulation (PBM) employment by clinicians.

A deep comprehension of molecular mechanisms at the basis of PBM properties and of cellular repercussion of light absorption, as delineated in this PhD work, can be useful to extend the knowledge in the PBM flied. Moreover, a broad insight of PBM can lead to a more justified and rationale application of PBM with an evidence based medicine approach. The variety of possible

PBM treatments that takes into account also the subjective characteristic of patients allows the personalization of the protocols of irradiation. PBM treatment is also safe without any side effect, therefore the results obtained in laboratory can easily translated to patients for the optimization of clinical protocols in order to achieve the maximum effectiveness [Moskvin, 2017]. New applications of PBM is arising continuously, just for instance, the delivery of light to head for brain disorders [Hamblin, 2016].
In this research novel clinical usages of PBM were proposed, for the modulation of innate immune response (i.e. hBDs regulation) and for the fighting against bacterial and viral infection using the blue light. Moreover, it describes the anti-oxidant activities of PBM, proposing a combination protocol that can be adopted in the clinical practice; meanwhile, the investigation of pain pathways allows to understand the molecular basis of analgesic effect, showing the differential effect of the wavelengths in the NIR range. Thus, this work is able to fulfill the above cited objectives of the study.

It is even more important to consider that PBM is also a rapid treatment, since a session lasts only few minutes, it is painless, not invasive and it can be a useful choice for the management of pediatric patients.
Pediatric age requires special attention in the oncologic field, in fact, OM can negatively impact on nutrition affecting the normal growth, but also on daily normal activities, such as speaking compromising the social relationship [Bryant, 2003]. Moreover, in young children the OM related pain is often misunderstood, leading to an inadequate analgesic medical care [World Health Organization, 2012].

Besides, after the cost of instrument equipment and of personnel training, PBM is quite inexpensive and it can impact positively on the economy of public health service. It can also permit the reduction of analgesic drug administration and of parental nutrition, allowing also to not suspend the CRT, plausibly augmenting patients' survival.
Furthermore, from our data, blue PBM can be employed, in support to antimicrobial therapy, to decrease the administration of antibiotic and antiviral drugs, so impacting positively on the microorganisms' resistance towards these type of interventions, a worldwide serious challenge [El Zowalaty et al., 2015].

So, taken together, these findings corroborated the useful medical interventions based on laser light, possibly helping to increment a clinical thoughtful and justified usage of PBM in OM patients for routinely applications, especially in pediatric oncologic subjects.

References

Ablon G: Phototherapy with Light Emitting Diodes: Treating a Broad Range of Medical and Aesthetic Conditions in Dermatology. J Clin Aesthet Dermatol 2018;11:21–27.

Albers RW, Siegel GJ: The ATP-Dependent Na+,K+ Pump [Internet]. . Basic Neurochemistry: Molecular, Cellular and Medical Aspects 6th edition 1999 [cited 2018 Sep 22];Available from: https://www.ncbi.nlm.nih.gov/books/NBK28174/

AlGhamdi KM, Kumar A, Moussa NA: Low-level laser therapy: a useful technique for enhancing the proliferation of various cultured cells. Lasers Med Sci 2012;27:237–249.

Amin RM, Bhayana B, Hamblin MR, Dai T: Antimicrobial blue light inactivation of Pseudomonas aeruginosa by photo-excitation of endogenous porphyrins: In vitro and in vivo studies. Lasers Surg Med 2016;48:562–568.

Anders JJ, Lanzafame RJ, Arany PR: Low-level light/laser therapy versus photobiomodulation therapy. Photomed Laser Surg 2015;33:183–184.

Anderson RR, Parrish JA: The optics of human skin. J Invest Dermatol 1981;77:13–19.

Arimura Y, Ashitani J, Yanagi S, Tokojima M, Abe K, Mukae H, Nakazato M: Elevated serum beta-defensins concentrations in patients with lung cancer. Anticancer Res 2004;24:4051–4057.

Ashkenazi H, Malik Z, Harth Y, Nitzan Y: Eradication of Propionibacterium acnes by its endogenic porphyrins after illumination with high intensity blue light. FEMS Immunol Med Microbiol 2003;35:17–24.

Avci P, Gupta A, Sadasivam M, Vecchio D, Pam Z, Pam N, Hamblin MR: Low-level laser (light) therapy (LLLT) in skin: stimulating, healing, restoring. Semin Cutan Med Surg 2013;32:41–52.

Ayuk SM, Abrahamse H, Houreld NN: The Role of Matrix Metalloproteinases in Diabetic Wound Healing in relation to Photobiomodulation. J Diabetes Res 2016;2016:2897656.

Baer A, Kehn-Hall K: Viral concentration determination through plaque assays: using traditional and novel overlay systems. J Vis Exp 2014;e52065.

Batandier C, Fontaine E, Kériel C, Leverve XM: Determination of mitochondrial reactive oxygen species: methodological aspects. J Cell Mol Med 2002;6:175–187.

Bensadoun R-J, Nair RG: Low-level laser therapy in the prevention and treatment of cancer therapy-induced mucositis: 2012 state of the art based on literature review and meta-analysis. Curr Opin Oncol 2012;24:363–370.

Bogdan Allemann I, Kaufman J: Laser principles. Curr Probl Dermatol 2011;42:7–23.

Bomfin LE, Braga CM, Oliveira TA, Martins CS, Foschetti DA, Santos AAQA, Costa DVS, Leitão RFC, Brito GAC: 5-Fluorouracil induces inflammation and oxidative stress in the major salivary glands affecting salivary flow and saliva composition. Biochem Pharmacol 2017;145:34–45.

Bryant R: Managing side effects of childhood cancer treatment. J Pediatr Nurs 2003;18:113–125.

Carmody RJ, Chen YH: Nuclear factor-kappaB: activation and regulation during toll-like receptor signaling. Cell Mol Immunol 2007;4:31–41.

Carrega G, Castagnola E, Canessa A, Argenta P, Haupt R, Dini G, Garaventa A: Herpes simplex virus and oral mucositis in children with cancer. Support Care Cancer 1994;2:266–269.

Cerdeira CD, Lima Brigagão MRP, Carli ML, de Souza Ferreira C, de Oliveira Isac Moraes G, Hadad H, Costa Hanemann JA, Hamblin MR, Sperandio FF: Low-level laser therapy

stimulates the oxidative burst in human neutrophils and increases their fungicidal capacity. J Biophotonics 2016;9:1180–1188.

Chen AC-H, Arany PR, Huang Y-Y, Tomkinson EM, Sharma SK, Kharkwal GB, Saleem T, Mooney D, Yull FE, Blackwell TS, Hamblin MR: Low-level laser therapy activates NF-kB via generation of reactive oxygen species in mouse embryonic fibroblasts. PLoS ONE 2011;6:e22453.

Chen X, Kim P, Farinelli B, Doukas A, Yun S-H, Gelfand JA, Anderson RR, Wu MX: A novel laser vaccine adjuvant increases the motility of antigen presenting cells. PLoS ONE 2010;5:e13776.

Cheng KK-F: Oral mucositis, dysfunction, and distress in patients undergoing cancer therapy. J Clin Nurs 2007;16:2114–2121.

Cheng KKF, Chang AM, Yuen MP: Prevention of oral mucositis in paediatric patients treated with chemotherapy; a randomised crossover trial comparing two protocols of oral care. Eur J Cancer 2004;40:1208–1216.

Chermetz M, Gobbo M, Ronfani L, Ottaviani G, Zanazzo GA, Verzegnassi F, Treister NS, Di Lenarda R, Biasotto M, Zacchigna S: Class IV laser therapy as treatment for chemotherapy-induced oral mucositis in onco-haematological paediatric patients: a prospective study. Int J Paediatr Dent 2014;24:441–449.

Chow R, Armati P, Laakso E-L, Bjordal JM, Baxter GD: Inhibitory effects of laser irradiation on peripheral mammalian nerves and relevance to analgesic effects: a systematic review. Photomed Laser Surg 2011;29:365–381.

Chow RT, Armati PJ: Photobiomodulation: Implications for Anesthesia and Pain Relief. Photomed Laser Surg 2016;34:599–609.

Chow RT, David MA, Armati PJ: 830 nm laser irradiation induces varicosity formation, reduces mitochondrial membrane potential and blocks fast axonal flow in small and medium diameter rat dorsal root ganglion neurons: implications for the analgesic effects of 830 nm laser. J Peripher Nerv Syst 2007;12:28–39.

Chung H, Dai T, Sharma SK, Huang Y-Y, Carroll JD, Hamblin MR: The nuts and bolts of low-level laser (light) therapy. Ann Biomed Eng 2012;40:516–533.

Cidral-Filho FJ, Mazzardo-Martins L, Martins DF, Santos ARS: Light-emitting diode therapy induces analgesia in a mouse model of postoperative pain through activation of peripheral opioid receptors and the L-arginine/nitric oxide pathway. Lasers Med Sci 2014;29:695–702.

Collins LM, Dawes C: The surface area of the adult human mouth and thickness of the salivary film covering the teeth and oral mucosa. J Dent Res 1987;66:1300–1302.

Corey L: Chapter 179. Herpes Simplex Virus Infections [Internet]; in Longo DL, Fauci AS, Kasper DL, Hauser SL, Jameson JL, Loscalzo J (eds): Harrison's Principles of Internal Medicine, ed 18. New York, NY, The McGraw-Hill Companies, 2012, [cited 2018 Sep 22].Available from: accessmedicine.mhmedical.com/content.aspx?aid=9123167

Curra M, Pellicioli ACA, Filho NAK, Ochs G, Matte Ú, Filho MS, Martins MAT, Martins MD: Photobiomodulation reduces oral mucositis by modulating NF-kB. J Biomed Opt 2015;20:125008.

Dai T, Gupta A, Huang Y-Y, Yin R, Murray CK, Vrahas MS, Sherwood ME, Tegos GP, Hamblin MR: Blue light rescues mice from potentially fatal Pseudomonas aeruginosa burn infection: efficacy, safety, and mechanism of action. Antimicrob Agents Chemother 2013;57:1238–1245.

Dai T, Gupta A, Murray CK, Vrahas MS, Tegos GP, Hamblin MR: Blue light for infectious

diseases: Propionibacterium acnes, Helicobacter pylori, and beyond? Drug Resist Updat 2012;15:223–236.

Dai Y: TRPs and pain. Semin Immunopathol 2016;38:277–291.

Dale BA, Fredericks LP: Antimicrobial peptides in the oral environment: expression and function in health and disease. Curr Issues Mol Biol 2005;7:119–133.

De Prá SDT, Ferro PR, Milioli AM, Rigo FK, Chipindo OJ, Camponogara C, Casoti R, Manfron MP, de Oliveira SM, Ferreira J, Trevisan G: Antinociceptive activity and mechanism of action of hydroalcoholic extract and dichloromethane fraction of Amphilophium crucigerum seeds in mice. J Ethnopharmacol 2017;195:283–297.

Donnarumma G, De Gregorio V, Fusco A, Farina E, Baroni A, Esposito V, Contaldo M, Petruzzi M, Pannone G, Serpico R: Inhibition of HSV-1 replication by laser diode-irradiation: possible mechanism of action. Int J Immunopathol Pharmacol 2010;23:1167–1176.

Donnelly JP, Bellm LA, Epstein JB, Sonis ST, Symonds RP: Antimicrobial therapy to prevent or treat oral mucositis. Lancet Infect Dis 2003;3:405–412.

Ebrahimi T, Moslemi N, Rokn A, Heidari M, Nokhbatolfoghahaie H, Fekrazad R: The influence of low-intensity laser therapy on bone healing. J Dent (Tehran) 2012;9:238–248.

Eduardo C de P, Bezinelli LM, Eduardo F de P, da Graça Lopes RM, Ramalho KM, Bello-Silva MS, Esteves-Oliveira M: Prevention of recurrent herpes labialis outbreaks through low-intensity laser therapy: a clinical protocol with 3-year follow-up. Lasers Med Sci 2012;27:1077–1083.

El Zowalaty ME, Al Thani AA, Webster TJ, El Zowalaty AE, Schweizer HP, Nasrallah GK, Marei HE, Ashour HM: Pseudomonas aeruginosa: arsenal of resistance mechanisms, decades of changing resistance profiles, and future antimicrobial therapies. Future Microbiol 2015;10:1683–1706.

Erel O: A new automated colorimetric method for measuring total oxidant status. Clin Biochem 2005;38:1103–1111.

Feuerstein O, Ginsburg I, Dayan E, Veler D, Weiss EI: Mechanism of visible light phototoxicity on Porphyromonas gingivalis and Fusobacterium nucleatum. Photochem Photobiol 2005;81:1186–1189.

Fila G, Kawiak A, Grinholc MS: Blue light treatment of Pseudomonas aeruginosa: Strong bactericidal activity, synergism with antibiotics and inactivation of virulence factors. Virulence 2017;8:938–958.

Foote CS: Definition of type I and type II photosensitized oxidation. Photochem Photobiol 1991;54:659.

de Freitas LF, Hamblin MR: Proposed Mechanisms of Photobiomodulation or Low-Level Light Therapy. IEEE J Sel Top Quantum Electron 2016;22. DOI: 10.1109/JSTQE.2016.2561201

Frobert E, Cortay J-C, Ooka T, Najioullah F, Thouvenot D, Lina B, Morfin F: Genotypic detection of acyclovir-resistant HSV-1: characterization of 67 ACV-sensitive and 14 ACV-resistant viruses. Antiviral Res 2008;79:28–36.

Geneva II: Photobiomodulation for the treatment of retinal diseases: a review. Int J Ophthalmol 2016;9:145–152.

Genina EA, Titorenko VA, Belikov AV, Bashkatov AN, Tuchin VV: Adjunctive dental therapy via tooth plaque reduction and gingivitis treatment by blue light-emitting diodes tooth brushing. J Biomed Opt 2015;20:128004.

Giuliani A, Lorenzini L, Gallamini M, Massella A, Giardino L, Calzà L: Low infra red laser

light irradiation on cultured neural cells: effects on mitochondria and cell viability after oxidative stress. BMC Complement Altern Med 2009;9:8.

Glenny AM, Gibson F, Auld E, Coulson S, Clarkson JE, Craig JV, Eden OB, Khalid T, Worthington HV, Pizer B, Children's Cancer and Leukaemia Group (CCLG)/Paediatric Oncology Nurses Forum's (CCLG-PONF) Mouth Care Group: The development of evidence-based guidelines on mouth care for children, teenagers and young adults treated for cancer. Eur J Cancer 2010;46:1399–1412.

Gobbo M, Verzegnassi F, Ronfani L, Zanon D, Melchionda F, Bagattoni S, Majorana A, Bardellini E, Mura R, Piras A, Petris MG, Mariuzzi ML, Barone A, Merigo E, Decembrino N, Vitale MC, Berger M, Defabianis P, Biasotto M, Ottaviani G, Zanazzo GA: Multicenter randomized, double-blind controlled trial to evaluate the efficacy of laser therapy for the treatment of severe oral mucositis induced by chemotherapy in children: laMPO RCT. Pediatr Blood Cancer 2018;65:e27098.

Gogvadze V, Orrenius S, Zhivotovsky B: Multiple pathways of cytochrome c release from mitochondria in apoptosis. Biochim Biophys Acta 2006;1757:639–647.

Gregory NS, Harris AL, Robinson CR, Dougherty PM, Fuchs PN, Sluka KA: An overview of animal models of pain: disease models and outcome measures. J Pain 2013;14:1255–1269.

Hagiwara S, Iwasaka H, Okuda K, Noguchi T: GaAlAs (830 nm) low-level laser enhances peripheral endogenous opioid analgesia in rats. Lasers Surg Med 2007;39:797–802.

Hamblin MR: The role of nitric oxide in low level light therapy [Internet]; in : Mechanisms for Low-Light Therapy III. International Society for Optics and Photonics, 2008, p 684602.

Hamblin MR: Shining light on the head: Photobiomodulation for brain disorders. BBA Clin 2016;6:113–124.

Hamblin MR: Mechanisms and applications of the anti-inflammatory effects of photobiomodulation. AIMS Biophys 2017;4:337–361.

Harris DJ: Cancer treatment-induced mucositis pain: strategies for assessment and management. Ther Clin Risk Manag 2006;2:251–258.

Hawker GA, Mian S, Kendzerska T, French M: Measures of adult pain: Visual Analog Scale for Pain (VAS Pain), Numeric Rating Scale for Pain (NRS Pain), McGill Pain Questionnaire (MPQ), Short-Form McGill Pain Questionnaire (SF-MPQ), Chronic Pain Grade Scale (CPGS), Short Form-36 Bodily Pain Scale (SF-36 BPS), and Measure of Intermittent and Constant Osteoarthritis Pain (ICOAP). Arthritis Care Res (Hoboken) 2011;63 Suppl 11:S240-252.

Hawkins D, Abrahamse H: Biological effects of helium-neon laser irradiation on normal and wounded human skin fibroblasts. Photomed Laser Surg 2005;23:251–259.

Hawkins D, Houreld N, Abrahamse H: Low level laser therapy (LLLT) as an effective therapeutic modality for delayed wound healing. Ann N Y Acad Sci 2005;1056:486–493.

He M, Zhang B, Shen N, Wu N, Sun J: A systematic review and meta-analysis of the effect of low-level laser therapy (LLLT) on chemotherapy-induced oral mucositis in pediatric and young patients. Eur J Pediatr 2018;177:7–17.

Held K, Ramage E, Jacobs M, Gallagher L, Manoil C: Sequence-verified two-allele transposon mutant library for Pseudomonas aeruginosa PAO1. J Bacteriol 2012;194:6387–6389.

Holanda VM, Chavantes MC, Wu X, Anders JJ: The mechanistic basis for photobiomodulation therapy of neuropathic pain by near infrared laser light. Lasers Surg Med 2017;49:516–524.

Hsieh Y-L, Chou L-W, Chang P-L, Yang C-C, Kao M-J, Hong C-Z: Low-level laser therapy alleviates neuropathic pain and promotes function recovery in rats with chronic constriction

injury: possible involvements in hypoxia-inducible factor 1α (HIF-1α). J Comp Neurol 2012;520:2903–2916.

Huang Y-Y, Chen AC-H, Carroll JD, Hamblin MR: Biphasic dose response in low level light therapy. Dose Response 2009;7:358–383.

Huang Y-Y, Nagata K, Tedford CE, Hamblin MR: Low-level laser therapy (810 nm) protects primary cortical neurons against excitotoxicity in vitro. J Biophotonics 2014;7:656–664.

Huang Y-Y, Nagata K, Tedford CE, McCarthy T, Hamblin MR: Low-level laser therapy (LLLT) reduces oxidative stress in primary cortical neurons in vitro. J Biophotonics 2013;6:829–838.

Huang Y-Y, Sharma SK, Carroll J, Hamblin MR: Biphasic dose response in low level light therapy - an update. Dose Response 2011;9:602–618.

Hungerer C, Troup B, Römling U, Jahn D: Cloning, mapping and characterization of the Pseudomonas aeruginosa hemL gene. Mol Gen Genet 1995;248:375–380.

Jara-Oseguera A, Simon SA, Rosenbaum T: TRPV1: on the road to pain relief. Curr Mol Pharmacol 2008;1:255–269.

Jasovský D, Littmann J, Zorzet A, Cars O: Antimicrobial resistance-a threat to the world's sustainable development. Ups J Med Sci 2016;121:159–164.

Jiang YQ, Oblinger MM: Differential regulation of beta III and other tubulin genes during peripheral and central neuron development. J Cell Sci 1992;103 (Pt 3):643–651.

Jimbo K, Noda K, Suzuki K, Yoda K: Suppressive effects of low-power laser irradiation on bradykinin evoked action potentials in cultured murine dorsal root ganglion cells. Neurosci Lett 1998;240:93–96.

Karu T: Primary and secondary mechanisms of action of visible to near-IR radiation on cells. J Photochem Photobiol B, Biol 1999;49:1–17.

Karu TI: Mitochondrial signaling in mammalian cells activated by red and near-IR radiation. Photochem Photobiol 2008;84:1091–1099.

Katsetos CD, Legido A, Perentes E, Mörk SJ: Class III beta-tubulin isotype: a key cytoskeletal protein at the crossroads of developmental neurobiology and tumor neuropathology. J Child Neurol 2003;18:851–866; discussion 867.

Kennedy L, Diamond J: Assessment and management of chemotherapy-induced mucositis in children. J Pediatr Oncol Nurs 1997;14:164–174; quiz 175–177.

Kesting MR, Loeffelbein DJ, Hasler RJ, Wolff K-D, Rittig A, Schulte M, Hirsch T, Wagenpfeil S, Jacobsen F, Steinstraesser L: Expression profile of human beta-defensin 3 in oral squamous cell carcinoma. Cancer Invest 2009;27:575–581.

Kleinpenning MM, Smits T, Frunt MHA, van Erp PEJ, van de Kerkhof PCM, Gerritsen RMJP: Clinical and histological effects of blue light on normal skin. Photodermatol Photoimmunol Photomed 2010;26:16–21.

Kuffler DP: Photobiomodulation in promoting wound healing: a review. Regen Med 2016;11:107–122.

Lalla RV, Bowen J, Barasch A, Elting L, Epstein J, Keefe DM, McGuire DB, Migliorati C, Nicolatou-Galitis O, Peterson DE, Raber-Durlacher JE, Sonis ST, Elad S, Mucositis Guidelines Leadership Group of the Multinational Association of Supportive Care in Cancer and International Society of Oral Oncology (MASCC/ISOO): MASCC/ISOO clinical practice guidelines for the management of mucositis secondary to cancer therapy. Cancer 2014;120:1453–1461.

Langtry J a. A: Lasers in plastic surgery and dermatology: By B. M. Achauer, V. M. Vander Kam, M. W. Berns, 1992. Thieme Medical Publishers Inc, New York. pp202. Price £72. ISBN: 0-86577-426-9. British Journal of Oral and Maxillofacial Surgery 1994;32:265.

Latz E, Xiao TS, Stutz A: Activation and regulation of the inflammasomes. Nat Rev Immunol 2013;13:397–411.

Lee CI, Liu X, Zweier JL: Regulation of xanthine oxidase by nitric oxide and peroxynitrite. J Biol Chem 2000;275:9369–9376.

Lerman MA, Laudenbach J, Marty FM, Baden LR, Treister NS: Management of oral infections in cancer patients. Dent Clin North Am 2008;52:129–153, ix.

Liebert AD, Chow RT, Bicknell BT, Varigos E: Neuroprotective Effects Against POCD by Photobiomodulation: Evidence from Assembly/Disassembly of the Cytoskeleton. J Exp Neurosci 2016;10:1–19.

Lim WB, Kim JS, Ko YJ, Kwon H, Kim SW, Min HK, Kim O, Choi HR, Kim OJ: Effects of 635nm light-emitting diode irradiation on angiogenesis in CoCl(2) -exposed HUVECs. Lasers Surg Med 2011;43:344–352.

Livak KJ, Schmittgen TD: Analysis of relative gene expression data using real-time quantitative PCR and the 2(-Delta Delta C(T)) Method. Methods 2001;25:402–408.

Loeser JD, Treede R-D: The Kyoto protocol of IASP Basic Pain Terminology. Pain 2008;137:473–477.

Longley DB, Harkin DP, Johnston PG: 5-fluorouracil: mechanisms of action and clinical strategies. Nat Rev Cancer 2003;3:330–338.

Lopes NNF, Plapler H, Lalla RV, Chavantes MC, Yoshimura EM, da Silva MAB, Alves MTS: Effects of low-level laser therapy on collagen expression and neutrophil infiltrate in 5-fluorouracil-induced oral mucositis in hamsters. Lasers Surg Med 2010;42:546–552.

Lubart R, Lipovski A, Nitzan Y, Friedmann H: A possible mechanism for the bactericidal effect of visible light. Laser Ther 2011;20:17–22.

Maclean M, Macgregor SJ, Anderson JG, Woolsey GA: The role of oxygen in the visible-light inactivation of Staphylococcus aureus. J Photochem Photobiol B, Biol 2008;92:180–184.

Malin SA, Davis BM, Molliver DC: Production of dissociated sensory neuron cultures and considerations for their use in studying neuronal function and plasticity. Nat Protoc 2007;2:152–160.

Mallick S, Benson R, Rath GK: Radiation induced oral mucositis: a review of current literature on prevention and management. Eur Arch Otorhinolaryngol 2016;273:2285–2293.

Martius F: Das Amdt-Schulz Grandgesetz. Munch Med Wschr 1923;70:1005–1006.

Mason MG, Nicholls P, Cooper CE: Re-evaluation of the near infrared spectra of mitochondrial cytochrome c oxidase: Implications for non invasive in vivo monitoring of tissues. Biochim Biophys Acta 2014;1837:1882–1891.

Matsunaga T, Tsuji Y, Kaai K, Kohno S, Hirayama R, Alpers DH, Komoda T, Hara A: Toxicity against gastric cancer cells by combined treatment with 5-fluorouracil and mitomycin c: implication in oxidative stress. Cancer Chemother Pharmacol 2010;66:517–526.

McDougald D, Klebensberger J, Tolker-Nielsen T, Webb JS, Conibear T, Rice SA, Kirov SM, Matz C, Kjelleberg S: Pseudomonas aeruginosa: A Model for Biofilm Formation [Internet]; in : Pseudomonas. Wiley-Blackwell, 2008, pp 215–253.

McGuire DB, Yeager KA, Dudley WN, Peterson DE, Owen DC, Lin LS, Wingard JR: Acute oral pain and mucositis in bone marrow transplant and leukemia patients: data from a pilot study.

Cancer Nurs 1998;21:385–393.

Mester E, Nagylucskay S, Döklen A, Tisza S: Laser stimulation of wound healing. Acta Chir Acad Sci Hung 1976;17:49–55.

Mester E, Spiry T, Szende B, Tota JG: Effect of laser rays on wound healing. Am J Surg 1971;122:532–535.

Mester E, Szende B, Gärtner P: [The effect of laser beams on the growth of hair in mice]. Radiobiol Radiother (Berl) 1968;9:621–626.

Mester E, Szende B, Spiry T, Scher A: Stimulation of wound healing by laser rays. Acta Chir Acad Sci Hung 1972;13:315–324.

Migliorati C, Hewson I, Lalla RV, Antunes HS, Estilo CL, Hodgson B, Lopes NNF, Schubert MM, Bowen J, Elad S, Mucositis Study Group of the Multinational Association of Supportive Care in Cancer/International Society of Oral Oncology (MASCC/ISOO): Systematic review of laser and other light therapy for the management of oral mucositis in cancer patients. Support Care Cancer 2013;21:333–341.

Miller MM, Donald DV, Hagemann TM: Prevention and treatment of oral mucositis in children with cancer. J Pediatr Pharmacol Ther 2012;17:340–350.

Miriyala S, Holley AK, St Clair DK: Mitochondrial superoxide dismutase--signals of distinction. Anticancer Agents Med Chem 2011;11:181–190.

Moskvin SV: Only lasers can be used for low level laser therapy. Biomedicine (Taipei) 2017;7. DOI: 10.1051/bmdcn/2017070422

Nalamachu S: An overview of pain management: the clinical efficacy and value of treatment. Am J Manag Care 2013;19:s261-266.

Nilius B, Voets T, Peters J: TRP channels in disease. Sci STKE 2005;2005:re8.

Oberoi S, Zamperlini-Netto G, Beyene J, Treister NS, Sung L: Effect of prophylactic low level laser therapy on oral mucositis: a systematic review and meta-analysis. PLoS ONE 2014;9:e107418.

de Oliveira RF, de Andrade Salgado DMR, Trevelin LT, Lopes RM, da Cunha SRB, Aranha ACC, de Paula Eduardo C, de Freitas PM: Benefits of laser phototherapy on nerve repair. Lasers Med Sci 2015;30:1395–1406.

Omi T, Kawana S, Sato S, Takezaki S, Honda M, Igarashi T, Hankins RW, Bjerring P, Thestrup-Pedersen K: Cutaneous immunological activation elicited by a low-fluence pulsed dye laser. Br J Dermatol 2005;153 Suppl 2:57–62.

Opstelten W, Neven AK, Eekhof J: Treatment and prevention of herpes labialis. Can Fam Physician 2008;54:1683–1687.

Otmani N, Alami R, Hessissen L, Mokhtari A, Soulaymani A, Khattab M: Determinants of severe oral mucositis in paediatric cancer patients: a prospective study. Int J Paediatr Dent 2011;21:210–216.

Ottaviani G, Gobbo M, Sturnega M, Martinelli V, Mano M, Zanconati F, Bussani R, Perinetti G, Long CS, Di Lenarda R, Giacca M, Biasotto M, Zacchigna S: Effect of class IV laser therapy on chemotherapy-induced oral mucositis: a clinical and experimental study. Am J Pathol 2013;183:1747–1757.

Ottaviani G, Martinelli V, Rupel K, Caronni N, Naseem A, Zandonà L, Perinetti G, Gobbo M, Di Lenarda R, Bussani R, Benvenuti F, Giacca M, Biasotto M, Zacchigna S: Laser Therapy Inhibits Tumor Growth in Mice by Promoting Immune Surveillance and Vessel Normalization. EBioMedicine 2016;11:165–172.

Passarella S, Karu T: Absorption of monochromatic and narrow band radiation in the visible and near IR by both mitochondrial and non-mitochondrial photoacceptors results in photobiomodulation. J Photochem Photobiol B, Biol 2014;140:344–358.

de Paula Eduardo C, Aranha ACC, Simões A, Bello-Silva MS, Ramalho KM, Esteves-Oliveira M, de Freitas PM, Marotti J, Tunér J: Laser treatment of recurrent herpes labialis: a literature review. Lasers in Medical Science 2013; DOI: 10.1007/s10103-013-1311-8

Peplow PV, Chung T-Y, Ryan B, Baxter GD: Laser photobiomodulation of gene expression and release of growth factors and cytokines from cells in culture: a review of human and animal studies. Photomed Laser Surg 2011;29:285–304.

Ponnudurai RN, Zbuzek VK, Wu WH: Hypoalgesic effect of laser photobiostimulation shown by rat tail flick test. Acupunct Electrother Res 1987;12:93–100.

Poyton RO, Ball KA: Therapeutic photobiomodulation: nitric oxide and a novel function of mitochondrial cytochrome c oxidase. Discov Med 2011;11:154–159.

Prado WA: Involvement of calcium in pain and antinociception. Braz J Med Biol Res 2001;34:449–461.

Prindeze NJ, Moffatt LT, Shupp JW: Mechanisms of action for light therapy: a review of molecular interactions. Exp Biol Med (Maywood) 2012;237:1241–1248.

Quatromoni JG, Eruslanov E: Tumor-associated macrophages: function, phenotype, and link to prognosis in human lung cancer. Am J Transl Res 2012;4:376–389.

Rai V: Role of Reactive Oxygen Species in Low-Level Laser Therapy [Internet]. Handbook of Low-Level Laser Therapy 2016; DOI: 10.1201/9781315364827-15

Ramphal R: Chapter 152. Infections Due to Pseudomonas Species and Related Organisms [Internet]; in Longo DL, Fauci AS, Kasper DL, Hauser SL, Jameson JL, Loscalzo J (eds): Harrison's Principles of Internal Medicine, ed 18. New York, NY, The McGraw-Hill Companies, 2012, [cited 2018 Sep 22].Available from: accessmedicine.mhmedical.com/content.aspx?aid=9121755

Rapf RJ, Vaida V: Sunlight as an energetic driver in the synthesis of molecules necessary for life. Phys Chem Chem Phys 2016;18:20067–20084.

Rizzi CF, Mauriz JL, Freitas Corrêa DS, Moreira AJ, Zettler CG, Filippin LI, Marroni NP, González-Gallego J: Effects of low-level laser therapy (LLLT) on the nuclear factor (NF)-kappaB signaling pathway in traumatized muscle. Lasers Surg Med 2006;38:704–713.

Rose-Ped AM, Bellm LA, Epstein JB, Trotti A, Gwede C, Fuchs HJ: Complications of radiation therapy for head and neck cancers. The patient's perspective. Cancer Nurs 2002;25:461–467; quiz 468–469.

Rubenstein EB, Peterson DE, Schubert M, Keefe D, McGuire D, Epstein J, Elting LS, Fox PC, Cooksley C, Sonis ST, Mucositis Study Section of the Multinational Association for Supportive Care in Cancer, International Society for Oral Oncology: Clinical practice guidelines for the prevention and treatment of cancer therapy-induced oral and gastrointestinal mucositis. Cancer 2004;100:2026–2046.

Rupniak HT, Rowlatt C, Lane EB, Steele JG, Trejdosiewicz LK, Laskiewicz B, Povey S, Hill BT: Characteristics of four new human cell lines derived from squamous cell carcinomas of the head and neck. J Natl Cancer Inst 1985;75:621–635.

Ryu J-J, Yoo S, Kim KY, Park J-S, Bang S, Lee SH, Yang T-J, Cho H, Hwang SW: Laser modulation of heat and capsaicin receptor TRPV1 leads to thermal antinociception. J Dent Res 2010;89:1455–1460.

Salehpour F, Mahmoudi J, Kamari F, Sadigh-Eteghad S, Rasta SH, Hamblin MR: Brain

Photobiomodulation Therapy: a Narrative Review. Molecular Neurobiology 2018;55:6601–6636.

Santinoni CDS, Oliveira HFF, Batista VE de S, Lemos CAA, Verri FR: Influence of low-level laser therapy on the healing of human bone maxillofacial defects: A systematic review. J Photochem Photobiol B, Biol 2017;169:83–89.

Saunders DP, Epstein JB, Elad S, Allemano J, Bossi P, van de Wetering MD, Rao NG, Potting C, Cheng KK, Freidank A, Brennan MT, Bowen J, Dennis K, Lalla RV, Mucositis Study Group of the Multinational Association of Supportive Care in Cancer/International Society of Oral Oncology (MASCC/ISOO): Systematic review of antimicrobials, mucosal coating agents, anesthetics, and analgesics for the management of oral mucositis in cancer patients. Support Care Cancer 2013;21:3191–3207.

Sharma SK, Kharkwal GB, Sajo M, Huang Y-Y, De Taboada L, McCarthy T, Hamblin MR: Dose response effects of 810 nm laser light on mouse primary cortical neurons. Lasers Surg Med 2011;43:851–859.

Shiva S, Gladwin MT: Shining a light on tissue NO stores: near infrared release of NO from nitrite and nitrosylated hemes. J Mol Cell Cardiol 2009;46:1–3.

da Silva BR, de Freitas VAA, Nascimento-Neto LG, Carneiro VA, Arruda FVS, de Aguiar ASW, Cavada BS, Teixeira EH: Antimicrobial peptide control of pathogenic microorganisms of the oral cavity: a review of the literature. Peptides 2012;36:315–321.

Silveira PCL, Silva LA, Freitas TP, Latini A, Pinho RA: Effects of low-power laser irradiation (LPLI) at different wavelengths and doses on oxidative stress and fibrogenesis parameters in an animal model of wound healing. Lasers Med Sci 2011;26:125–131.

Simone DA, Baumann TK, Collins JG, LaMotte RH: Sensitization of cat dorsal horn neurons to innocuous mechanical stimulation after intradermal injection of capsaicin. Brain Res 1989;486:185–189.

Simpson AWM: Fluorescent measurement of [Ca2+]c: basic practical considerations. Methods Mol Biol 2006;312:3–36.

Sommer AP, Pinheiro AL, Mester AR, Franke RP, Whelan HT: Biostimulatory windows in low-intensity laser activation: lasers, scanners, and NASA's light-emitting diode array system. J Clin Laser Med Surg 2001;19:29–33.

Sonis ST: The pathobiology of mucositis. Nat Rev Cancer 2004;4:277–284.

Sonis ST: Pathobiology of oral mucositis: novel insights and opportunities. J Support Oncol 2007;5:3–11.

Soukos NS, Stultz J, Abernethy AD, Goodson JM: Phototargeting human periodontal pathogens in vivo. Lasers Med Sci 2015;30:943–952.

de Sousa NTA, Santos MF, Gomes RC, Brandino HE, Martinez R, de Jesus Guirro RR: Blue Laser Inhibits Bacterial Growth of Staphylococcus aureus, Escherichia coli, and Pseudomonas aeruginosa. Photomed Laser Surg 2015;33:278–282.

Spanemberg JC, Figueiredo MAZ, Cherubini K, Salum FG: Low-level Laser Therapy: A Review of Its Applications in the Management of Oral Mucosal Disorders. Altern Ther Health Med 2016;22:24–31.

Sperandio FF, Simões A, Corrêa L, Aranha ACC, Giudice FS, Hamblin MR, Sousa SCOM: Low-level laser irradiation promotes the proliferation and maturation of keratinocytes during epithelial wound repair. J Biophotonics 2015;8:795–803.

Streeter K, Neuman C, Thompson J, Hatje E, Katouli M: The characteristics of genetically related Pseudomonas aeruginosa from diverse sources and their interaction with human cell lines.

Can J Microbiol 2016;62:233–240.

Sung L, Robinson P, Treister N, Baggott T, Gibson P, Tissing W, Wiernikowski J, Brinklow J, Dupuis LL: Guideline for the prevention of oral and oropharyngeal mucositis in children receiving treatment for cancer or undergoing haematopoietic stem cell transplantation. BMJ Support Palliat Care 2017;7:7–16.

Tang E, Khan I, Andreana S, Arany PR: Laser-activated transforming growth factor-β1 induces human β-defensin 2: implications for laser therapies for periodontitis and peri-implantitis. J Periodont Res 2017;52:360–367.

Tatmatsu-Rocha JC, Ferraresi C, Hamblin MR, Damasceno Maia F, do Nascimento NRF, Driusso P, Parizotto NA: Low-level laser therapy (904nm) can increase collagen and reduce oxidative and nitrosative stress in diabetic wounded mouse skin. J Photochem Photobiol B, Biol 2016;164:96–102.

Tricarico PM, Zupin L, Ottaviani G, Pacor S, Jean-Louis F, Boniotto M, Crovella S: Photobiomodulation therapy promotes in vitro wound healing in nicastrin KO HaCaT cells. J Biophotonics 2018;e201800174.

Tsai S-R, Hamblin MR: Biological effects and medical applications of infrared radiation. J Photochem Photobiol B, Biol 2017;170:197–207.

Tsen S-WD, Chapa T, Beatty W, Tsen K-T, Yu D, Achilefu S: Inactivation of enveloped virus by laser-driven protein aggregation. J Biomed Opt 2012;17:128002.

Tunér J, Hode L: It's all in the parameters: a critical analysis of some well-known negative studies on low-level laser therapy. J Clin Laser Med Surg 1998;16:245–248.

Turvey SE, Broide DH: Chapter 2: Innate Immunity. J Allergy Clin Immunol 2010;125:S24–S32.

Wainwright M: Local treatment of viral disease using photodynamic therapy. Int J Antimicrob Agents 2003;21:510–520.

Wang L, Hu L, Grygorczyk R, Shen X, Schwarz W: Modulation of extracellular ATP content of mast cells and DRG neurons by irradiation: studies on underlying mechanism of low-level-laser therapy. Mediators Inflamm 2015;2015:630361.

Wang Y, Huang Y-Y, Wang Y, Lyu P, Hamblin MR: Photobiomodulation of human adipose-derived stem cells using 810nm and 980nm lasers operates via different mechanisms of action. Biochim Biophys Acta Gen Subj 2017a;1861:441–449.

Wang Y, Wang Y, Wang Y, Murray CK, Hamblin MR, Hooper DC, Dai T: Antimicrobial blue light inactivation of pathogenic microbes: State of the art. Drug Resist Updat 2017b;33–35:1–22.

Wegiel B, Nemeth Z, Correa-Costa M, Bulmer AC, Otterbein LE: Heme oxygenase-1: a metabolic nike. Antioxid Redox Signal 2014;20:1709–1722.

Wong HM: Oral complications and management strategies for patients undergoing cancer therapy. ScientificWorldJournal 2014;2014:581795.

World Health Organization: WHO Handbook for Reporting Results of Cancer Treatment 1979;

World Health Organization: WHO guidelines on the pharmacological treatment of persisting pain in children with medical illnesses, Geneva, World Health Organization, 2012.

World Health Organization: Herpes simplex virus [Internet]. World Health Organization 2017 [cited 2018 Sep 22];Available from: http://www.who.int/news-room/fact-sheets/detail/herpes-simplex-virus

Yan X, Liu J, Zhang Z, Li W, Sun S, Zhao J, Dong X, Qian J, Sun H: Low-level laser irradiation modulates brain-derived neurotrophic factor mRNA transcription through calcium-dependent activation of the ERK/CREB pathway. Lasers Med Sci 2017;32:169–180.

Yang H, Inokuchi H, Adler J: Phototaxis away from blue light by an Escherichia coli mutant accumulating protoporphyrin IX. Proc Natl Acad Sci USA 1995;92:7332–7336.

Yoshino F, Yoshida A, Nakajima A, Wada-Takahashi S, Takahashi S, Lee MC: Alteration of the redox state with reactive oxygen species for 5-fluorouracil-induced oral mucositis in hamsters. PLoS ONE 2013;8:e82834.

Funding

This work was supported by University of Trieste – "University funding for scientific research project" (U22SCFRA15, "Effects of laser therapy on innate immune response in oncologic paediatric patients with oral mucositis") and by IRCCS Burlo Garofolo /Italian Ministry of Health (RC 15/2017 "Terapia Laser in pazienti oncologici pediatrici: analisi dei meccanismi molecolari responsabili della riduzione del dolore e del miglioramento della mucosite orale").

Acknowledgments

A special thanks to my supervisor prof. Sergio Crovella and to all my colleagues that supported me in the development of the research project:

Genetic Immunology Laboratory, Institute for Maternal and Child Health, IRCCS Burlo Garofolo: dr. Fulvio Celsi, dr. Paola Maura Tricarico, dr. Rossella Gratton

Division of Oral Medicine and Pathology, Dental Clinic, Maggiore Hospital: prof. Roberto Di Lenarda, prof. Matteo Biasotto, dr. Giulia Ottaviani, dr. Katia Rupel, dr. Augusto Poropat, Jacopo Dus

Cardiovascular Biology Laboratory, International Centre for Genetic Engineering and Biotechnology (ICGEB): dr. Serena Zacchigna, dr. Simone Vodret

Department of Medicine, Surgery and Health Sciences, University of Trieste: Prof. Pierlanfranco D'Agaro, dr. Ilaria Caracciolo